PALACKÝ UNIVERSITY OLOMOUC
Faculty of Science
Laboratory of growth regulators

Study of subcellular localization of auxin-inactivating enzymes in *Arabidopsis thaliana*: from cloning to fusion protein expression in plants

MASTER THESIS

Author:	**Anna Chesnokova, BSc**
Study program:	N1501 Biology
Field of study:	Experimental biology
Form of study:	Full-time
Thesis supervisor:	Federica Brunoni, Ph.D.
Thesis co-supervisor:	Anita Ament, MSc
Thesis submission deadline:	2024

Bibliografická identifikace

Jméno a příjmení autora	Anna Chesnokova
Název práce	Studium subcelulární lokalizace enzymů inaktivujících auxin u *Arabidopsis thaliana*: od klonování po expresi fúzního proteinu v rostlinách
Typ práce	Diplomová
Pracoviště	Laboratoř růstových regulátorů
Vedoucí práce	Federica Brunoni, Ph.D.
Rok obhajoby práce	2024
Abstrakt	Auxiny jsou rostlinné hormony, které hrají klíčovou roli v růstu a vývoji rostlin. Některé aspekty metabolismu auxinů však stále vyžadují další zkoumání. Jedním z takových aspektů je inaktivace pomocí konjugace s aminokyselinami prostřednictvím enzymů patřících do rodiny GRETCHEN HAGEN 3 (GH3). Cílem práce je určit prostorovou lokalizaci enzymů GH3s řízených jejich nativním promotorem v rostlinách *Arabidopsis thaliana*. Za tímto účelem byly enzymy GH3s fúzovány se zeleným fluorescenčním proteinem (GFP) a vytvořeny expresní konstrukty. Pomocí konfokální laserové skenovací mikroskopie byla analyzována subcelulární lokalizace konstruktů AtGH3s-GFP. Připravené vektory pro transformaci rostlin a výsledné transgenní linie by mohly přispět k dalšímu výzkumu zaměřenému na pochopení metabolismu auxinu v rostlinách.
Klíčová slova	*Arabidopsis thaliana*; auxin; GH3s; klonovací metody; konfokální laserová mikroskopie
Počet stran	58
Počet příloh	18
Jazyk	Angličtina

Bibliographical identification

Author's first name and surname	Anna Chesnokova
Title of thesis	Study of subcellular localization of auxin-inactivating enzymes in *Arabidopsis thaliana*: from cloning to fusion protein expression in plants
Type of thesis	Master
Department	Laboratory of Growth Regulators
Supervisor	Federica Brunoni, Ph.D.
The year of presentation	2024
Abstract	Auxin is a plant hormone that plays a key role in plant growth and development. Several mechanisms, such as auxin biosynthesis, transport, and inactivation regulate cellular auxin homeostasis in plants. Conjugation of auxin with amino acids by amido synthetases belonging to the GRETCHEN HAGEN 3 (GH3) family is one of the main inactivation pathways. This thesis aims to uncover the spatial localization of GH3 enzymes in *Arabidopsis thaliana* plants. This was achieved by expressing GH3 enzymes as fusion proteins with green fluorescent protein (GFP) to create expression constructs. The subcellular localization of the GH3-GFP fusion protein was analyzed using confocal laser microscopy. Prepared plant transformation vectors and resulting transgenic lines could contribute to setting up a baseline for further research to understand how GH3 enzymes contribute to auxin metabolism in plants.
Keywords	*Arabidopsis thaliana*; auxin; GH3s; cloning; protein localization; fluorescent tags; confocal laser microscopy
Number of pages	58
Number of appendices	18
Language	English

„Prohlašuji, že jsem předloženou diplomovou práci vypracovala samostatně za použití citované literatury.“

V Olomouci dne 07.05.2024 *Anna Chesnokova*

Acknowledgment

I want to thank my supervisors Federica Brunoni, PhD, and Anita Ament, MSc, for their valuable advice and guidance during the experiments. I also thank the Laboratory of Growth Regulators for providing me with educational opportunities in science. Special thanks to the entire laboratory team for their unwavering support in every aspect. My heartfelt appreciation also to my family and friends for their moral support and motivation.

The list of contents

List of abbreviations

4-Cl-IAA - 4-chloroindole-3-acetic acid

AMI - Amidase

AMP - Adenosine Monophosphate

ARF - Auxin Response Factor

ATP - Adenosine Triphosphate

AtNIT - *Arabidopsis thaliana* nitrilase

A.thaliana - *Arabidopsis thaliana*

BSA - Bovine serum albumin

bp - base pairs

CYP - Cytochrome

dNTPs - Deoxynucleotide triphosphates

E. coli - *Escherichia coli*

EDTA - Ethylenediaminetetraacetic acid

ELFO - Electrophoresis

ER - Endoplasmic reticulum

ERF13 - Ethylene Responsive Factor 13

Fw - Forward

g - gravitational force

gDNA – genomic DNA

GFP - Green fluorescent protein

GH3s - GRETCHEN HAGEN 3 enzymes

GMOs - Genetically Modified Organisms

HDGS - homology-dependent gene silencing

IAA - Indole-3-acetic acid

IAA-aa - IAA-amino acid conjugates

IAOx - Indole-3-acetaldoxime

IAM - Indole-3-acetamide

IAMT1 - IAA Carboxyl Methyltransferase

IAN - Indole-3-acetonitrile

IBA - Indole-3-butyric acid

ILR/ILL - IAA-Leu-Resistant1/ILR1-like

IpyA - Indole-3-pyruvic acid

INS - Indole Synthase

JA - Jasmonate

JA-Ile - Jasmonoyl-isoleucine

KO - Knockout

LB - Luria-Bertani

MES - 2-(N-morpholine)ethane sulfonic acid

MCS - Multiple Cloning Site

mQH2O - Milli-Q water

MPK - Mitogen-Activated Protein Kinase

MS - Murashige and Skoog medium

MW - Molecular weight

NAP - Nuclear Auxin Pathways

ORI - Origin of Replication

oxIAA - 2-oxindole-3-acetic acid

PAT - Polar auxin transport

PBC - Pelleted bacterial culture

PCR - Polymerase Chain Reaction

PAA - Phenylacetic acid

RT - Room temperature

rpm - Revolutions per minute

TAA - Tryptophan aminotransferase

TARs - tryptophan aminotransferase-related proteins

T-DNA - Transferred DNA

TAE - Tris-acetate-EDTA

Ti plasmid - Tumor-inducing plasmid

Tris - 2-amino-2-hydroxymethylpropane-1,3-diol

Trp - Tryptophan

TMK - Transmembrane Kinases

UMAMiT – Multiple Acids Move In And Out proteins

WAT - Walls Are Thin group of proteins

X-gal - 5-bromo-4-chloro-3-indolyl-beta-D-galactopyranoside

1. Introduction

Phytohormones are small molecular weight signaling molecules that are produced within the plant. In extremely low concentrations, they can regulate all aspects of plant growth and development. One of the most important plant hormones is the auxin indole-3-acetic acid (IAA) that is essential for optimal plant growth, development and it responds to environmental stimuli such as light and gravity. Auxin exert its function through concentration gradients within organs, tissues, and cells. These gradients result from coordinated local biosynthesis, metabolism, and transport.

Subgroup II members of the GRETCHEN HAGEN 3 (GH3) protein family typically conjugate amino acids to IAA. This reaction is the plant's primary inactivation response to excess auxin cellular concentrations and takes place in the cytoplasm. As a small molecule, IAA could potentially enter the nucleus via diffusion through the nuclear pores without restriction to activate the auxin-signaling cascade. However, auxin fluxes are instead mediated by specific efflux and influx carriers that are localized at the endoplasmic reticulum (ER) membrane, where they are predicted to regulate cellular IAA homeostasis *via* their transportation in and out of the ER compartment. While this is an emerging model for regulating auxin movement to the nucleus, it still needs to be fully understood how inactivation pathways contribute to maintaining auxin balance within the cell.

Determining the GH3 spatial localization could help advance our understanding of GH3-mediated mechanisms. To date, synthesis of IAA-amino acid conjugates is believed to occur in the cytosol, as cytosolic localization was demonstrated for GH3.17 by isopycnic glucose gradient. While this method allows inspecting the proteins' presence in a specific cellular compartment, getting comprehensive information about the protein's subcellular localization may be challenging as each subcellular compartment needs to be individually verified. If not, it may result in incomplete, misleading information. Therefore, in this work we have utilized commonly used GFP tagging of the protein approach. The main advantage of this method is the *in vivo* localization of the protein of interest. The main goal of this work is to determine the subcellular localization of GH3 proteins by generating *Arabidopsis thaliana* stable transgenic lines expressing GFP-fusion proteins under their native genomic locus.

2. Goals of the thesis

The goals of the thesis:

- Literature review that is focused on molecular cloning techniques, as well as auxin synthesis, metabolism, and signaling;
- Design and preparation of plant transformation vectors for the expression of *Arabidopsis* GH3-GFP fusion proteins for subcellular localization studies in *planta*;
- Generation of *Arabidopsis* transgenic lines by *Agrobacterium*-mediated transformation with transgenic line selection;
- Subcellular localization study of GFP-tagged proteins by confocal laser scanning microscopy.

3. Theoretical part

3.1 Auxin role and biosynthesis

The existence of auxin was famously inferred by Darwin's work on coleoptile phototropism. He showed that the seedling's response to unidirectional light producing a growth stimulus originated at the coleoptile tip. When the stimulus was traveling downward, it caused lower cells on the shaded side to grow faster compared to those on the illuminated side. The mobile growth regulator hypothesized by Darwin with these experiments was later identified by Went in 1928 as indole-3-acetic acid (IAA), the most abundant active auxin form in plants[1]. Besides IAA, several other naturally occurring molecules exhibit auxin-like activity: indole-3-butyric acid (IBA), 4-chloroindole-3-acetic acid (4-Cl-IAA), and phenylacetic acid (PAA) (Figure 1). Auxin and its derivates act like morphogens; their gradient determines developmental patterns. At the same time, auxin is transported from cell to cell, similar to mammalian hormones, and triggers plants' response to environmental stimuli[2]. Auxins regulate various physiological processes during plant development, including the formation of bilateral symmetry in the embryo, root emergence, apical dominance, as well as environmental responses, such as gravitropism and phototropism[2,3].

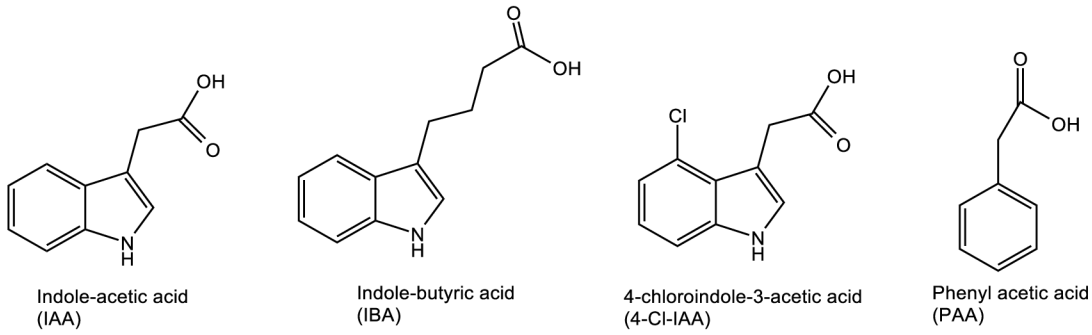

Figure 1. Chemical structures of most common natural auxins in plants.

The phenyl acetic acid (PAA) (Figure 1) is a less studied type of auxins. The PAA is synthesized from amino acid phenylalanine *via* the phenylpyruvate pathway[4]. Some data show its involvement in the formation of root primordial cells in some terrestrial plants[5]. Next, 4-chloroindole-3-acetic acid (4-Cl-IAA) was exclusively found in ovaries without growing embryos. These findings indicate that 4-Cl-IAA is a key signaling molecule in floret senescence[6]. The particular mechanisms of action of these hormones are unknown. While 4-Cl-AA is involved in fruit and seed formation, IAA and indole-butyric acid (IBA) affect mainly root development[7]. IBA is a precursor molecule that serves as a storage form of IAA[8]. Furthermore, IBA produces plant responses independent of IAA or it is converted to IAA, where it contributes to IAA function in plant development, stress responses, or both[7].

As auxin plays a pivotal role in almost all aspects of plant growth and development, regulating optimal levels of active auxin within cells is necessary. The levels of free IAA can be controlled by transport, interconversion of modified auxin forms, and biosynthesis[7]. The aromatic amino acid L-tryptophan (Trp) has been solidly established as a key precursor of auxin biosynthesis. However, two main IAA production routes exist: Trp-dependent and Trp-independent[9]. The existence of multiple IAA biosynthetic pathways ensures redundancy and robustness in auxin production. If one pathway is disturbed or inhibited, plants could still produce auxin and maintain essential growth and developmental processes in non-optimal conditions.

3.1.1 Tryptophan-dependent pathway

The tryptophan-dependent pathway occurs in two distinct compartments of the cell. First, aromatic amino acids, including tryptophan, are synthesized in plastids. Then tryptophan is translocated to the cytoplasm where downstream reactions can occur[9]. Trp-dependent auxin biosynthesis includes several parallel pathways (Figure 2) named after intermediate molecules: IAOx (indole-3-acetaldoxime), IAM (indole-3-acetamide), and IpyA (indole-3-pyruvic acid)[4].

Tryptophan deamination results in the synthesis of IpyA by tryptophan aminotransferase (TAA1) and TAA1-related proteins (TARs). Afterward, the YUCCA (YUC) family of flavin monooxygenases converts IpyA to IAA[4].

The conversion from Trp to IAOx is mediated by two cytochrome isozymes of the Monooxygenase P450 (CYP) family, CYP79B2 and CYP79B3[9]. IAOx is converted to IAN (indole-3-acetonitrile) by another enzyme of the P450 family – CYP71A13. AtNIT1, AtNIT2, and AtNIT3 are gene products with nitrilase activity. They take part in the conversion of IAN to IAA[10]. Specifically, they convert nitriles to carboxylic acids.

Although whether the conversion of Trp to IAM occurs is still unknown, IAM can be converted to active IAA through the action of AMIDASE1 (AMI1)[7,11].

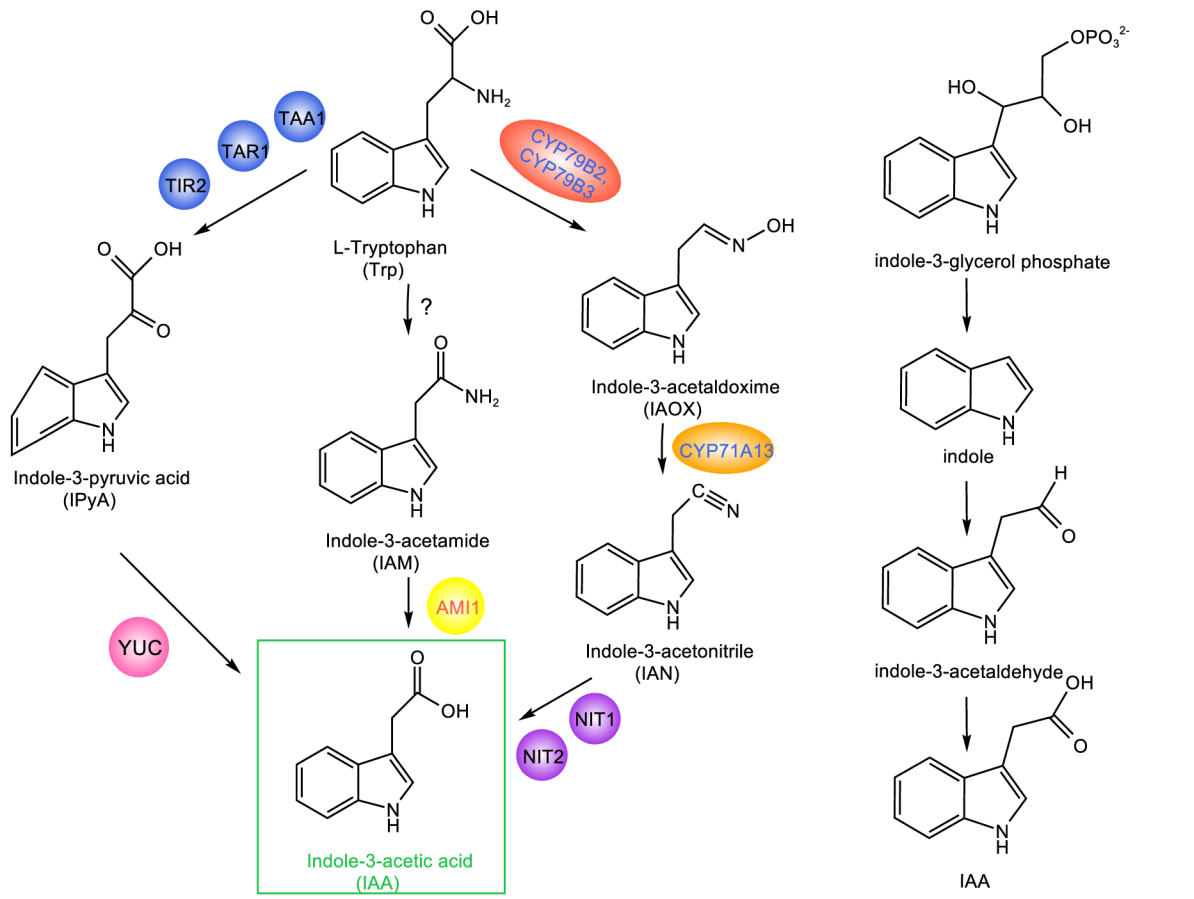

Figure 2. Potential IAA Trp-dependent and Trp-independent biosynthetic pathways[7,9,12].

So far, IpyA pathway is the only complete Trp-dependent auxin biosynthesis pathway, and it is considered the main pathway for IAA synthesis in plants. The role of IAOx and IAM pathways still has to be further elucidated[9].

3.1.2. Tryptophan-independent pathway

After discovering that maize and *Arabidopsis* mutants lacking in Trp biosynthesis were still producing IAA, a Trp-independent mechanism for auxin production was proposed[13]. Later research[14] suggested that cytosolic indole synthase (INS) mediates Trp-independent IAA production by converting indole-3-glycerolphosphate to indole (Figure 2). However, the molecular mechanism behind the indole to IAA conversion is unknown[12].

3.2. Auxin transport in plants

Typically, auxin is synthesized in flowers and leaves and then is transported by phloem to target tissues. One type of transport unique to auxin is polar auxin transport (PAT)[15]. This transport includes both active and passive ways of auxin movement and is mediated through influx and efflux carriers[16]. According to the chemiosmotic hypothesis, all auxins are weak acids in either proton-dissociated or nondissociated state[17]. Therefore, their movement

between cells depends on pH, and the transport of cellular IAA relies on the collective action of auxin transporters. In the apoplast's slightly acidic conditions (around pH 5.5), a small portion of IAA is in the nondissociated form (IAAH) and can enter cells by passive lipophilic diffusion. Most IAA exists in a proton-dissociated form (IAA-), requiring transporters for active uptake into cells. Since the cytoplasm has a higher pH than the apoplast (around pH 7.0), the equilibrium shifts towards the proton-dissociated form, which cannot passively diffuse across the plasma membrane. To exit the cell, IAA relies on efflux transporters. Since then, candidates for auxin carrier proteins have been identified[15,18].

The PIN-formed (PIN) family of proteins is a significant class of efflux transporters. They are frequently distributed polarly within cells, resulting in directed auxin transport only *via* membranes with PINs. The PIN family consists of eight members divided into two subclades based on the lengths of the hydrophilic loop[19]. Canonical or "long" PINs (PIN1, PIN2, PIN3, PIN4 and PIN7 proteins) have subcellular polar localization finely corresponding to the directionality of auxin movement and explaining auxin asymmetrical distribution at intercellular level[20–23]. It seems that auxin alone is one of the most important regulators of its transport, but regulation of carrier-mediated transport can take effect on a few different levels[17,24]. The role of PINs in various developmental processes, such as vascular differentiation, apical dominance, patterning, organ polarity, embryogenesis, organogenesis, phyllotaxis, and tropisms, have been reported and widely discussed[25,26].

Another group of proteins involved in auxin transport is the AUX1/LIKE AUX1 family of permeases. In *Arabidopsis*, this small gene family consists of four members: *AUX1*, *LAX1*, *LAX2* and *LAX3*. Unlike PINs, AUX proteins facilitate the influx of auxin into cells. Similarly to PINs, AUX protein activity and localization are tightly regulated to ensure proper auxin transport and response. These proteins typically contain several transmembrane domains that ensure selective transport of auxin molecules from the extracellular space into the cytoplasm of cells. The expression and activity of AUX proteins are influenced by various factors such as hormones, environmental cues, and developmental signals. One of the critical regulators of AUX protein activity is auxin itself. Mutants that lack functional AUX proteins often exhibit defects in various auxin-dependent processes, further highlighting the importance of these proteins in auxin transport and plant development[27].

3.2.1. Auxin transport on subcellular level

Contrary to cell-to-cell auxin transport driven by plasma membrane PINs, the ER-localized PIN5 and PIN8 („short", noncanonical PINs) ensure the compartmentalization of intracellular auxin pools[28,29]. Studies have shown that PIN5 and PIN8 act antagonistically.

Opposite values in analogous experiments indicate that PIN5 may convey auxin transport from the cytoplasm to the ER, whereas PIN8 conveys transport in the opposite direction[28,29].

PIN-like transporters (PILS) are yet another ER-localized family of transporters contributing to subcellular auxin distribution[30–32]. It is believed that auxin transport in the ER would sequester molecules in the cell compartment, restricting the abundance of signaling molecules in the nucleus[31].

WALLS ARE THIN1 (WAT1/UmamiT5) of the UmamiT (USUALLY MULTIPLE ACIDS MOVE IN AND OUT) family of proteins is considered to harbor auxin transport, which was demonstrated in *Arabidopsis* vacuoles[33].

3.3 Auxin signaling

The understanding of auxin signaling has significantly improved in the past decades. Auxin effects through the nuclear auxin pathways (NAP) consist of protein-protein interactions. There are three groups of them: TRANSPORT INHIBITOR RESPONSE1/AUXIN SIGNALING F-BOX (TIR1/AFB) family of coreceptors, AUXIN/INDOLE-3-ACETIC ACID INDUCIBLE (Aux/IAA) family of transcriptional repressors, and AUXIN RESPONSE FACTORS (ARF) transcription factors family[34].

One of the most critical pathways in auxin metabolism is the inhibition pathway, which prevents overstimulation by auxin in plants. The TIR1/AFB/IAA pairs act as coreceptors for auxin. The binding of the TIR1/AFBs pair to auxin triggers ubiquitination and further degradation of Aux/IAA transcriptional repressors. Without Aux/IAAs, ARFs (ARF10, ARF16) are no longer inhibited and start the transcription of auxin target genes[35].

Auxin has alternative signaling pathways, controlled by TRANSMEMBRANE KINASEs (TMKs) and MITOGEN-ACTIVATED PROTEIN KINASE (MPKs). TMK1 protein plays a role in extracellular auxin signaling by massive protein phosphorylation[34]. However, the precise roles of TMK2 and TMK3 in auxin signaling remain unclear. Another key protein for plant development and later root growth is Ethylene Responsive Factor 13 (ERF13). It is proved[36] that its degradation, carried by MPK14-mediated phosphorylation, is essential to regulating the auxin signaling cascade.

TMKs and TIR1/AFBs participate in general auxin signaling and are also crucial in keeping the balance between apoplastic acidification and alkalization[34]. The right balance is the main condition for effective auxin-mediated cell proliferation and plant growth.

3.4 Auxin metabolism

The main IAA inactivation mechanisms include oxidation, glycosylation, amino acid conjugation, and methylation. The last three processes are reversible. Therefore, they allow adjustable auxin release without the necessity for *de novo* auxin production[37]. However, some auxin forms, such as 2-oxindole-3-acetic acid (oxIAA), are irreversibly changed and safeguard against auxin toxicity in the presence of auxin overflow[38].

The key catabolic mechanism for inactivating auxin is the oxidation of IAA to oxIAA, which is mediated by DIOXIGENASE FOR AUXIN OXIDATION (DAO) enzyme, with further glycosylation to oxIAA-glc[22]. This pathway is considered a major route for auxin inactivation, as oxIAA-glc is the most prevalent IAA metabolite in *A.thaliana*[39]. A recent study showed[39] that IAA inactivation is coordinately regulated by a GH3-ILR1-DAO framework. According to this model, GH3 proteins first conjugate IAA. This reaction is reversible as ILR/ILL (IAA-Leu-Resistant/ILR1-like) amidohydrolases can hydrolyze conjugates back to the active form. Alternatively, IAA amino acid conjugates can be irreversibly oxidized by DAO and oxIAA-aa can be further hydrolyzed to form oxIAA[39].

In the past, it was thought that linking IAA with either aspartate (Asp) or glutamate (Glu) would mark these molecules for degradation. In contrast, conjugation with other amino acids would create storage forms of the hormone[40]. However, it has been recently shown that the production of IAA-Asp and IAA-Glu does not lead to degradation; instead, these conjugates also serve as storage forms of auxin[39].

Furthermore, the differences in expression levels between *DAO* and *GH3* genes suggest that DAO has slower enzyme kinetics compared to GH3 proteins[42], which helps to keep basal auxin concentrations in standard growth conditions. In contrast, GH3 proteins rapidly increase cellular IAA concentrations in response to environmental factors[43].

The last proposed type of auxin inactivation is methylation *via* IAA CARBOXYL METHYLTRANSFERASE 1 (IAMT1), which converts IAA to IAA methyl ester (MeIAA). However, the exact metabolism and function of MeIAA remain unknown[44].

3.4.1. Gretchen Hagen 3 (GH3) protein family

Gretchen Hagen 3 (*GH3*) genes encode acyl acid amido synthetases that catalyze ATP-dependent conjugation of phytohormones. Their mechanism consists of two steps. Firstly, acidic phytohormone is adenylated, forming an intermediate molecule with AMP. Then, amino acid nucleofilically attacks AMP, creating conjugated amino acid product (Figure 3)[45,46]. This mechanism contributes to maintening active phytohormone levels by balancing

the synthesis of the hormone and formation of amide-linked conjugates. The genome of *Arabidopsis* consists of 19 *GH3* genes, the exact role of which is difficult to determine due to their genetic redundancy[45]. However, these 19 members of *GH3* family can be classified into three subgroups based on their sequence similarity and substrate preference. Subgroup I consists of two members, GH3.10 and GH3.11, which catalyze the conjugation of jasmonate (JA) with isoleucine, resulting in the formation of jasmonoyl-isoleucine (JA-Ile)[47]. Next, subgroup II consists of eight members: *GH3.1*, *GH3.2*, *GH3.3*, *GH3.4*, *GH3.5*, *GH3.6*, *GH3.9* and *GH3.17*. All subgroup II proteins effectively conjugate auxin with amino acids, resulting in temporary auxin inactivation[48,49]. Lastly, subgroup III comprises nine members: *GH3.7*, *GH3.8*, *GH3.12*, *GH3.13*, *GH3.14*, *GH3.15*, *GH3.16*, *GH3.18*, *GH3.19*[50]. Some members, such as GH3.12, have been demonstrated to conjugate isochlorismate with glutamate, that can be converted to salicylic acid[49].

Three members belonging to Subgroup II of the GH3 protein family, such as GH3.3, GH3.4 and GH3.17, will be investigated in this thesis. Recent studies[45] showed that GH3.17 may play prominent role in root elongation, while GH3.3 an GH3.4 may contribute to lateral root formation and affect the primary root growth[45].

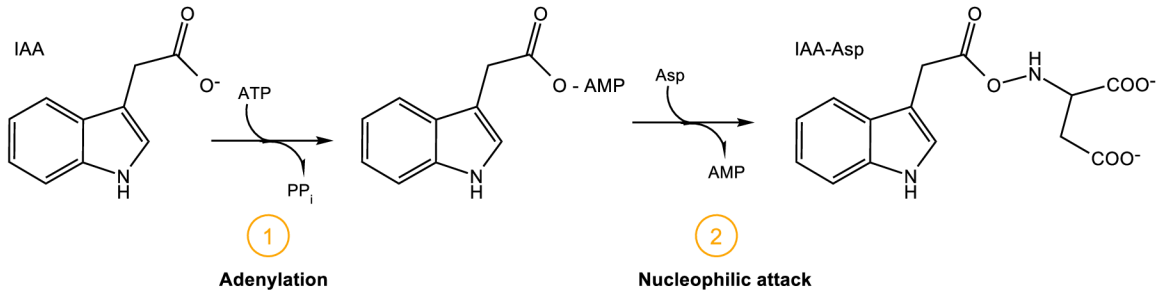

Figure 3. General reaction catalyzed by IAA-amido synthetases belonging to the GH3 family[47].

3.5. Molecular cloning

Gene cloning comprises the *in vitro* creation of new DNA molecules containing unique combinations of genes or oligonucleotides and the propagation of recombinant DNA molecules *in vivo via* the replication mechanisms of bacteria and other microorganisms. The term "clone" comes from the Greek word for "bud" or "twig"[51]. It was initially used in biomedical sciences as a term for a set of genetically identical organisms. As they derive from a single organism, clones are supposed to be identical. The ability to make numerous identical clones of a DNA molecule ("molecular cloning", achievable both *in vivo* or *in vitro*) or a cell is referred to as cloning[52].

Molecular cloning includes specific, unique tools and terminology. A DNA construct is created by a segment of DNA carried on a vector that can be used to insert genetic material into a target tissue or cell. A vector is any particle (such as plasmids, cosmids, Lambda phages) used to transport a foreign nucleic sequence artificially - usually DNA - into another cell, where it can be duplicated and/or expressed[53]. Recombinant DNA is a vector that contains foreign DNA. Plasmids are the most widely used vectors. Typically, the vectors used in DNA constructs contain several essential features: an origin of replication (ORI), a multiple cloning site (MCS), and a selectable marker[53].

In general, there are five main steps of molecular cloning: preparation of the insert and vector, ligation, transformation, screening of the clones, and selection of the transformants[51].

3.5.1. Cloning vectors

The most well-known double-stranded vectors are plasmids. They can replicate independently of the host chromosome. Naturally, plasmids contain genes that benefit the survival of the organism[54]. A plasmid cloning vector is commonly used to clone DNA fragments of up to 15 kbp. The pBR322 plasmid was one of the first commonly used as a cloning vector[55]. There are five main categories of plasmids by original function. Howeve, one plasmid can belong to more than one group[56]: fertility F-plasmids, resistance plasmids (R), Col plasmids, degradative plasmids, and virulence plasmids.

One of the main parts of vector is the ORI, which is responsible for the self-replication and sharing plasmid copies to the daughter cells. MCS is a specific DNA sequence for restriction enzymes used to insert the target DNA into the plasmid. MCS plays a significant role in the cloning methods. The promoter region is a sequence located upstream of inserted gene and directs to start of transcription. Promoters come in various types: native, constitutive, inducible and repressible[54]. Native promoters initially consist of a single fragment from the 5' region of a given gene. An inducible promoter controls the expression of the target gene in specific circumstances. They activate gene transcription when exposed to a certain small chemical, such as lactose and galactose. Opposite to inducible promoters, repressible promoters are inhibiting gene expression in the presence of specific small chemicals, such as tryptophan or ethanol. The next part of the vector is the terminator. It defines the end of transcription. Therefore, only the gene of interest will be transcribed. Another type of the vector sequence is the primer binding site, which is complementary to the sequence of a PCR (polymerase chain reaction) primer used for amplification of the region of interest[54]. Last but not least, is a selectable marker. It is a gene that brings

identifiable characteristic to a vector. The most used ones are antibiotic resistance genes and genes encoding fluorescent proteins.

3.5.2. GreenGate cloning

GreenGate is a cloning technique for the fast building of plant transformation constructs. It relies on the Golden Gate technique. Ready-to-use plant transformation vectors are constructed from six pre-cloned entry modules and a destination vector in a single-tube reaction. The method includes release of DNA fragments from entry modules using the type IIS restriction endonuclease *Bsa*I[57]. Each DNA fragment is flanked at its 5'-end by the same overhang as the 3'-end of its previous neighbor. All overhangs vary from each other by at least two of the four nucleotides. Once DNA fragments are released, they can be ligated in specific order between the destination vector's left and right border sequences by *T4* DNA ligase (Figure 4). These six pUSC19-based modules include plant promoter, N-terminal tag, coding sequence (*i.e.*. the gene of interest), C-terminal tag, plant terminator and plant resistance cassette[57]. All modules can be modified, and the gene's coding region should be inserted in the module designed for coding sequence. In addition, the pGreen-IIS-based destination vector encodes a different antibiotic resistance than the entry vectors. It carries recognition sites in an orientation that removes them from the backbone after type IIS digestion, exposing overhangs compatible with those of the outer insert modules[57].

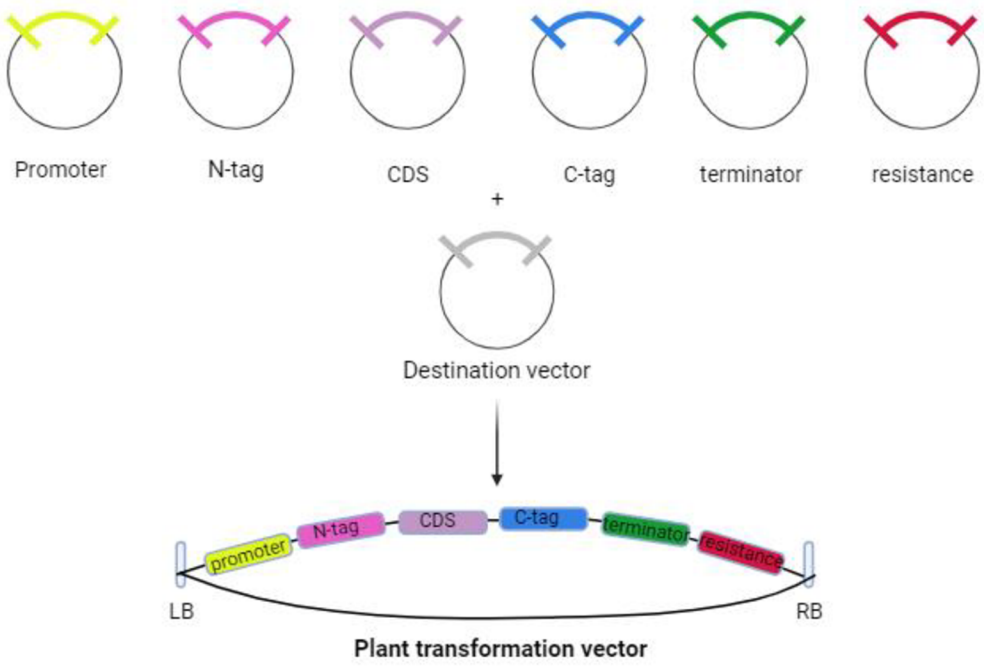

Figure 4. The process of generating a plant transformation vector by GreenGate cloning strategy, created in Biorender.

3.5.3. TA cloning

TA cloning is a technique that creates complementary single-stranded overhangs between the insert and vector using Taq polymerase's terminal transferase activity. Taq polymerase adds a single deoxyadenosine (dA) to the 3'-ends of double-stranded DNA, a unique feature not found in all thermostable DNA polymerases[58]. Vectors with T overhangs (overhangs with the deoxythymidine on 3'-end) can be bought or prepared individually by using a blunt-end restriction enzyme, mixing with terminal transferase enzyme and dideoxythymidine triphosphate (ddTTP), which lacks the 3' hydroxyl group. The lack of the hydroxyl group guarantees that only one T is attached to the vector ends. Alternatively, the vector can be cleaved using restriction enzymes that produce T overhang straightly[58].

The TA cloning process starts with generating the insert in a PCR reaction using Taq polymerase, which attaches a single A to the 3`-ends of the PCR product. Subsequently, the PCR products are fused with a vector containing complementary 3' deoxythymidine (T) overhangs. DNA ligase is then utilized to join the vector and insert together. The disadvantage of this method is that proofreading DNA polymerases cannot be used, as they are incapable of producing A-overhangs[59]. However, this limitation could be solved by incubating the PCR reaction with Taq polymerase after performing the PCR reaction with the DNA-proofreading polymerase.

3.5.4. PCR

A straightforward enzymatic procedure called PCR enables the *in vitro* amplification of a particular DNA region from a complex DNA pool. PCR can produce enough copies of DNA from minimal levels. Therefore, DNA can be examined with standard laboratory techniques. As a result, PCR is considered a sensitive assay[60]. The critical component of PCR is the Taq polymerase, a thermostable DNA polymerase, which utilizes DNA primers made especially for the target DNA region to be amplified. After first step, denaturation, which breaks double-stranded DNA into two separated strands, follows primers annealing. Thermostable Taq polymerase recognizes primers and production of DNA amplicons begins in 5’ to 3’ orientation[61]. The final phase is called elongation and occurs after the last cycle. Its purpose is to guarantee that every amplicon will have their second strand produced[62]. The target region can be created in significant quantities by the PCR process, as with every cycle, the number of DNA molecules is doubled[63].

3.5.5. Screening Strategies

Selection and screening strategies are used to validate if transformation of foreign DNA into host cells was effective. There are two main types of selection: positive and negative.

The most often used negative selection method is blue-white selection. β-galactosidase is a naturally occurring protein in *E.coli* encoded by the *lacZ* gene of the *lac* operon. In its native form, it forms a homotetramer, which cuts lactose into glucose and galactose[64]. N-terminal deletion makes a mutant β-galactosidase from the M15 strain of *E.coli* inactive, as the ω-peptide cannot form a tetramer. However, in the presence of the protein's N-terminal part, the *α*-peptide, in this mutant form of the protein, may fully rebound to its active tetrameric structure. The ω-peptide-containing *lacZ* deletion (*lacZΔM15*) is carried by the host *E.coli* strain in this screening approach, whereas the plasmids utilized carry the *lacZα* sequence, which encodes the *α*-peptide[65]. Both are ineffective, but when both peptides are expressed simultaneously, they combine to generate a functioning β-galactosidase enzyme. X-gal is a colorless lactose analog that may be cut down by β-galactosidase to produce an insoluble pigment that is vivid blue. Growing bacteria on X-Gal may produce blue and white colonies. Blue colonies suggest that the vector may have an unbroken *lacZα* (no DNA insert present), but white colonies, where X-gal is not hydrolyzed, indicate the presence of an insert in lacZα that prevents the β-galactosidase from being active[66].

The other well-studied method is antibiotic selection. When the inserted plasmid has a marker for antibiotic resistance, selection is straightforward. Transformed cells are placed on a medium containing the appropriate antibiotic. The cells that proliferate should be those harboring plasmids containing selected antibiotic resistance[67].

The most precise ways of selection are PCR methods, such as Colony PCR and Sanger sequencing. These techniques use specific primers to identify the presence of the inserted gene. Colony PCR is a technique for detecting an inserted construct or plasmid into bacteria or yeast. In colony PCR, primers are designed to produce a specific, known-size product only in the presence of the wanted construct. Ideally, the product will have a different size if the desired DNA insertion did not occur[68]. By using a very crude cell preparation, the tiny quantity of template DNA produces an easily visible band on an agarose gel after PCR amplification. Consequently, colony PCR is an effective method for quick and striaghtforward sorting through a potentially huge number of positive colonies from false ones[69].

3.5.6. Competent cells transformation

The majority of techniques for transforming bacteria are based on the findings of Mandel and Higa[70] and Cohen *et al*[71], who demonstrated the possibility of transfecting bacteria with bacteriophage and DNA plasmids by incubating them with an ice-cold $CaCl_2$ solution and briefly heating them after that. Through this process, bacterial cells are brought into a brief stage of "competence" that allows them to absorb DNA. After transformation, cells are incubated into a recovery medium to refurbish the cell membrane and the cell wall[72]. Other methods of transformation are electroporation and heat shock.

The electroporation method uses an electric pulse, which produces an irregular electric field and creates pores in the plasma membrane. That helps the foreign DNA to move into a host cell. After that, the cell membrane locks itself again and traps the DNA inside. A comparison between electroporation and the heat shock method demonstrates that electroporation is more efficient, in terms of higher colony numbers and faster procedure[73]. One of the method's limitations is that it requires electroporation cuvettes and an electroporator, a specialized piece of instrumentation, while the heat shock method can be performed using standard Eppendorf tubes and a conventional thermoblock. Furthermore, a common issue with electroporation is the existence of air bubbles or salts lasted because of wrong competent cell preparation, which might lead to an arcing in the cuvette and in that case losing the sample[73].

In the heat shock transformation, the membrane potential of competent cells is reduced by the temperature pulse, which reduces the potential barrier for negatively charged DNA to enter the cytoplasm[74]. Chemically competent cells are frequently formed in pellets by adding salt, such as $CaCl_2$. The negative charge on the phospholipid and DNA is eliminated by applying salt, which helps the DNA to move toward the cell[75].

3.5.7. Molecular cloning impact

The advancement of genetic engineering techniques has enabled the manipulation of microbe genomes to produce substances with little intrinsic value but significant medical or commercial benefit to mankind. Small portions of DNA could be replicated with great precision using molecular cloning. The high number of copies makes it easier to analyze the DNA sequence, content, and genes within specific DNA fragments. Molecular cloning has excellent benefits in areas such as gene function analysis, recombinant protein production and generation of genetically modified organisms (GMOs).

To investigate the function of a gene, either gain-of-function or interference studies using microRNA can be performed by cloning the cDNA into an expression vector to induce overexpression in the target organism. Besides RNA interference, there are other ways to inhibit gene function, such as the CRISPR/Cas9 editing method, Zinc-Finger Nucleases (ZFNs), and transcription activator-like (TAL) effector nucleases (TALENs)[76]. Furthermore, adding particular mutations can determine genes' effectiveness in gene function, whether through site-directed mutations or the creation of protein mutants[53].

Molecular biology and the production of relevant proteins have been revolutionized by cloning. By cloning the gene that encodes a specific protein into an appropriate expression system, scientists can generate substantial quantities of this protein for research, therapeutic or industrial purposes. For example, extraneous genes have been inserted into the DNA of *E.coli* to enable the creation of beneficial proteins such as interferons, human hormones insulin, somatostatin, and somatotropin[52].

Molecular cloning techniques have enabled scientists to insert certain genes into organisms, creating GMOs. This has resulted in agricultural breakthroughs such as the producing crops with better features such as insect resistance, disease resistance, and nutritional value[77].

3.6. *Agrobacterium*-mediated plant transformation

Among the various techniques used to introduce foreign genetic material into plants, *Agrobacterium*-mediated plant transformation, known as the floral dip method, is commonly used. With this method, a naturally occurring bacteria in soil, *Agrobacterium tumefaciens*, is used as vector to deliver foreign DNA into the plant cells leading to heritable changes in the plant genome. The process includes growing *Arabidopsis* to the flowering stage, dipping plant floral buds in a *Agrobacterium* growth culture medium containing sucrose or hormones, gathering seeds several weeks later, and identifying transformed progeny by selection on media containing antibiotic or herbicide[78]. The optimal period for conducting the floral dip is when plants have a substantial number of unopened flower buds. The fact that transformed progeny are usually hemizygous for the transgene at a particular locus indicates that transformation takes place subsequent to the divergence of the ovarian and anther cell types[79]. *Agrobacterium*-mediated transformation is suitable not only for introducing certain gene constructs into plants, but also for a random mutagenesis technique for gene-tagging as transformed plants can be obtained at high numbers[80]. Beside sucrose media there is a second crucial component - surfactant Silwet - which allows chemicals and *Agrobacterium* to enter a plant tissue, particularly female gametes[81].

In detail, the plant is infected by *Agrobacterium via* its *Ti* plasmid. The *Ti* plasmid incorporates T-DNA, a portion of its DNA, into the chromosomal DNA of its host plant cells. The periplasmic space contains a chvE protein, which is encoded by a chromosomal gene and serves for recognizing sugars[82]. Attachment occurs in two stages. This mechanism is mediated by four major genes: *chvA*, *chvB*, *pscA*, and *att*. The first three genes' proteins appear to be responsible for the creation of cellulose fibrils. These fibrils also serve as anchors for the bacteria, assisting in forming a microcolony. VirC2 ensures proper processing and is also essential for single-copy system integration[83].

3.7. Confocal microscopy

Confocal laser scanning microscopy is an optical imaging technique that uses a spatial pinhole to exclude out-of-focus light during image generation to increase the optical resolution and contrast of a micrograph[84]. The optical sectioning method, which allows for reconstructing three-dimensional structures within an object, is made possible by taking many two-dimensional photographs of the object (z-stack) at different depths in the sample. A traditional microscope allows light to penetrate as far into the material as possible. In contrast, a confocal microscope only concentrates a smaller beam of light at one particular depth level. A confocal microscope focuses both illumination and detection lenses on a single, diffraction-limited point in the sample. This particular spot is the only spot imaged by the detector throughout a scan[84]. While the original design's pinholes, objective lenses, and low-noise detectors remain the fundamental elements of a conventional confocal microscope, fast scanning mirrors, wavelength selection filters, and laser illumination are also commonly included. Usually, the laser is focused on two scanning mirrors that move the beam in x and y directions over a single field of view[85], creating an image.

In this diploma thesis, confocal microscopy was used to observe the subcellular localization of proteins fused to a green fluorescent protein (GFP). GFP is a fluorophore, originally isolated from the jellyfish *Aequorea victoria*[86]. The cell generates the fluorophore spontaneously by cyclizing the tripeptide Ser65-Tyr66-Gly67, forming a heterocyclic imidazolinone ring and oxidizing Tyr66 with molecular oxygen[86].

4. Experimental part

4.1 Material and equipment

4.1.1 Chemicals

2-(N-morpholine)ethane sulfonic acid (MES) - Duchefa Biochemie (Netherlands)

2-amino-2-hydroxymethylpropane-1,3-diol (Tris) - Duchefa Biochemie (Netherlands)

5x Green GoTaq Flexi Reaction Buffer – Promega (Czech Republic)

Acetic acid – Penta (Czech Republic)

Agarose - Merck Life Science (Germany)

Alfa Aesar Gellan Gum - Thermo Fisher Scientific (USA)

10 mM ATP – Thermo Fisher Scientific (USA)

Bacteriological agar - Sigma-Aldrich (USA)

dNTPs - Thermo Fisher Scientific (USA)

DreamTaq Green PCR Master Mix (2x) - Thermo Fisher Scientific (USA)

E.Z.N.A. ® Plant DNA Kit – Omega Bio-tek (USA)

Ethanol - Lachner (Czech Republic)

Ethylenediaminetetraacetic acid (EDTA) - Penta (Czech Republic)

10x FastDigest Green buffer - Thermo Fisher Scientific (USA)

GelRed - Sigma-Aldrich (USA)

Glycerol - Sigma-Aldrich (USA)

Hydrochloric acid 37% (HCl) – Penta (Czech Republic)

Isopropanol - Lachner (Czech Republic)

LB Broth - Sigma-Aldrich (USA)

Magnesium Chloride - Penta (Czech Republic)

Milli-Q water (from Milli-Q Reference Water Purification System) - Merck Life Science (Germany)

Murashige & Skoog including vitamins - Duchefa Biochemie (Netherlands)

NucleoSpin® Gel and PCR Clean-up – Takara Bio (USA)

GeneRuler 1 kB Plus DNA Ladder - Thermo Fisher Scientific (USA)

Polyoxyethylene sorbitan monolaurate 20 (Tween 20) - Sigma-Aldrich (USA)

Phusion HF Buffer Pack - Thermo Fisher Scientific (USA)

Silwet L-77 - Sigma-Aldrich (USA)

Sodium hypochloride – Carl Roth (Germany)

Sucrose - Lachner (Czech Republic)

TriTrack DNA Loading Dye (6x) - Thermo Fisher Scientific (USA)

QIAprep Spin Miniprep Kit – Qiagen (USA)

4.1.2 Enzymes

DreamTaq DNA Polymerase - Thermo Fisher Scientific (USA)

Eco31I (*Bsa*I) 10 U- Thermo Fisher Scientific (USA)

GoTaq G2 Flexi DNA polymerase - Promega (Czech Republic)

Phusion High-Fidelity DNA Polymerase - Thermo Fisher Scientific (USA)

T4 DNA Ligase 30 U - Thermo Fisher Scientific (USA)

4.1.3 Instruments

Airstream Gen 3 Horizontal Laminar Flow Cabinet - Esco Micro Pte. Ltd. (Singapore)

Confocal microscope LSM 900 - Zeiss (Germany)

Electroporator ECM 399 - BTX (USA)

Fume cupboard - MERCI (Czech Republic)

ICT incubator - P-Lab (Czech Republic)

INCU-Line incubator - VWR International, Avantor (USA)

IKA IKAMAG Magnetic Mixer - IKA (Germany)

Mega Star 600R refrigerated centrifuge - VWR International, Avantor (USA)

Memmert incubator - VWR International, Avantor (USA)

Microcentrifuge/vortex Combi-spin PCV-2400 - Keison products (UK)

Microwave oven - Sencor (Japan)

Milli-Q Reference Water Purification System - Merck Life Science (Germany)

NanoDrop OneC - Thermo Fisher Scientific (USA)

pH Meter Ultra-Basic Bench-top Meter - Biotech (France)

POS-300 Orbital Shaking Platform - Keison products (UK)

Precision Balances - Mettler Toledo (USA)

Plant Growth Chamber Sanyo MLR-351H - SANYO Electric Co., Ltd. (Japan)

SANOclav Laboratory autoclave La-MCS - SANOclav (Germany)

Thermocycler Doppio - VWR International, Avantor (USA)

ThermoMixer Temperature Control Device - Eppendorf AG (Hamburg, Germany)

Transilluminator Gel Doc EZ System - Bio-Rad Laboratories (USA)

UV-1600PC Spectrophotometer - VWR International, Avantor (USA)

XSR analytical balances - Mettler Toledo (USA)

4.1.4 Software

Geneious Prime – Dotmatics (New Zealand)

ImageLab – Bio-Rad (USA)

ZEN blue/black – Zeiss (Germany)

4.1.5 Biological material

Arabidopsis thaliana, ecotype Columbia (Col-0)

Escherichia coli NEB5α

Escherichia coli TOP 10

Agrobacterium tumefaciens GV3101 (pSoup)

4.1.6 Antibiotics

Kanamycin - Duchefa Biochemie (Netherlands)

Carbenicillin - Duchefa Biochemie (Netherlands)

Rifampicin - Duchefa Biochemie (Netherlands)

Spectinomycin - Duchefa Biochemie (Netherlands)

Tetracycline - Duchefa Biochemie (Netherlands)

4.2 Methods

4.2.1 Genomic DNA extraction

Genomic DNA (gDNA) was extracted by E.Z.N.A. ® Plant DNA Kit or DNA extraction buffer.

Arabidopsis leaves were ground in liquid nitrogen, and 100 mg of the sample was transferred to a nuclease-free 1,5-ml microcentrifuge tube. Six hundred µl of the P1 Buffer was added to the sample following vortexing until all clumps disappeared. Samples were incubated at 65 °C for 10 minutes, and mixed twice during the incubation by inverting the tube. Afterward, 140 µl of the P2 Buffer was added, followed by thorough vortexing. Samples were centrifugated at 10,000 *g* for 10 minutes. The cleared lysate was transferred to a new 1,5-ml microcentrifuge tube, 0,7 volumes of 100 % isopropanol were added, and

samples were thoroughly mixed. Centrifugation at 14,000 *g* for 2 minutes was performed to pellet DNA. The supernatant was discarded. The tube containing DNA was inverted on a paper towel for 1 minute to allow any residual liquid to drain. Three hundred µl of sterile deionized water heated to 65 °C was added and pellet was resuspended by vortexing. Next, 4 µl of RNase A was added, and samples were vortexed briefly. One hundred and fifty µl of P3 Buffer and 300 µl of absolute ethanol were added, and samples were vortexed immediately to obtain a homogeneous mixture. A HiBind® DNA mini-column was inserted into a collection tube. The entire sample was transferred to the column and was centrifuged at 10,000 *g* for 1 minute. The flow-through was discarded, and 650 µl DNA washing buffer was added. Centrifugation at 10,000 *g* for one minute was carried out, and the washing step was repeated. The column was centrifuged at 10,000 *g* for two minutes to dry. The HiBind® DNA mini-column was transferred into a new 1,5-ml microcentrifuge tube with the addition of 50 µl mQH_2O heated to 65 °C. Samples were incubated at room temperature for five minutes. The DNA was eluted by centrifugation at 10000 *g* for one minute.

Alternatively, DNA was extracted using a genomic DNA extraction buffer containing 50 mM of Tris-HCl (pH 7,2), 300 mM NaCl, and 10 % sucrose. The solution was topped up to ten ml with mQH_2O and autoclaved on a liquid cycle (121 °C for 15-20 minutes). Approximately 100 mg of fresh leaves with 500 µl of genomic DNA extraction buffer were homogenized with beadmill (3 beads, 27 Hz, 3 minutes) and incubated at 95 °C for one minute. Samples was centrifuged at 3000 *g*, at 22 °C for two minutes. One µl of supernatant was used for the PCR reaction.

4.2.2 Plasmid isolation

Isolation of plasmids was performed using a QIAprep® Miniprep kit. Selected colonies were inoculated in 6 ml of LB medium supplemented with the corresponding antibiotic, and grown at 37 °C overnight. The day after, the bacterial culture was pelleted at 6800 *g* for three minutes, and the pellet was resuspended in 250 µl of buffer P1. Then, 250 µl buffer P2 were added, and the mixture was mixed by inverting the tube 4–6 times. Next, 350 µl buffer N3 was added, and the mixture was gently remixed. Samples were centrifuged for ten minutes at 17,900 *g*, forming a compact white pellet. The supernatant was transferred to the QIAprep spin column. Centrifugation at 17,900 *g* for one minute was carried out, and the flow-through was discarded. The column was washed by adding 700 µl PE Buffer, followed by one minute centrifugation at 17,900 *g*. The flow-through was discarded, and centrifugation was performed for two minutes to remove residual washing buffer. The column was placed in a clean 1,5-ml microcentrifuge tube, and samples were incubated in a preheated thermoblock

at 70 °C for 5 minutes. Fifty µl of mQH2O water was added to the colum, incubated at RT (room temperature) for five minutes, and then centrifuged for two minutes to elute.

4.2.3 Preparation of Luria-Broth (LB) medium

LB medium was prepared by dissolving 25 g of LB Broth in 900 ml of mQH_2O. pH was adjusted to 7-7,2, and the solution was topped up to 1000 ml with mQH_2O. To prepare LB agar plates, 1,5% bactoagar was added into the LB medium. The medium was autoclaved on a liquid cycle (121 °C for 15 minutes). LB medium containing bactoagar was supplemented with either 60 µg/ml spectinomycin, 100 µg/ml carbenicillin, or 50 µg/ml kanamycin. For *Agrobacterium* selection, LB agar plates were supplemented with 60 µg/ml spectinomycin, 50 µg/ml rifampicin, and 5 µg/ml tetracycline and poured into Ø 90mm round Petri dishes.

4.2.4 Preparation of MS agar plates

Half-strength MS medium was prepared by dissolving 4,4 g of MS salts + vitamins, 0,5 g of MES, and 10 g of saccharose in 900 ml of mQH_2O. Reagents were stirred until completely dissolved. pH was adjusted on 5,7, and the solution was topped up to 1000 ml with mQH_2O. After pH adjustment, 0,57 % of Gellan Gum was added, and the medium was autoclaved on a liquid cycle (121 °C for 15 minutes). The medium was supplemented with 30 µg/ml of Hygromycin B and poured in Ø145 mm round Petri dishes.

4.2.5 PCR amplification and PCR clean-up

PCR was used to amplify coding regions of *AtGH3.3*, *AtGH3.4* and *AtGH3.17* genes. Ten µl of gDNA were mixed with 0,5 µl of the Phusion DNA polymerase, 10 µl of 5xPhusion HF buffer, 1 µl of 10 µM dNTPs, 2,5 µl of 10 µM forward (Fw) and reverse (Rv) primer pairs (Table 2) and 21,5 µl of mQH_2O. After mixing, samples were spun down and transferred to a thermocycler to initiate PCR amplification. The PCR amplification parameters are described in Table 1. If amplicons were used for TA cloning strategy, 0,7 units of GoTaq Polymerase were added to the mixture and additional ten-minute incubation at 72 °C was performed.

Table 1. Thermocycler parameters for PCR amplification

Temperature (°C)	**Time (minutes)**	**Cycles (number)**
98	0:30	1
98	0:30	35
55	0:30	35
72	4	35

72	10	1
8	60	

Table 2. Primers used for amplification of the coding region of GH3s from genomic DNA

Primer name	Primer sequence
AtGH3.3_GG_Fw	AACAGGTCTCAGGCTCAACAATGACCGTTGATTCAGCTCTGCG
AtGH3.3_GG_Rv	AACAGGTCTCTCTGAACGACGACGTTCTGGTGACCA
AtGH3.4_GG_Fw	AACAGGTCTCAGGCTCAACAATGGCTGTTGATTCGCTTCTTCA
AtGH3.4_GG_Rv	AACAGGTCTCTCTGAATGACGTCGTTCTGGCGACCA
AtGH3.17_GG_Fw	AACAGGTCTCAGGCTCAACAATGATACCAAGTTACGAC
AtGH3.17_GG_Rv	AACAGGTCTCTCTGAAGAATCTAAACCAAGTGG

The size of PCR amplicons was verified using agarose electrophoresis, and PCR products were processed using NucleoSpin® Gel and PCR Clean-up Kit.

The 40 µl of the PCR reaction were mixed with 80 µl of NTI buffer, loaded in the NucleoSpin® Column, and centrifuged for 30 seconds at 11,000 *g*. The flow-through was discarded, and 650 µl of NT3 buffer were added. The sample was centrifuged under the same conditions as in the previous step. To dry silica membrane, centrifugation was performed at 11,000 *g* for one minute to remove the remaining Buffer NT3. All columns were additionally incubated for five minutes at 70 °C. The NucleoSpin column was placed into a new tube and 35 µl of mQH_2O were added to the center of the column, and further incubated for five-minute at RT. The samples were eluted by centrifugation at 11,000 *g* for two minutes.

4.2.6 Electrophoresis

In 80 ml of the 1 % agarose in TAE buffer, 6 µl of GelRed was added. The agarose-GelRed mixture was poured into an electrophoresis gel caster, and wells for sample loading were prepared using a comb. The gel solidifies in approximately 10-15 minutes. The gel was placed into the electrophoresis chamber, and the chamber was filled with 1x TAE buffer. GeneRuler 1 kB Plus DNA Ladder was used as a marker. If a PCR reaction buffer did not contain any loading dye, 1,2 µl of TriTrack dye was added to 10 µl of each sample. The electrophoresis run was performed for 30 minutes at 100V. After 30 minutes, the gel was placed on a UV transilluminator tray, and the GelDoc EZ Gel Documentation system visualized the bands.

The 50x TAE contained 50 mM EDTA dipotassium salt, 2 M Tris-base, and 1 M glacial acetic acid. The pH was adjusted to 8,5 by KOH . TAE working buffer (1x) was prepared by mixing 20 ml of 50x TAE buffer with 980 ml of mQH_2O.

4.2.7 *Bsa*I/T4 ligation

The coding region of *AtGH3.3*, *AtGH3.4* and *AtGH3.17* was inserted into the *pGGC000* GreenGate entry vector by mixing 9 µl of PCR product with 1,5 µl of *pGGC000* plasmid, 1,5 µl of 10x FD Buffer, 1 µl of 10 mM ATP, 1 µl of *Bsa*l and 1 µl T4 DNA ligase. Samples were spun down and incubated in a thermocycler, with cycling parameters described in Table 3.

Table 3. Thermocycler parameters for Bsa1/T4 ligation

Temperature (°C)	**Time (minutes)**	**Cycles (number)**
37	5	50
16	5	50
50	5	1
80	5	1
10	1 hour	

TOP 10 competent cells were transformed with the generated constructs, transformed bacterial cells were plated on LB media supplemented with carbenicillin and plates were incubated at 37 °C. Positive bacterial colonies were selected by colony PCR method (Table 4). Primers used for colony PCR were designed with the forward primer specific for each insert and the T7 reverse primer specific for the vector.

Table 4. The list of primers used for the colony PCR and Sanger sequencing of pDrive and pGGC000 vectors harboring AtGH3.3, AtGH3.4, and AtGH3.17 coding regions.

Primer name	**Primer sequence**
T7_prom_Rv	AATACGACTCACTATAGG
AtGH3.3_Fw	GACGTCCTAACGATCCGTACA
AtGH3.3_Rv	ATAACGGTTAAGCCCAGCATA
AtGH3.4_Fw	CTTCAGGACGTCGGATTCAGA
AtGH3.4_Rv	ACGGTAGAGCCCCGCGTAGGT
AtGH3.17_Fw	TTTCAGAAACAGACCATTCAA
AtGH3.17_Rv	ACAGAGTAGGCGATATTCTAA
SP6_prom_Fw	ATTTAGGTGACACTATAGA

4.2.8 Colony PCR

For colony PCR, eight colonies were picked from selective plates to verify the presence of DNA insert in the plasmid harboring the resistance to the antibiotic. A small portion of the

colony surface was rubbed with the pipette tip. Then, the tip was incubated in the PCR tube containing the PCR reaction mixture: 4 µl of 5x GoTaq Flexi Buffer, 3 µl of $MgCl_2$ (25 $mmol \cdot l^{-1}$), 0,4 µl of dNTPs (10 $mmol \cdot l^{-1}$), 0,1 µl of GoTaq G2 Flexi DNA polymerase, 10,5 µl of mQH_2O and 1 µl of each forward and reverse primers (Table 4). Pipette tips were removed and samples were incubated in a thermocycler following the cycling paramenters described in Table 5.

Table 5. Thermocycler parameters for colony PCR program

Temperature (°C)	Time (min)	Cycles (nr)
95	5	1
95	0:30	30
55	0:30	30
72	4	30
72	5	1
8	15	1

3.2.9 TA cloning

The amplified coding regions of *AtGH3.3*, *AtGH3.4* and *AtGH3.17* genes were cloned into a *pDrive* vector by TA cloning. Approximately 150 ng of amplified DNA (Table 8) was mixed with 1 µl of *pDrive* vector (50 ng/µl) and 5 µl of 2x Ligation Master Mix. The mixture was spun down and incubated at 4 °C for 2 hours. After two hours, TOP10 competent cells were transformed with *pDrive* vectors containing coding regions of *AtGH3.3*, *AtGH3.4* or *AtGH3.17* genes. Transformed competent cells were plated on LB agar plates containing kanamycin, 1 mM IPTG and 20 µg/ml X-Gal.

A colony PCR was carried out to verify the presence of *pDrive* plasmid carrying the desired insert in positive bacterial colonies. Primers used for colony PCR were designed with the forward primer specific for each insert and the T7 reverse primer specific for the vector (Table 4). For positive colonies, liquid cultures were prepared and corresponding plasmids were isolated. The plasmids, along with the primers listed in Table 4, were sent for Sanger sequencing at SEQme in Dobriš, Czech Republic. The sequencing reaction consisted of 5 µl of purified plasmid, 2,5 µl of mQH_2O, and 2,5 µl of the specific primer.

3.2.10 Green Gate reaction

pDrive-AtGH3.3, *pDrive-AtGH3.4*, and *pDrive-AtGH3.17* plasmids were used as entry modules to assembly the final plant transformation vectors. The coding region of every gene was cloned under the control of the corresponding native promoter (pN, previously cloned),

followed by C-terminal GFP tag, plant terminator and plant resistance cassette (Table 6). For the assembly, modules and reagents were mixed in corresponding volumes: 1,5 µl of 10x FD Buffer, 1,5 µl of 10 mM ATP, 1,5 µl of *pGGA-pNAtGH3s* (100 ng/µl), 1,5 µl of *pGGB003* (100 ng/µl), 1,5 µl of *pDrive-AtGH3s* (concentrations are in Table 9), 1,5 µl of *pGGD001* (100 ng/µl), 1,5 µl of *pGGE001* (100 ng/µl), 1,5 µl of *pGGF005* (100 ng/µl), 1 µl of *pGGZ003* (100 ng/µl), 1 µl of *Bsa*I (10 U/µl), 1 µl of T4 DNA ligase (30 U/µl). Afterward, samples were incubated in a thermocycler following the cycling parameters described in Table 3.

Table 6. Description of GreenGate modules

GreenGate modules	Type
pGGA-pNAtGH3s	Native promoter sequence of the specific gene
pGGB003	B-dummy (empty vector if no N-tag is needed)
pDrive-AtGH3s	coding region of the specific gene
pGGD001	GFP-linker
pGGE001	Terminator sequence
pGGF005	Plant resistance cassette
pGGZ003	Destination vector

Ligation reactions were used to transform competent cells, and transformed cells were plated on selective LB agar plates. To verify the correctness of the final assembly, colony PCR was performed on positive bacterial colonies using gene-specific Fw primer and eGFP Rv primer (Table 7). Confirmed positive colonies were grown in liquid LB medium, and corresponding plasmids were isolated. These plasmids, along with primers specified in Table 7, were subsequently sent for Sanger sequencing. The sequencing reaction consisted of 5 µl of purified plasmid, mixed with 2,5 µl of mQH2O and 2,5 µl of the primer.

Table 7. The list of primers used for colony PCR and Sanger sequencing of final transformation vectors

Primer name	Primer sequence
AtGH3.3_Fw	GACGTCCTAACGATCCGTACA
AtGH3.3_Rv	ATAACGGTTAAGCCCAGCATA
AtGH3.4_Fw	CTTCAGGACGTCGGATTCAGA
AtGH3.4_Rv	ACGGTAGAGCCCCGCGTAGGT
AtGH3.17_Fw	TTTCAGAAACAGACCATTCAA
AtGH3.17_Rv	ACAGAGTAGGCGATATTCTAA

Hygr_Fw	CTTGACCAACTCTATCAGAGC
Hygr_Rv	ATCGACCCTGCGCCCAAGCTG
E9_Fw	CGCTATCGAACTGTGAAATGG
E9_Rv	GCCTAGTGAATAAGCATAATGG
LB_T-DNA_Rv	TGGCAGGATATATTGTGGTGTAA
RB_T-DNA_Fw	TTTACCCGCCAATATATCCTGTCA
eGFP_Fw	GCAGCGTGCAGCTCGCCGACC
eGFP_Rv	TTGTACAGCTCGTCCATGCCG
pUBQ10_Fw	AACAATACCCAAAGAGCTC
pUBQ10_Rv	ATACGAAATTGGGATCGAACG

4.2.11 Competent cells transformation

TOP 10 competent cells were thawed on ice and gently mixed with 10 µl of the ligation reaction. After mixing, the tubes were kept in ice for 30 minutes. Afterward, the tube containing the mixture was heated at 42 °C for 45 seconds, placed on ice for two minutes, and resuspended with 800 µl of liquid LB medium. Bacteria were grown at 37 °C in a shaking incubator for 60 minutes. The competent cells were pelleted at 2000 *g* for 5 minutes. About 700 µl of supernatant was discarded, the remaining 100 µl was used to resuspend pellet and plated to LB agar plates supplemented with antibiotics. The plates were incubated at 37 °C overnight to allow bacterial growth. Single bacterial colonies were used for colony PCR and plasmid isolation.

Agrobacterium-competent cells were transformed by electroporation. Electroporation consisted of combining 50 µl of electrocompetent agrobacteria with 1 µl of either *pNAtGH3.3:GH3.3cdr:GFP:HygR*, *pNAtGH3.4:GH3.4cdr:GFP:HygR* or *pNAtGH3.17:GH3.17cdr:GFP:HygR* vectors. The mixture was transferred to an ice-cooled cuvette and subjected to electroporation at 1800 V. The cells were transferred to 1,5 ml tube with 1 ml of LB medium and incubated for 3 hours on a shaker at 28 °C. Subsequently, bacterial cells were plated on LB agar plates containing antibiotics (*i.e.*, spectinomycin, rifampicin, gentamicin, and tetracycline). After a 48-hour incubation at 28 °C, individual colonies were grown in liquid LB selective medium containing identical antibiotic mixture as mentioned above. A 10-ml liquid culture was prepared and incubated on a shaker for 24 hours at 28 °C.

4.2.12 Floral dip method

Four-six weeks old *Arabidopsis* plants, ecotype Columbia (Col-0), still carrying unopened floral buds, were used for floral dip transformation. *Agrobacterium* cells harboring *pNAtGH3.3:GH3.3cdr:GFP:HygR*, *pNAtGH3.4:GH3.4cdr:GFP:HygR* or *pNAtGH3.17:GH3.17cdr:GFP:HygR* were grown overnight at 28 °C, 130 rpm in 200 ml of LB medium supplemented with spectinomycin, rifampicin, gentamycin, and tetracycline. The next day, the bacterial cultures were pelleted at 3000 *g* for 15 minutes, and pellet was resuspended in a 5% sucrose solution containing 0,03% Silwet L-77. Afterward, floral buds were dipped in the mixture for two minutes. Transformed plants were kept in the dark overnight. The next day plants were transferred to a growth chamber and grown under long-day conditions (16 h photoperiod; 22 ± 1 °C), and the floral dip was repeated after five days. Once siliques were dry, seeds were harvested.

4.2.13 Selection of primary transformants (T1)

Seeds were sterilized by chlorine gas method. Tubes containing approximately 200 mg of seeds were placed with an open lid in a desiccator, and exposed to a mixture of 15 ml of mQH_2O, 25 ml of bleach (NaClO) and 10 ml of 37% HCl for 2 hours. Sterilized seeds were transferred to the flowbox, and 1 ml of sterile mQH_2O was added to each tube. Next, water was removed, 0,1 % agarose solution was added, and seeds were sowed on hygromycin B-containing half-strength MS plates. Plates were sealed and kept in the dark at 4 °C for 48 hours for stratification. Seeds were germinated under long-day conditions (16 h photoperiod; 22 ± 1 °C) in a growth cabinet. After ten days, the presence of hygromycin-resistant transformants was inspected. Hygromycin-resistant seedlings were larger than non-resistant seedlings, as hygromycin causes growth retardation of sensitive seedlings. Selected resistant seedlings were transferred to the soil, and grown under long-day conditions. Collected seeds represented the first generation of transformants (T_1).

4.2.14 Confocal microscopy

GFP signal from selected T_1 hygromycin-resistant seedlings harboring *pNAtGH3.4:GH3.4cdr:GFP:HygR* or *UBQ10:AtGH3.3-GFP:HygR* (positive control), and *A. thaliana* (Col-0) (negative control) was inspected by confocal microscopy. Ten-day-old seedlings grown under long-day conditions (16 h photoperiod, 22 ± 1 °C) were mounted on a glass slide with approximately 150 µl of mQH_2O and with a coverslip. Visualization was conducted using a Zeiss confocal microscope with a 20x objective. The fluorescent signal was visualized as eGFP (excitation wavelength 488 nm, emission wavelength 509 nm).

5. Results

5.1 Genomic DNA extraction and PCR amplification

Genomic DNA extraction is a method aimed at isolating DNA from other cellular components. The isolated gDNA was quantified using a micro-volume Nanodrop spectrophotometer (Table 8). “gDNA_1” and “gDNA_2” samples were extracted by E.Z.N.A. ® Plant DNA kit, while “gDNA_3” and “gDNA_4” samples were extracted by genomic DNA extraction buffer.

The $A_{260/280}$ and $A_{260/230}$ values are critical to determine the DNA quality, as they refer to DNA purity and contaminants presence. The A260/280 ratio is used to evaluate residual protein contamination from the nucleic acid isolation process, as nucleic acids absorb at 260 nm and proteins absorb at 280 nm. Absorption at 230 nm can indicate contamination by organic compounds such as phenolate ions or thiocyanates. An $A_{260/280}$ ratio of approximately 1,8 is considered indicative of "pure" DNA. Expected 260/230 absorbance values would typically range from 2,0 to 2,2.

The highest DNA concentrations were obtained for DNA extracted using genomic DNA extraction buffer (gDNA_3 = 231,6 ng/µl, gDNA_4 = 114,4 ng/µl), while “gDNA_1” and “gDNA_2”, isolated with E.Z.N.A. ® Plant DNA kit, exhibited approximately three times lower concentrations. The “gDNA_2” sample displayed the best $A_{260/280}$ ratio with a value of 1,74, whereas the lowest ratio was observed for “gDNA_4” with 1,51. The $A_{260/230}$ ratio values were relatively low for all samples, ranging from 0,22 for “gDNA_4" to 1,3 for “gDNA_2”.

Table 8. gDNA concentrations and purity, isolated from A.thaliana Col-0 plants.

Name	Concentration (ng/µl)	A260/280	A260/230
gDNA_1	50,2	1,87	0,59
gDNA_2	78,7	1,74	1,30
gDNA_3	231,6	1,65	0,26
gDNA_4	114,4	1,51	0,22

PCR amplification was carried out to amplify the coding regions of *GH3.3*, *GH3.4*, *GH3.17* genes. Primers contained *Bsa*I restriction sites, and the stop codon was removed for the reverse primers (Figure 5). To check the integrity of the isolated DNA, electrophoresis

on agarose gel was performed (Figure 6). The expected sizes of the *GH3.3*, *GH3.4*, and *GH3.17* amplicons were 2410 bp, 2154 bp, and 2446 bp, respectively. Figure 6 displays bands corresponding to the estimated sizes of the DNA amplicons. However, there are also additional bands, which could correspond to non-specific amplification, DNA contamination, or other experimental artifacts.

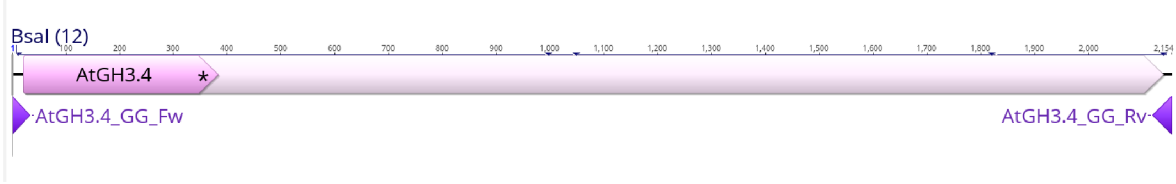

Figure 5. Representation of the GH3.4 PCR product, created in Geneious Prime. Overhanging primers were used for the addition of the BsaI restriction site to both ends of the gene.

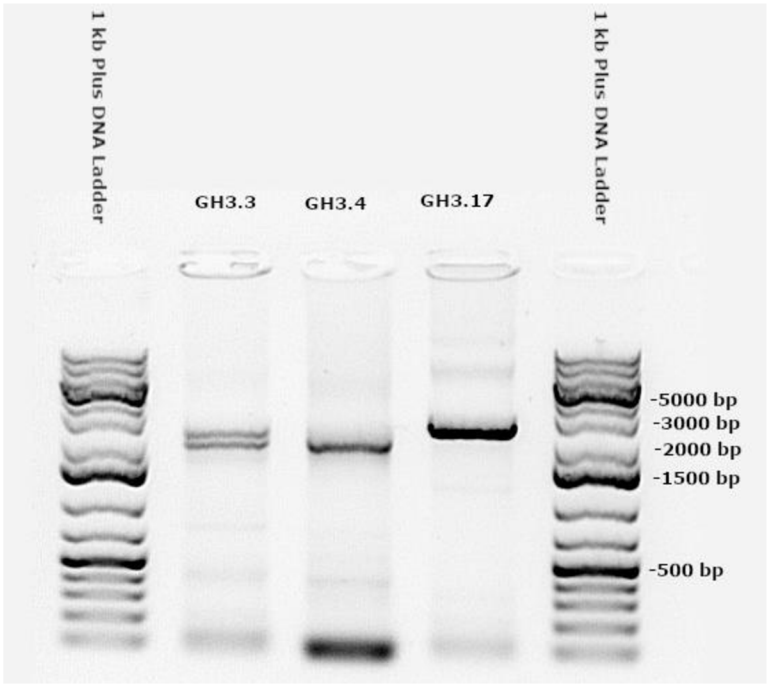

Figure 6. Agarose gel electropherogram of amplified coding regions. Lane 2, AtGH3.3; Lane 3, AtGH3.4; Lane 4, AtGH3.17. Lane 1 and 5, 1 kB Plus DNA Ladder (marker).

5.2 *Bsa*I/T4 ligation in *pGGC000* Green Gate module

Plasmid *pGGC000* carries resistance to ampicillin and was used as the GreenGate module to carry inserts. Insertion of the three genes *GH3.3, GH3.4, GH3.17* in respective vectors was performed by *Bsa*I/T4 ligation (Attachments 1-2, Figure 7).

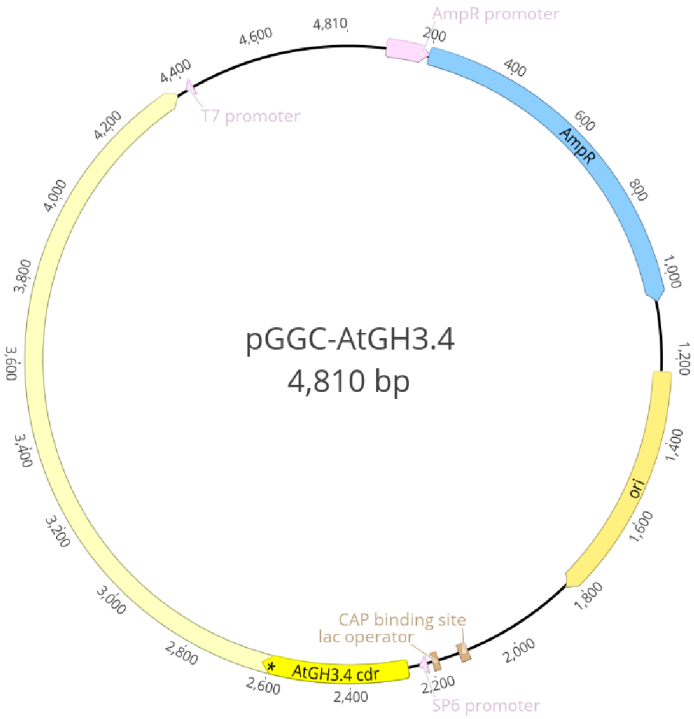

Figure 7. Representation of pGGC000 plasmid with inserted AtGH3.4 gene, created in Geneious Prime. The plasmid is 4,810 bp and carries the origin of replication ORI, lac operator (required for lactose metabolism), CAP binding site (positive regulator of lac operon), SP6 promoter, AtGH3.4 inserted gene sequence, T7 promoter, and ampicillin resistance cassette.

Colony PCR was conducted on transformed bacteria to confirm the presence of the target gene in the recombinant plasmid. Results of colony PCR were visualized by electrophoresis (Figure 8). The expected size of the amplicons was around 2000 bp. Multiple bands corresponding to the expected size were detected for all three constructs on the agarose gel. Besides them, there were additional bands around 5000 bp and 500 bp. However, Sanger sequencing confirmed unsuccessful transformation.

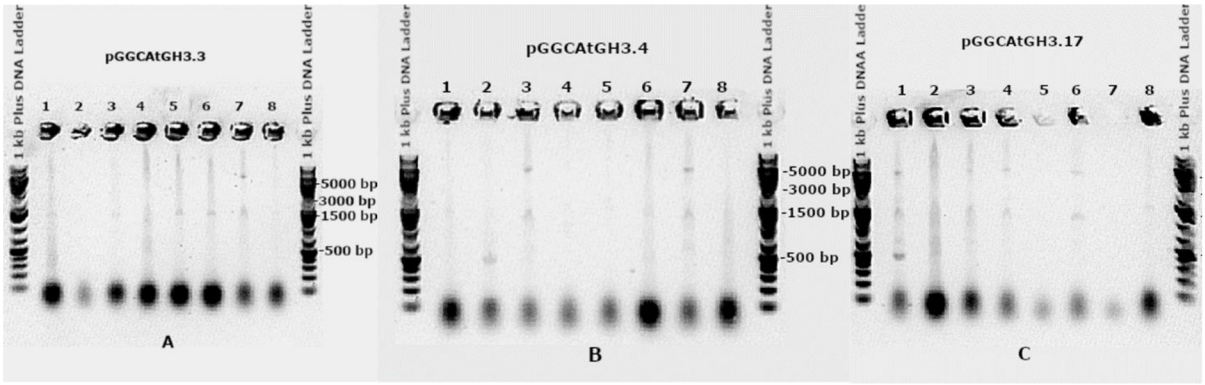

Figure 8. Agarose gel electropherograms of pGGCAtGH3.3 (A), pGGCAtGH3.4 (B), and pGGCAtGH3.17 (C) PCR amplicons. In each electropherogram, the 1 kB Plus DNA Ladder (marker) was loaded in the first and last lanes. Lanes 2-9 exhibit colony-PCR products obtained from transformed TOP 10 E.coli colonies grown on LB medium.

5.3 TA cloning with *pDrive*

TA cloning method is used to insert amplified DNA fragments harboring A-overhangs directly into a linearized vector. Coding regions of three distinct genes *AtGH3.3, AtGH3.4,* and *AtGH3.17* were inserted into *pDrive* vectors (Attachments 3-4, Figure 9).

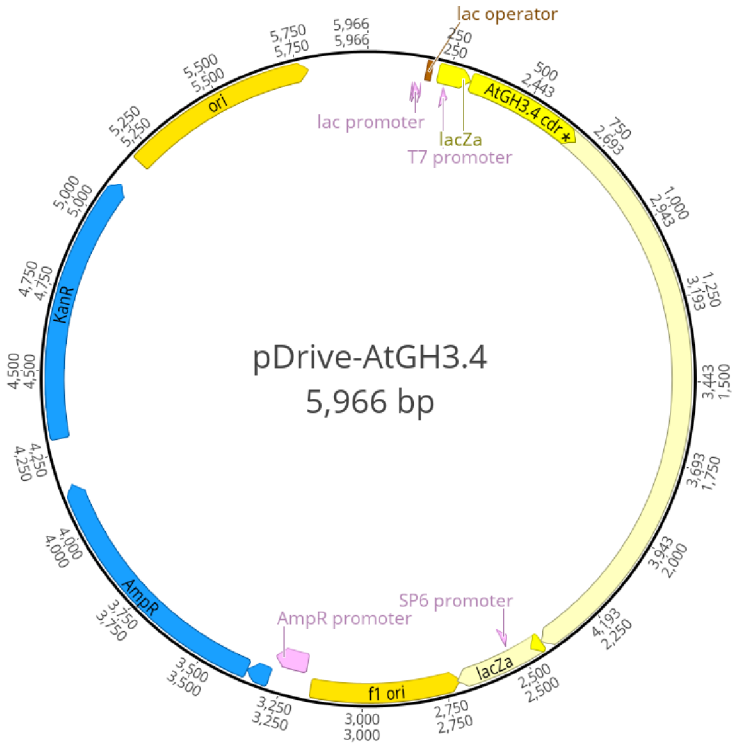

Figure 9. Representation of pDrive vector with inserted AtGH3.4 gene, created in Geneious Prime. The plasmid is 5,966 bp and carries the origin of replication ORI, f1 ORI, lac operator with LacZa (required for lactose metabolism), CAP binding site (positive regulator of lac operon), SP6 promoter, AtGH3.4 inserted gene sequence, T7 promoter, ampicillin, and kanamycin resistance

To verify the presence of target genes in a plasmid, transformed bacteria were subjected to colony PCR. Eight white colonies from every construct (*pDrive-AtGH3.3*, *pDrive-AtGH3.4*, *pDrive-AtGH3.17*) were inspected (Figure 10). Results of colony PCR were visualized by electrophoresis (Figure 11). The transformation was successful, as amplicons of the expected size (around 2000 bp) were obtained from all picked colonies for each construct. However, colonies 3 and 4 from *pDrive-AtGH3.17*-transformed *E.coli* population did not return a clear amplicon. The electropherogram of *pDrive-AtGH3.*3 (Figure 11A)

illustrated several additional bands around 1000 bp. The first positive colony was selected for further experiments for all three constructs.

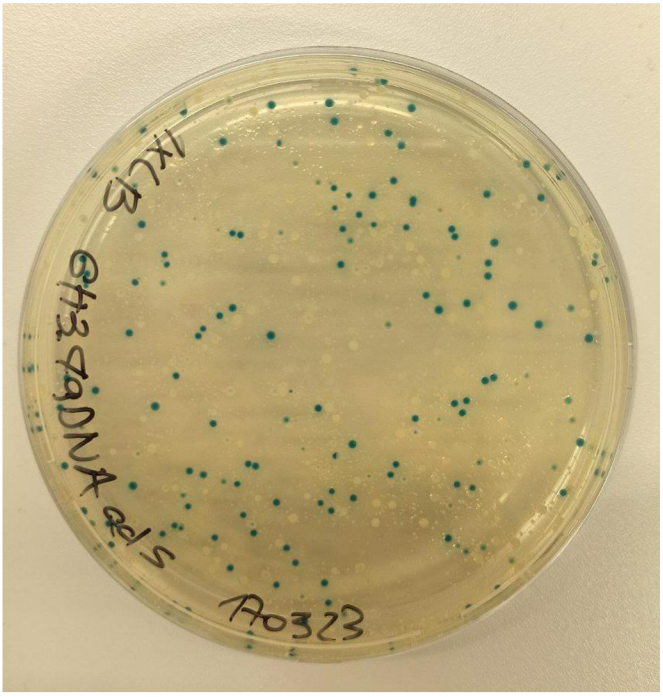

Figure 10. The example of blue-white screening for transformed TOP10 competent cells carrying pDrive-AtGH3.4. The colonies carrying recombinant protein appear white.

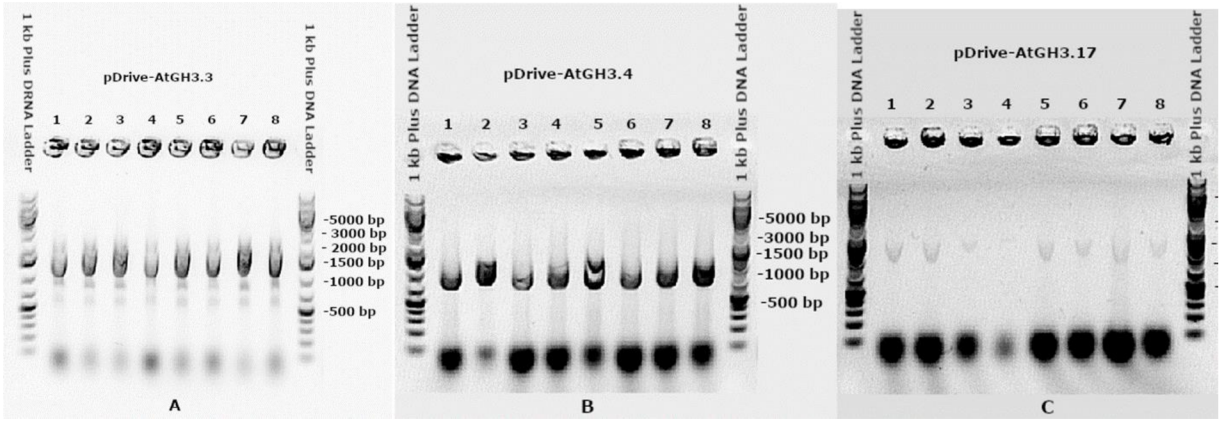

Figure 11. Agarose gel electropherograms of pDrive-AtGH3.3 (A), pDrive-AtGH3.4 (B), and pDrive-AtGH3.17 (C) PCR amplicons. In each electropherogram, the 1 kB Plus DNA Ladder (marker) was loaded in the first and last lanes. Lanes 2-9 show colony-PCR products obtained from transformed TOP 10 E.coli colonies grown on LB medium.

The DNA concentration and purity of plasmids containing the gene inserts was quantified to ensure optimal sequencing results (Table 9). The *pDrive-AtGH3.3* plasmid exhibited the highest concentration at 409,2 ng/µl, whereas the lowest concentration was observed for *pDrive-AtGH3.17* at 253,3 ng/µl. In terms of purity, all three vectors displayed an average $A_{260/280}$ ratio of 1,85, indicating their high purity. The *pDrive-AtGH3.3* plasmid also demonstrated the best $A_{260/230}$ purity ratio.

Table 9. Recombinant pDrive vectors' concentrations and purity

Name	Concentration (ng/µl)	A260/280	A260/230
pDrive-AtGH3.3	409,2	1,85	2,20
pDrive-AtGH3.4	342,5	1,87	2,32
pDrive-AtGH3.17	253,3	1,84	2,19

Sequencing results confirmed the presence of the target gene sequences within the recombinant plasmids without nucleotide alterations, thereby validating the efficiency of TA cloning (Attachment 5-7). Figure 12 illustrates sequencing results of the *GH3.4* coding region, inserted to the *pDrive* vector.

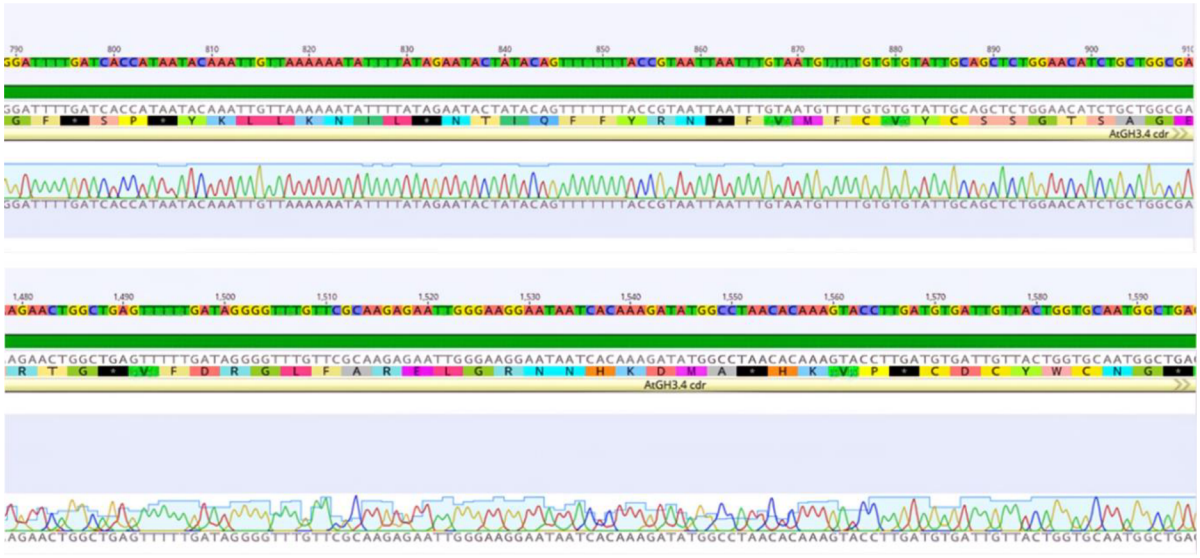

Figure 12. Representation of the GH3.4 gene sequence inserted into pDrive vector, created in Geneious Prime.

5.4 Green Gate cloning

Green Gate cloning is a technique that allows assembling several DNA elements into a single destination vector. Six entry vectors (*pGGA-pNAtGH3s*, *pGGB003*, *pDrive-AtGH3s*, *pGGD001*, *pGGE001*, *pGGF005*) were used in a reaction with the destination vector *pGGZ003* carrying spectinomycin resistance to generate the final assembly vector (Attachments 8-9, Figure 13).

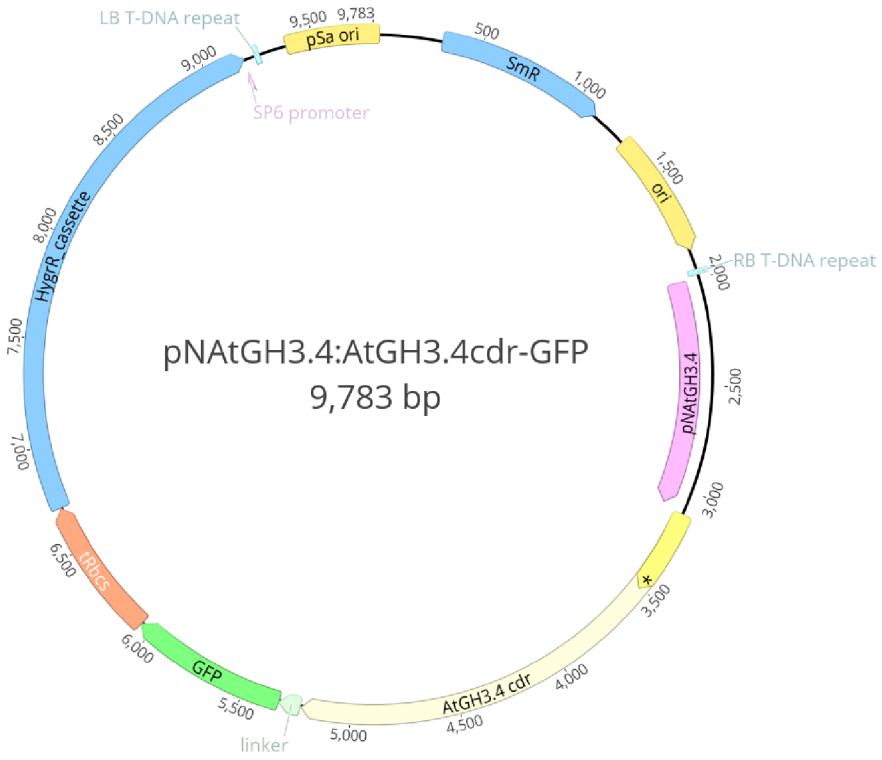

Figure 13. Representation of pNAtGH3.4:AtGH3.4cdr-GFP vector, created in Geneious Prime. The plasmid is 9,783 bp and carries origin of replication ORI, native promoter pNAtGH3.4, AtGH3.4 inserted gene sequence, GFP sequence with a linker, tRbcs (terminator), HygrR (hygromycin resistance cassette), pSa ori (origin of replication for bacteria), SmR (spectinomycin resistance cassette)

To confirm the correct assembly of the plant transformation vector, colony PCR was carried out. Eight colonies from each construct (*pNAtGH3.3:AtGH3.3cdr-GFP*, *pNAtGH3.4:AtGH3.4cdr-GFP*, *pNAtGH3.17:AtGH3.17cdr-GFP*) were selected. The results of the colony PCR were visualized by electrophoresis (Figure 14). The expected amplicon size was approximately 2000 bp for all three constructs, and amplicons of this size indicated possible successful assembly. Figure 14 shows that each colony from each construct returned a band of expected size, confirming the efficiency of the Green Gate cloning method. For further experiments the first positive colony of each construct was inoculated, plasmid was isolated and sent for sequence validation.

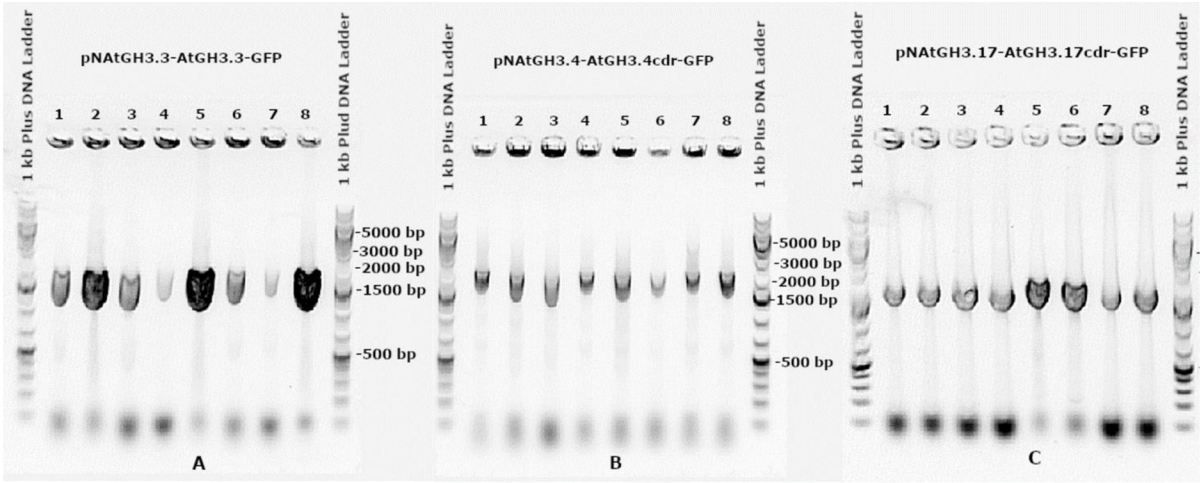

Figure 14. Agarose gel electropherograms of pNAtGH3.3:AtGH3.3cdr-GFP (A), pNAtGH3.4:AtGH3.4cdr-GFP (B), and pNAtGH3.17:AtGH3.17cdr-GFP (C) PCR amplicons. In each electropherogram, the 1 kB Plus DNA Ladder (marker) was loaded in the first and last lanes. Lanes 2-9 exhibit colony-PCR products obtained from transformed TOP 10 E.coli colonies grown on LB medium.

Concentrations and purity of recombinant vectors pNAtGH3.3:AtGH3.3cdr-GFP, *pNAtGH3.4:AtGH3.4cdr-GFP*, and *pNAtGH3.17:AtGH3.17cdr-GFP* were validated to ensure optimal sequencing results (Table 10). The *pNAtGH3.3:AtGH3.3cdr-GFP* vector had the highest concentration at 927,6 ng/µl, while the *pNAtGH3.4:AtGH3.4cdr-GFP* vector had the lowest concentration at 475,7 ng/µl. The purity ratios for all three constructs showed minimal deviation, with an average $A_{260/280}$ value of 1,85, and an average $A_{260/230}$ value of 2,3.

Table 10. Final Green Gate recombinant pGGZ003 vectors' concentrations and purity

Name	Concentration (ng/µl)	A260/280	A260/230
pNAtGH3.3:AtGH3.3cdr-GFP	927,6	1,87	2,34
pNAtGH3.4:AtGH3.4cdr-GFP	475,7	1,90	2,40
pNAtGH3.17:AtGH3.17cdr-GFP	502,0	1,77	2,10

Sequencing results confirmed the correctness of the assembly of all modules and the sequence (Attachments 10-21). Figure 15 illustrates sequencing results of the *pNAtGH3.4:AtGH3.4cdr-GFP* vector, highlighting the correct assembling of the *GH3.4* coding region and GFP coding sequence.

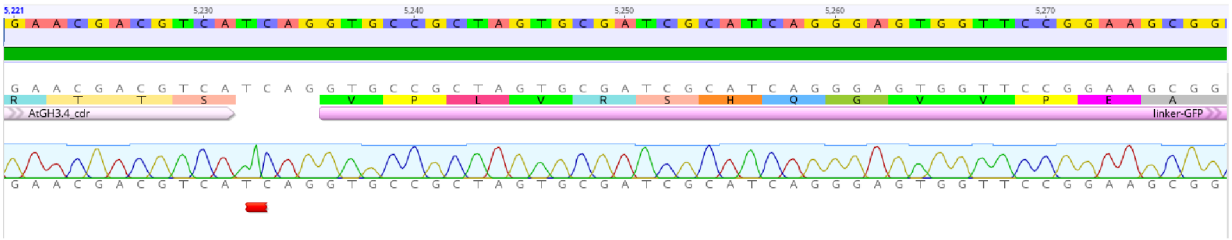

Figure 15. Representation of the GH3.4 gene sequence, assembled to a GFP sequence via the GFP linker, created in Geneious Prime.

5.5 Selection of transformants

Selection of transformed seeds was performed on ½ MS plates supplemented with 30 µg/ml hygromycin B. After a ten-day growth period, the identification of hygromycin-resistant seedlings was based on cotyledon size and vigor. Seedlings exibiting robust growth and larger cotyledons were considered as transgenic. Larger seedlings were observed in *pNAtGH3.4:AtGH3.4cdr-GFP* plant population. These seedlings were transferred to the soil for continued growth and development (Figure 16). In contrast, no transformants were detected for the plants transformed with *pNAtGH3.3:AtGH3.3cdr-GFP* and *pNAtGH3.17:AtGH3.17cdr-GFP*. The seeds collected from this initial screening give rise to the first generation of transformants T_1.

Figure 16. Selection of T_0 transformants on ½ MS round plates supplemented with 30 µg/ml hygromycin B. Transformant harboring pNAtGH3.4:AtGH3.4cdr-GFP construct is highlighted by an orange circle. The transgenic seedling displayed a different morphology to non-transformant seedlings, such as larger size, hypocotyl, and cotyledon growth.

5.6 Confocal imaging

Confocal microscopy was used to visualize and compare the fluorescence signals from the negative control Col-0, a transgenic line expressing the *pNAtGH3.4:AtGH3.4cdr-GFP*, and the positive control *UBQ10::AtGH3.3-GFP* (Figure 17). All images were obtained using uniform imaging parameters to ensure comparability across the samples.

The GFP fluorescence signal was detected in the positive control, confirming the successful expression of the transgene and validating the reliability of the imaging setup. In contrast, the negative control samples did not show any GFP fluorescence signal, indicating the absence of the transgene and the specificity of the observed signal.

Confocal imaging of the T_1 generation of the *pNAtGH3.4:AtGH3.4cdr-GFP* transgenic line revealed a fluorescence profile similar to the negative control, meaning that the GFP fluorescence was not detected in the transgenic line.

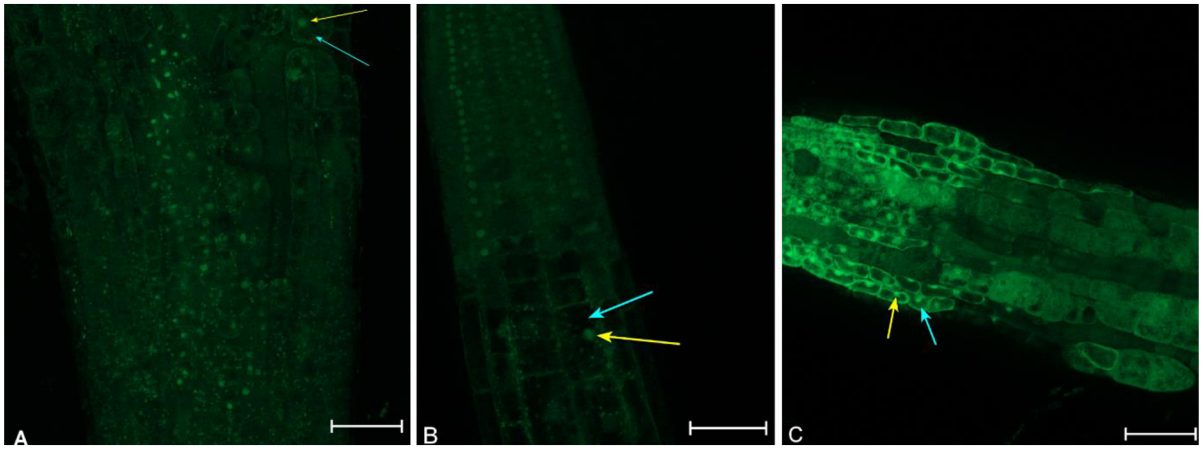

Figure 17. Confocal images from negative Col-0 control (A), pNAtGH3.4:AtGH3.4cdr-GFP (B), and positive control UBQ10-GH3.3-GFP (C) in 10-day seedlings of A.thaliana. Observed with standard settings at 20 times magnification. The yellow arrow (↑) indicates nucleus, blue arrow (↑) indicates cytosol. Scale bar is 50 µm.

6. Discussion

Auxin is an essential plant hormone, whose metabolism is tightly regulated by several mechanisms, such as biosynthesis, degradation, and inactivation. This thesis focused on three *Arabidopsis* proteins belonging to the GRETCHEN HAGEN 3 family that directly play a role in the conjugation of auxin to amino acids, which leads to temporary auxin inactivation[87]. Since the first *GH3* gene was isolated from soybean in 1984[88], not all the genes from this family have been fully characterized. This diploma thesis contributed to the creation of three plant transformation vectors containing the coding regions of three *Arabidopsis* genes *GH3.3*, *GH3.4*, and *GH3.17*. These genes were placed under their corresponding native promoters, followed by a C-terminal GFP tag, plant terminator, and plant resistance cassette. Those vectors were used to transform *A.thaliana* Col-0 plants, leading to a selection of transformed progeny for the *pNAtGH3.4:AtGH3.4cdr-GFP* line. The transgenic line underwent confocal microscopy analysis, providing data that might contribute to understanding the native localization of the GH3.4 protein in *Arabidopsis*.

In the first part of this thesis, the experiments were performed to prepare plant transformation vectors. The first step was to extract the gDNA from *Arabidopsis* leaves using gDNA extraction buffer. Although the extracted DNA had sufficient concentrations (231,6 ng/µl and 114,4 ng/µl), the purity of extracted DNA was low and DNA amplification of selected gene region did not lead to a result. According to P. Desjardins[89], pure nucleic acids usually have a 260/280 ratio of around 2.0 and 260/230 typically ranges from 1.8 to 2.2. The sufficient purity of extracted DNA was accomplished by using the E.Z.N.A.® Plant DNA Kit (Table 8). DNA extracted by this method was used in downstream applications.

Onwards, extracted gDNA was used as a template for PCR amplification of the coding regions of *GH3.3*, *GH3.4* and *GH3.17* genes. The genes of interest were amplified using overhanging primers that contained *Bsa*I recognition sites (Figure 5). Additionally, for reverse primers, the stop codon was removed, to ensure GH3-GFP fusion proteins in frame translation. PCR products were checked *via* agarose gel electrophoresis, which visualized bands corresponding to the expected sizes of the DNA amplicons (Figure 6). Amplified DNA was used for the *Bsa*I/T4 ligation cloning with a *pGGC000* vector. This entry vector advantageously had T7 and SP6 bacteriophage promoters and *lac* operon for the blue-white screening[57] (Attachments 1-2, Figure 7). The prepared vectors were first inserted into TOP 10 *E.coli,* and transformation was verified by colony PCR and sequencing. The amplicons were expected to be roughly 2000 bp. On the agarose gel, bands of the expected size were observed in all three cases (Figure 8). Besides bands of expected sizes, additional bands

around 5000 bp and 500 bp were also observed on electropherograms. Those bands could appear due to incomplete DNA amplification cycles, which can be the result of shorter DNA fragments, such as primer dimers, heteroduplexes, chimeras or hairpin structures[90]. Another possible reason of unspecific bands is DNA thermal damage[91]. There are three main negative effects of thermal damage: A+G depurination, the oxidation of guanine to 8-oxoG, and cytosine deamination to uracil. In addition to causing incorrect nucleotide incorporation during replication, high temperatures increase DNA degradation, resulting in lower yield[91]. Sanger sequencing confirmed that the transformation was unsuccessful. During the second repetition of the same experiment, troubleshooting steps were undertaken. This included optimizing the concentration of the gDNA amplicon, using unopened buffers, and preparing fresh solutions (dNTPs). Additionally, a different competent cell strain for transformation was tested; TOP 10 was used for the first trial, while NEB5α for the second attempt. The troubleshooting steps did not have an effect on the outcome of the cloning. The exact reason for the unsuccessful outcome remained unclear. The most frequent reasons of unsuccessful cloning are damaged template or a template with low purity[92], irrelevantly chosen polymerases and restriction endonucleases[93], long sequence of the cloning gene and repeated sequences[94].

Following the first unsuccessful cloning attempt, a different strategy was adopted. A TA cloning with a *pDrive* vector was tested. This vector also had T7 and SP6 bacteriophage promoters and *lac* operon, but contained kanamycin and ampicillin resistance cassettes (Attachments 3-4, Figure 9). Taq-polymerase amplified coding regions of three genes with T-overhangs were inserted into *pDrive* vectors with complementary A-overhangs. The ligation products were then transformed into the TOP 10 competent cells, followed by blue-white screening. Screening divided all bacterial colonies into two groups: white - recombinant ones and blue – non-recombinant ones (Figure 10). White colonies were picked for colony PCR. Results of the colony PCR were visualized by agarose gel electrophoresis, and amplicons were observed as bands around 2000 bp for each vector (Figure 11). Additional bands of unexpected size were considered impurities or false primers' aligning[95]. Sanger sequencing confirmed the successful transformation (Attachments 5-7, Figure 12).

The subsequent step involved GreenGate cloning method, which was chosen by efficiency in saving time and effort, since both digestion and ligation steps carry out simultaneously in a single-tube reaction[57]. Comparing to conventual cloning methods, such as traditional restriction enzyme cloning, Gateway cloning or TOPO cloning, GreenGate allows to assemble six modules at the same time with no need to purify insert DNA fragments and vector[57]. GreenGate was successfully used in gene expression analysis[96],

protein subcellular localization[97], and generating transgenic lines[98]. The *pDrive* vectors containing the coding regions of either *GH3.3*, *GH3.4* or *GH3.17* were used as alternative module C and assembled with *pGGA-pNAtGH3s* (native promoter for each gene), *pGGB003*, *pGGD001* (GFP tag), *pGGE001*, and pGGF005 into the *pGGZ003* destination vector using *Bsa*I/T4 ligation cloning[57] (Attachments 8-9, Figure 13). TOP 10 competent cells were transformed with the final assembly vectors *pNAtGH3.3:AtGH3.3cdr-GFP*, *pNAtGH3.4:AtGH3.4cdr-GFP*, and *pNAtGH3.17:AtGH3.17cdr-GFP*, and subsequently subjected to colony PCR. Electrophoresis visualized the colony PCR results and confirmed the presence of the expected bands of 2000 bp for each vector (Figure 14). Three final vectors were sent for sequencing, which confirmed the correct assembly and sequence of *pNAtGH3.3:AtGH3.3cdr-GFP*, *pNAtGH3.4:AtGH3.4cdr-GFP*, *pNAtGH3.17:AtGH3.17cdr-GFP* (Attachments 10-21, Figure 15).

Three final vectors were transformed to the *Agrobacterium* electrocompetent cells. Plant transformation mediated by *Agrobacterium* through the floral-dip method is a widely used plant transformation technique, characterized by its simplicity, high-efficiency with reduced time and non-destructivity for plants[99]. Thus, transformation with the generated constructs of Col-0 *Arabidopsis* plants with unopened floral buds (4-6 weeks) was performed by floral dip. Seeds resulting from this transformation belonged to the T_0 generation and underwent a selection process, based on hygromycin-B antibiotic resistance. The genetically modified seedlings distinguished from non-transgenic seedlings by their larger size, hypocotyl and cotyledon growth, and overall resilience[100](Figure 16). Transformation on *Arabidopsis* with the the *pNAtGH3.4:AtGH3.4cdr-GFP* vector was successful, T_0 transgenic seedlings were selected and cultivated until the subsequent T_1 generation of seeds was collected. *Arabidopsis* plants with inserted *pNAtGH3.3:AtGH3.3cdr-GFP* and *pNAtGH3.17:AtGH3.17cdr-GFP* vectors did not contain any recombinant seedlings, so thetransformation process was repeated. Despite several floral dip repetitions, these lines failed to produce transgenic progeny. Study of the S. De Buck[101] states that floral dip transformation yields an average 4-6 recombinant T-DNA copies *per* transformant. Additionally, transgene after transformation can undergo different unexpected modifications, leading to gene silencing. The most well-studied silencing is homology-dependent gene silencing (HDGS)[102]. This phenomenon suggests that homology between the transgene, and either the native gene or another transgene leads to gene silencing. All of the above together with bad plant condition before transformation, such as weak or stressed plants, can be considered as the reason of the lack of the transgenic lines for *pNAtGH3.3:AtGH3.3cdr-GFP* and *pNAtGH3.17:AtGH3.17cdr-GFP* vectors.

Inspection of the GFP signal in the generated transgenic line by confocal laser scanning microscopy represented the last step of this thesis. Detection was performed with 10-day *Arabidopsis* seedlings of T_1 generation expressing *pNAtGH3.4:AtGH3.4cdr-GFP*. As positive control, *UBQ10::AtGH3.3-GFP* stable transgenic line was used, and as negative control *Arabidopsis* Col-0 was used (Figure 17). Highly intense GFP signal in roots was observed in the positive control, confirming the overexpression of the fusion protein due to constitutive promoter. Constitutive promoters ensure stable gene expression consistently across different tissues and developmental stages. They are especially beneficial in fluorescent microscopy of transgenes, as they provide prolonged expression of the fluorescently-tagged proteins[103]. Alongside, negative control didn't show any specific fluorescence signal besides autofluorescence, which is consistent with the expected result because the plants did not contain any GFP tag. Autofluorescence is the natural ability of certain biomolecules to emit fluorescent light when excited by specific wavelengths of light. Chlorophyll and multiple cell wall components can exhibit autofluorescence after excitation by ultraviolet, blue or green light[104]. The T_1 generation of plants transformed with the *pNAtGH3.4:AtGH3.4cdr-GFP* vector did not show any fluorescence signal besides autofluorescence, similar to the negative control, suggesting a lack of GFP signal in the transformed plant line. Generally, GFP signal may not be observed under a native promoter due to low protein expression levels, inappropriate observation timing and protein localization, unexpected protein post-translational modifications, or limitations of detection methods[105]. According to the *Arabidopsis* gene expression map (*Arabidopsis* eFP Browser)[106], the expression levels of the GH3.4 protein significantly vary across different stages of seed development. The main purpose of this diploma thesis was to inspect the localization of GH3s proteins, which was done on 10-day seedlings. At this developmental stage, GH3.4 protein expression in the root is lower compared to other stages. This could explain the low GFP signal detection by confocal microscopy, even though the seeds harbored a recombinant vector with a GFP tag. However, the *pNAtGH3.4:AtGH3.4cdr-GFP* transgenic line might have an important role in studying the key pathways of *Arabidopsis* and its response under different conditions. Changes in hormone levels during stress (surplus/the lack of water, chemicals, etc.) trigger the expression of other proteins in the plant that should help it survive the adverse conditions. Recent studies on ARFs group[107] of proteins and CLE9 peptide[108] show that they change their expression levels as a response to gradient concentration of abscisic acid, hydrogen peroxide, nitric oxide, and salt (NaCl) treatments. Using the tagged GH3.4 protein, it is possible to track its expression levels under

different conditions, which might extend the understanding of IAA metabolism and the possible interaction with other plant hormones.

7. Conclusion

In the theoretical part of the diploma thesis, in-depth literature review was conducted on auxins, particularly on biosynthesis, degradation, and inactivation mechanisms mediated by GH3s enzymes. The latter part of the theoretical section mainly explored cloning strategies and confocal laser microscopy.

The experimental section consisted of several steps. The initial step involved extracting gDNA from *Arabidopsis* using the E.Z.N.A.® Plant DNA Kit and a gDNA extraction buffer. It was experimentally demonstrated that the E.Z.N.A.® Plant DNA Kit yielded better results compared to the gDNA extraction buffer. The main goal of the subsequent step was to incorporate three *Arabidopsis* genes (*GH3.3*, *GH3.4*, *GH3.17*) into the *pGGC000* Green Gate module using *Bsa*I/T4 ligation.

After an unsuccessful transformation attempt, the cloning method was changed to TA cloning with a *pDrive* vector. This change led to the creation of three Green Gate entry vectors: *pDrive-AtGH3.3cdr*, *pDrive-AtGH3.4cdr*, and *pDrive-AtGH3.17cdr*. Subsequently, those vectors served as modules for the creation of final GreenGate assembly vector with a GFP tag: *pNAtGH3.3:AtGH3.3cdr-GFP*, *pNAtGH3.4:AtGH3.4cdr-GFP*, *pNAtGH3.17:AtGH3.17cdr-GFP*. The *Arabidopsis* transformation was achieved through the *Agrobacterium*-mediated floral dip method, with *Agrobacterium* carrying the corresponding vectors. The experiment succeeded in creation of a *pNAtGH3.4:AtGH3.4cdr-GFP Arabidopsis* transgenic line. No transgenic lines were obtained with the two other vectors.

Ten-day-old seedlings from the T_1 generation of *Arabidopsis* expressing *pNAtGH3.4:AtGH3.4cdr-GFP*, along with the positive control *Arabidopsis* expressing *UBQ10::AtGH3.3-GFP* and the negative control *Arabidopsis* Col-0, were used for GFP signal inspection by laser confocal microscopy. The transgenic line expressing *pNAtGH3.4:AtGH3.4cdr-GFP* did not exhibit any fluorescence, and its lack of signal was identical to that of the negative control. However, this line may be used for further studies related to IAA metabolism, such as for investigating changes in GH3.4 expression in response to specific hormones or alternated biotic and abiotic conditions.

Two additional vectors were designed to be used for plant transformation, and further protein localization driven by native promoter.

8. Literature

(1) Davies, P. J. (1987). Plant Hormones and Their Role in Plant Growth and Development. Leiden, Boston, MA: Martinus Nijhoff Publishers, 681 pp. http://dx.doi.org/10.1007/978-94-009-3585-3

(2) Gomes, G. L. B.; Scortecci, K. C. (2021) Auxin and Its Role in Plant Development: Structure, Signalling, Regulation and Response Mechanisms. *Plant Biology*. *23* (6), 894–904. https://doi.org/10.1111/plb.13303.

(3) Du, M.; Spalding, E. P.; Gray, W. M. (2020) Rapid Auxin-Mediated Cell Expansion. *Annual Review of Plant Biology*. 71 (1), 379–402. https://doi.org/10.1146/annurev-arplant-073019-025907.

(4) Cao, X.; Yang, H.; Shang, C.; Ma, S.; Liu, L.; Cheng, J. (2019) The Roles of Auxin Biosynthesis YUCCA Gene Family in Plants. *International Journal of Molecular Sciences.* 20 (24), 6343. https://doi.org/10.3390/ijms20246343.

(5) Schneider, E. A.; Kazakoff, C. W.; Wightman, F. (1985) Gas Chromatography-Mass Spectrometry Evidence for Several Endogenous Auxins in Pea Seedling Organs. *Planta.* 165 (2), 232–241. https://doi.org/10.1007/BF00395046.

(6) Dziurka, K.; Dziurka, M.; Warchoł, M.; Czyczyło-Mysza, I.; Marcińska, I.; Noga, A.; Kapłoniak, K.; Skrzypek, E. (2019) Endogenous Phytohormone Profile during Oat (Avena Sativa L.) Haploid Embryo Development. *In Vitro Cellular & Developmental Biology – Plant*. 55 (2), 221–229. https://doi.org/10.1007/s11627-019-09967-5.

(7) Korasick, D. A.; Enders, T. A.; Strader, L. C. (2013) Auxin Biosynthesis and Storage Forms. *Journal of Experimental Botany*. 64 (9), 2541–2555. https://doi.org/10.1093/jxb/ert080.

(8) Strader, L.; Monroe-Augustus, M.; Rogers. K.; Lin, G.; Bartel, B. (2008) *Arabidopsis* iba response5 Suppressors Separate Responses to Various Hormones. Genetics, Volume 180, Issue 4, Pages 2019–2031, https://doi.org/10.1534/genetics.108.091512

(9) Casanova-Sáez, R.; Mateo-Bonmatí, E.; Ljung, K. (2021) Auxin Metabolism in Plants. *Cold Spring Harbor Perspectives in Biology.* 13 (3), a039867. https://doi.org/10.1101/cshperspect.a039867.

(10) Vorwerk, S.; Biernacki, S.; Hillebrand, H.; Janzik, I.; Müller, A.; Weiler, E. W.; Piotrowski, M. (2001) Enzymatic Characterization of the Recombinant Arabidopsis Thaliana Nitrilase Subfamily Encoded by the NIT 2/ NIT 1/ NIT 3-Gene Cluster. *Planta*. 212 (4), 508–516. https://doi.org/10.1007/s004250000420.

(11) Mano, Y.; Nemoto, K.; Suzuki, M.; Seki, H.; Fujii, I.; Muranaka, T. (2010) The AMI1 Gene Family: Indole-3-Acetamide Hydrolase Functions in Auxin Biosynthesis in Plants. *Journal of Experimental Botany*. 61 (1), 25–32. https://doi.org/10.1093/jxb/erp292.

(12) Nonhebel, H. M. (2015) Tryptophan-Independent Indole-3-Acetic Acid Synthesis: Critical Evaluation of the Evidence. *Plant Physiology*. 169 (2), 1001–1005. https://doi.org/10.1104/pp.15.01091.

(13) Wright, A. D.; Sampson, M. B.; Neuffer, M. G.; Michalczuk, L.; Slovin, J. P.; Cohen, J. D. (1979) 1991 Indole-3-Acetic Acid Biosynthesis in the Mutant Maize *Orange Pericarp* , a Tryptophan Auxotroph. *Science*. 254 (5034), 998–1000. https://doi.org/10.1126/science.254.5034.998.

(14) Zhang, R.; Wang, B.; Ouyang, J.; Li, J.; Wang, Y. (2008) *Arabidopsis* Indole Synthase, a Homolog of Tryptophan Synthase Alpha, Is an Enzyme Involved in the Trp-Independent Indole-Containing Metabolite Biosynthesis. *Journal of Integrative Plant Biology*. 50 (9), 1070–1077. https://doi.org/10.1111/j.1744-7909.2008.00729.x.

(15) Petrášek, J.; Friml, J. (2009) Auxin Transport Routes in Plant Development. *Development*. 136 (16), 2675–2688. https://doi.org/10.1242/dev.030353.

(16) Friml, J.; Vieten, A.; Sauer, M.; Weijers, D.; Schwarz, H.; Hamann, T.; Offringa, R.; Jürgens, G. (2003) Efflux-Dependent Auxin Gradients Establish the Apical–Basal Axis of Arabidopsis. *Nature*. 426 (6963), 147–153. https://doi.org/10.1038/nature02085.

(17) Friml, J.; Palme, K. (2002) Polar Auxin Transport – Old Questions and New Concepts? *Plant Molecular Biology*. 49 (3/4), 273–284. https://doi.org/10.1023/A:1015248926412.

(18) Zazimalova, E.; Murphy, A. S.; Yang, H.; Hoyerova, K.; Hosek, P. (2010) Auxin Transporters--Why So Many? *Cold Spring Harbor Perspectives in Biology*. 2 (3), a001552–a001552. https://doi.org/10.1101/cshperspect.a001552.

(19) Vieten, A.; Sauer, M.; Brewer, P. B.; Friml, J. (2007) Molecular and Cellular Aspects of Auxin-Transport-Mediated Development. *Trends in Plant Science*. 12 (4), 160–168. https://doi.org/10.1016/j.tplants.2007.03.006.

(20) Gälweiler, L.; Guan, C.; Müller, A.; Wisman, E.; Mendgen, K.; Yephremov, A.; Palme, K. (1979) 1998 Regulation of Polar Auxin Transport by AtPIN1 in *Arabidopsis* Vascular Tissue. *Science*. 282 (5397), 2226–2230. https://doi.org/10.1126/science.282.5397.2226.

(21) Friml, J.; Vieten, A.; Sauer, M.; Weijers, D.; Schwarz, H.; Hamann, T.; Offringa, R.; Jürgens, G. (2003) Efflux-Dependent Auxin Gradients Establish the Apical–Basal Axis of Arabidopsis. *Nature*. 426 (6963), 147–153. https://doi.org/10.1038/nature02085.

(22) Benková, E.; Michniewicz, M.; Sauer, M.; Teichmann, T.; Seifertová, D.; Jürgens, G.; Friml, J. (2003) Local, Efflux-Dependent Auxin Gradients as a Common Module for Plant Organ Formation. *Cell*. 115 (5), 591–602. https://doi.org/10.1016/S0092-8674(03)00924-3.

(23) Swarup, R.; Bennett, M. (2003) Auxin Transport. *Developmental Cell*. 5 (6), 824–826. https://doi.org/10.1016/S1534-5807(03)00370-8.

(24) Adamowski, M.; Friml, J. (2015) PIN-Dependent Auxin Transport: Action, Regulation, and Evolution. *Plant Cell*. 27 (1), 20–32. https://doi.org/10.1105/tpc.114.134874.

(25) Sorefan, K.; Girin, T.; Liljegren, S. J.; Ljung, K.; Robles, P.; Galván-Ampudia, C. S.; Offringa, R.; Friml, J.; Yanofsky, M. F.; Østergaard, L. (2009) A Regulated Auxin Minimum Is Required for Seed Dispersal in Arabidopsis. *Nature*. 459 (7246), 583–586. https://doi.org/10.1038/nature07875.

(26) Vandenbussche, F.; Petrášek, J.; Žádníková, P.; Hoyerová, K.; Pešek, B.; Raz, V.; Swarup, R.; Bennett, M.; Zažímalová, E.; Benková, E.; Van Der Straeten, D. (2010) The Auxin Influx Carriers AUX1 and LAX3 Are Involved in Auxin-Ethylene Interactions during Apical Hook Development in *Arabidopsis Thaliana* Seedlings. *Development*. 137 (4), 597–606. https://doi.org/10.1242/dev.040790.

(27) Swarup, R.; Bhosale, R. (2019) Developmental Roles of AUX1/LAX Auxin Influx Carriers in Plants. *Frontiers in Plant Science*. 10:1306. doi:10.3389/fpls.2019.01306.

(28) Mravec, J.; Skůpa, P.; Bailly, A.; Hoyerová, K.; Křeček, P.; Bielach, A.; Petrášek, J.; Zhang, J.; Gaykova, V.; Stierhof, Y.-D.; Dobrev, P. I.; Schwarzerová, K.; Rolčík, J.; Seifertová, D.; Luschnig, C.; Benková, E.; Zažímalová, E.; Geisler, M.; Friml, J. (2009) Subcellular Homeostasis of Phytohormone Auxin Is Mediated by the ER-Localized PIN5 Transporter. *Nature*. 459 (7250), 1136–1140. https://doi.org/10.1038/nature08066.

(29) Ding, Z.; Wang, B.; Moreno, I.; Dupláková, N.; Simon, S.; Carraro, N.; Reemmer, J.; Pěnčík, A.; Chen, X.; Tejos, R.; Skůpa, P.; Pollmann, S.; Mravec, J.; Petrášek, J.; Zažímalová, E.; Honys, D.; Rolčík, J.; Murphy, A.; Orellana, A.; Geisler, M.; Friml, J. (2012) ER-Localized Auxin Transporter PIN8 Regulates Auxin Homeostasis and Male Gametophyte Development in Arabidopsis. *Nat Commun*. 3 (1), 941. https://doi.org/10.1038/ncomms1941.

(30) Béziat, C.; Barbez, E.; Feraru, M. I.; Lucyshyn, D.; Kleine-Vehn, J. (2017) Light Triggers PILS-Dependent Reduction in Nuclear Auxin Signalling for Growth Transition. *Nat Plants*. 3 (8), 17105. https://doi.org/10.1038/nplants.2017.105.

(31) Barbez, E.; Kubeš, M.; Rolčík, J.; Béziat, C.; Pěnčík, A.; Wang, B.; Rosquete, M. R.; Zhu, J.; Dobrev, P. I.; Lee, Y.; Zažímalovà, E.; Petrášek, J.; Geisler, M.; Friml, J.; Kleine-Vehn, J. (2012) A Novel Putative Auxin Carrier Family Regulates Intracellular Auxin Homeostasis in Plants. *Nature*. *485* (7396), 119–122. https://doi.org/10.1038/nature11001.

(32) Feraru, E.; Feraru, M. I.; Barbez, E.; Waidmann, S.; Sun, L.; Gaidora, A.; Kleine-Vehn, J. (2019) PILS6 Is a Temperature-Sensitive Regulator of Nuclear Auxin Input and Organ Growth in *Arabidopsis Thaliana*. *Proceedings of the National Academy of Sciences*. 116 (9), 3893–3898. https://doi.org/10.1073/pnas.1814015116.

(33) Ranocha, P.; Dima, O.; Nagy, R.; Felten, J.; Corratgé-Faillie, C.; Novák, O.; Morreel, K.; Lacombe, B.; Martinez, Y.; Pfrunder, S.; Jin, X.; Renou, J.-P.; Thibaud, J.-B.; Ljung, K.; Fischer, U.; Martinoia, E.; Boerjan, W.; Goffner, D. (2013) Arabidopsis WAT1 Is a Vacuolar Auxin Transport Facilitator Required for Auxin Homoeostasis. *Nature Communications*. 4 (1), 2625. https://doi.org/10.1038/ncomms3625.

(34) Caumon, H.; Vernoux, T. (2023) A matter of time: auxin signaling dynamics and the regulation of auxin responses during plant development. *Journal of Experimental Botany*. Volume 74, Issue 14, pages 3887–3902. https://doi.org/10.1093/jxb/erad132

(35) Ottoline Leyser. (2018) Auxin Signaling, *Plant Physiology*, Volume 176, Issue 1, Pages 465–479, https://doi.org/10.1104/pp.17.00765

(36) Bingsheng, L.; Kaijing, W.; Kongqin, H.; Te, T.; Feng, Z.; Zipeng,Y.; Dajian, Z.; Yinghua, S.; Yalin, S.; Xiansheng, Z.; Zhaojun, D. (2021) MPK14-mediated auxin signaling controls lateral root development via ERF13-regulated very-long-chain fatty acid biosynthesis. *Molecular Plant.* Volume 14, Issue 2, pages 285-297. https://doi.org/10.1016/j.molp.2020.11.011.

(37) Wang, Q.; De Gernier, H.; Duan, X.; Xie, Y.; Geelen, D.; Hayashi, K.; Xuan, W.; Geisler, M.; ten Tusscher, K.; Beeckman, T.; Vanneste, S. (2023) GH3-mediated Auxin Inactivation Attenuates Multiple Stages of Lateral Root Development. *New Phytologist*. https://doi.org/10.1111/nph.19284.

(38) Woodward, A. W. (2005) Auxin: Regulation, Action, and Interaction. *Ann Bot*. 95 (5), 707–735. https://doi.org/10.1093/aob/mci083.

(39) Hayashi, K.; Arai, K.; Aoi, Y.; Tanaka, Y.; Hira, H.; Guo, R.; Hu, Y.; Ge, C.; Zhao, Y.; Kasahara, H.; Fukui, K. (2021) The Main Oxidative Inactivation Pathway of the Plant Hormone Auxin. *Nat Commun*. 12 (1), 6752. https://doi.org/10.1038/s41467-021-27020-1.

(40) Östin, A.; Kowalyczk, M.; Bhalerao, R. P.; Sandberg, G. (1998) Metabolism of Indole-3-Acetic Acid in Arabidopsis. *Plant Physiol*. 118 (1), 285–296. https://doi.org/10.1104/pp.118.1.285.

(41) Ludwig-Müller, J. (2011) Auxin Conjugates: Their Role for Plant Development and in the Evolution of Land Plants. *J Exp Bot*. 62 (6), 1757–1773. https://doi.org/10.1093/jxb/erq412.

(42) Brunoni, F.; Collani, S.; Casanova-Sáez, R.; Šimura, J.; Karady, M.; Schmid, M.; Ljung, K.; Bellini, C. (2020) Conifers Exhibit a Characteristic Inactivation of Auxin to Maintain Tissue Homeostasis. *New Phytologist*. 226 (6), 1753–1765. https://doi.org/10.1111/nph.16463.

(43) Mellor, N.; Band, L. R.; Pěnčík, A.; Novák, O.; Rashed, A.; Holman, T.; Wilson, M. H.; Voß, U.; Bishopp, A.; King, J. R.; Ljung, K.; Bennett, M. J.; Owen, M. R. (2016) Dynamic Regulation of Auxin Oxidase and Conjugating Enzymes *AtDAO1* and *GH3* Modulates Auxin Homeostasis. *Proceedings of the National Academy of Sciences*. 113 (39), 11022–11027. https://doi.org/10.1073/pnas.1604458113.

(44) Fukui, K.; Arai, K.; Tanaka, Y.; Aoi, Y.; Kukshal, V.; Jez, J. M.; Kubes, M. F.; Napier, R.; Zhao, Y.; Kasahara, H.; Hayashi, K. (2022) Chemical Inhibition of the Auxin Inactivation Pathway Uncovers the Roles of Metabolic Turnover in Auxin Homeostasis. *Proceedings of the National Academy of Sciences*. 119 (32). https://doi.org/10.1073/pnas.2206869119.

(45) Guo, R.; Hu, Y.; Aoi, Y.; Hira, H.; Ge, C.; Dai, X.; Kasahara, H.; Zhao, Y. (2022) Local Conjugation of Auxin by the GH3 Amido Synthetases Is Required for Normal Development of Roots

and Flowers in Arabidopsis. *Biochemical and Biophysical Research Communications*. 589, 16–22. https://doi.org/10.1016/j.bbrc.2021.11.109.

(46) Chen, Q.F., Westfall, C.S., Hicks, L.M., Wang, S.P. and Jez, J.M. (2010) Kinetic basis for the conjugation of auxin by a GH3 family indoleacetic acid-amido synthetase. *Journal of biological chemistry*. 285: 29780–29786. https://doi.org/10.1074/jbc.M110.146431

(47) Staswick, P. E.; Tiryaki, I. (2004) The Oxylipin Signal Jasmonic Acid Is Activated by an Enzyme That Conjugates It to Isoleucine in Arabidopsis. *Plant Cell*. 16 (8), 2117–2127. https://doi.org/10.1105/tpc.104.023549.

(48) Delfin, J. C.; Kanno, Y.; Seo, M.; Kitaoka, N.; Matsuura, H.; Tohge, T.; Shimizu, T. (2022) AtGH3.10 Is Another Jasmonic Acid-amido Synthetase in *Arabidopsis Thaliana*. *The Plant Journal*. 110 (4), 1082–1096. https://doi.org/10.1111/tpj.15724.

(49) Okrent, R. A.; Brooks, M. D.; Wildermuth, M. C. (2009) Arabidopsis GH3.12 (PBS3) Conjugates Amino Acids to 4-Substituted Benzoates and Is Inhibited by Salicylate. *Journal of Biological Chemistry*. 284 (15), 9742–9754. https://doi.org/10.1074/jbc.M806662200.

(50) Westfall, C.; Herrmann, J.; Chen, Q.; Wang, S.; Jez, J. (2010) Modulating plant hormones by enzyme action: The GH3 family of acyl acid amido synthetases. *Plant signaling & behavior*. 5. 1607-12. https://doi.org/10.4161/psb.5.12.13941.

(51) Sgaramella, V.; Bernardi, A. (2001) DNA Cloning. *Brenner's Encyclopedia of Genetics: Second Edition*, 348–352. https://doi.org/10.1016/B978-0-12-374984-0.00417-4.

(52) Blackstock, J. C. (1989) Gene Cloning. *Guide to Biochemistry*. 230–241. https://doi.org/10.1016/B978-0-7236-1151-6.50025-X.

(53) Lessard, J. C. (2013) Molecular Cloning. *Methods in Enzymology*. 529, 85–98. https://doi.org/10.1016/B978-0-12-418687-3.00007-0.

(54) Esser, K.; Kück, U.; Lang-Hinrichs, C.; Lemke, P.; Osiewacz, H. D.; Stahl, U.; Tudzynski, P. (1986) *Plasmids of Eukaryotes*; Springer Berlin Heidelberg: Berlin, Heidelberg,. https://doi.org/10.1007/978-3-642-82585-9.

(55) Davis, L. G.; Dibner, M. D.; Battey, J. F. (1986) PBR322. In *Basic Methods in Molecular Biology*; Elsevier. pp 24–25. https://doi.org/10.1016/B978-0-444-01082-7.50010-2.

(56) Thomas, C. M.; Summers, D. (2008) Bacterial Plasmids. In *eLS*; Wiley, https://doi.org/10.1002/9780470015902.a0000468.pub2.

(57) Lampropoulos, A.; Sutikovic, Z.; Wenzl, C.; Maegele, I.; Lohmann, J. U.; Forner, J. (2013) GreenGate - A Novel, Versatile, and Efficient Cloning System for Plant Transgenesis. *PLoS One*. 8 (12), e83043. https://doi.org/10.1371/journal.pone.0083043.

(58) Clark, D. P.; Pazdernik, N. J.; McGehee, M. R. (2019) Cloning Genes for Synthetic Biology. *Molecular Biology*; Elsevier, pp 199–239. https://doi.org/10.1016/B978-0-12-813288-3.00007-0.

(59) Carson, S.; Heather, B.; Witherow, S.; Srougi, M.; (2019) Lab Session 3 - Completion of Vector Preparation and Polymerase Chain Reaction Amplification of egfp, Molecular Biology Techniques (Fourth Edition). *Academic Press*, 23-30 pages. https://doi.org/10.1016/B978-0-12-815774-9.00003-4.

(60) Garibyan, L.; Avashia, N. (2013) Polymerase Chain Reaction. *Journal of Investigative Dermatology*. 133 (3), 1–4. https://doi.org/10.1038/jid.2013.1.

(61) Gibbs, R. A. (1990) DNA Amplification by the Polymerase Chain Reaction. *Anal Chem*. 62 (13), 1202–1214. https://doi.org/10.1021/ac00212a004.

(62) Delidow, B. C.; Lynch, J. P.; Peluso, J. J.; White, B. A. (1996) Polymerase Chain Reaction: Basic Protocols. In *PCR Protocols*; Humana Press: New Jersey. pp 1–30. https://doi.org/10.1385/0-89603-244-2:1.

(63) Zhu, H.; Zhang, H.; Xu, Y.; Laššáková, S.; Korabečná, M.; Neužil, P. (2020) PCR Past, Present and Future. *Biotechniques*. 69 (4), 317–325. https://doi.org/10.2144/btn-2020-0057.

(64) Ullmann, A.; Jacob, F.; Monod, J. (1967) Characterization by in Vitro Complementation of a Peptide Corresponding to an Operator-Proximal Segment of the β-Galactosidase Structural Gene of Escherichia Coli. *J Mol Biol*. 24 (2), 339–343. https://doi.org/10.1016/0022-2836(67)90341-5.

(65) Langley, K. E.; Villarejo, M. R.; Fowler, A. V; Zamenhof, P. J.; Zabin, I. (1975) Molecular Basis of Beta-Galactosidase Alpha-Complementation. *Proceedings of the National Academy of Sciences*. 72 (4), 1254–1257. https://doi.org/10.1073/pnas.72.4.1254.

(66) Messing, J.; Gronenborn, B.; Müller-Hill, B.; Hans Hopschneider, P. (1977) Filamentous Coliphage M13 as a Cloning Vehicle: Insertion of a HindII Fragment of the Lac Regulatory Region in M13 Replicative Form in Vitro. *Proceedings of the National Academy of Sciences*. 74 (9), 3642–3646. https://doi.org/10.1073/pnas.74.9.3642.

(67) Martín, J. F.; Gil, J. A. (1984) Cloning and Expression of Antibiotic Production Genes. *Nat Biotechnol*. 2 (1), 63–72. https://doi.org/10.1038/nbt0184-63.

(68) Bergkessel, M.; Guthrie, C. (2013) Colony PCR. Methods Enzymol. pp 299–309. https://doi.org/10.1016/B978-0-12-418687-3.00025-2.

(69) Walch, G.; Knapp, M.; Rainer, G.; Peintner, U. (2016) Colony-PCR Is a Rapid Method for DNA Amplification of Hyphomycetes. *Journal of Fungi*. 2 (2), 12. https://doi.org/10.3390/jof2020012.

(70) Mandel, M.; Higa, A. (1970) Calcium-Dependent Bacteriophage DNA Infection. *J Mol Biol*. 53 (1), 159–162. https://doi.org/10.1016/0022-2836(70)90051-3.

(71) Cohen, S. N.; Chang, A. C. Y.; Hsu, L. (1972) Nonchromosomal Antibiotic Resistance in Bacteria: Genetic Transformation of *Escherichia Coli* by R-Factor DNA. *Proceedings of the National Academy of Sciences*. 69 (8), 2110–2114. https://doi.org/10.1073/pnas.69.8.2110.

(72) Aune, T. E. V.; Aachmann, F. L. (2010) Methodologies to Increase the Transformation Efficiencies and the Range of Bacteria That Can Be Transformed. *Appl Microbiol Biotechnol*. 85 (5), 1301–1313. https://doi.org/10.1007/s00253-009-2349-1.

(73) Carter, M.; Shieh, J. (2015) Gene Delivery Strategies. In *Guide to Research Techniques in Neuroscience*; Elsevier. pp 239–252. https://doi.org/10.1016/B978-0-12-800511-8.00011-3.

(74) Panja, S.; Saha, S.; Jana, B.; Basu, T. (2006) Role of Membrane Potential on Artificial Transformation of *E.coli* with Plasmid DNA. *J Biotechnol*. 127 (1), 14–20. https://doi.org/10.1016/j.jbiotec.2006.06.008.

(75) Asif, A.; Mohsin, H.; Tanvir, R.; Rehman, Y. (2017) Revisiting the Mechanisms Involved in Calcium Chloride Induced Bacterial Transformation. *Front Microbiol*. 8. https://doi.org/10.3389/fmicb.2017.02169.

(76) Kim, H.; Kim, J.-S. (2014) A Guide to Genome Engineering with Programmable Nucleases. *Nat Rev Genet*. 15 (5), 321–334. https://doi.org/10.1038/nrg3686.

(77) Bawa, A. S.; Anilakumar, K. R. (2013) Genetically Modified Foods: Safety, Risks and Public Concerns—a Review. *J Food Sci Technol*. 50 (6), 1035–1046. https://doi.org/10.1007/s13197-012-0899-1.

(78) Clough, S. J.; Bent, A. F. (1998) Floral Dip: A Simplified Method for *Agrobacterium* - mediated Transformation of *Arabidopsis Thaliana* . *The Plant Journal.* 16 (6), 735–743. https://doi.org/10.1046/j.1365-313x.1998.00343.x

(79) Bechtold, N.; Pelletier, G. (1998) In Planta *Agrobacterium*-Mediated Transformation of Adult Arabidopsis Thaliana Plants by Vacuum Infiltration. In *Arabidopsis Protocols*; Humana Press: Totowa, NJ. pp 259–266. https://doi.org/10.1385/0-89603-391-0:259.

(80) Azpiroz-Leehan, R. (1997) T-DNA Insertion Mutagenesis in Arabidopsis: Going Back and Forth. *Trends in Genetics*. 13 (4), 152–156. https://doi.org/10.1016/S0168-9525(97)01094-9.

(81) Desfeux, C.; Clough, S. J.; Bent, A. F. (2000) Female Reproductive Tissues Are the Primary Target of *Agrobacterium* -Mediated Transformation by the Arabidopsis Floral-Dip Method. *Plant Physiol*. 123 (3), 895–904. https://doi.org/10.1104/pp.123.3.895.

(82) Hwang, H.-H.; Yu, M.; Lai, E.-M. (2017) *Agrobacterium* -Mediated Plant Transformation: Biology and Applications. *Arabidopsis Book*. 15, e0186. https://doi.org/10.1199/tab.0186.

(83) Michielse, C. B.; Ram, A. F. J.; Hooykaas, P. J. J.; Hondel, C. A. M. J. J. van den. (2004) Role of Bacterial Virulence Proteins in *Agrobacterium*-Mediated Transformation of Aspergillus Awamori. *Fungal Genetics and Biology*. 41 (5), 571–578. https://doi.org/10.1016/j.fgb.2004.01.004.

(84) Vesely, P. (2006) 2007 Handbook of Biological Confocal Microscopy, 3rd Ed. By James B. Pawley, Editor. Springer Science + Business Media. 28 + 985 pages. *Scanning*. 29 (3), 91–91. https://doi.org/10.1002/sca.20059.

(85) Elliott, A. D. (2020) Confocal Microscopy: Principles and Modern Practices. *Curr Protoc Cytom*. 92 (1). https://doi.org/10.1002/cpcy.68.

(86) Heim, R.; Cubitt, A.; Tsien, R. (1995) Improved green fluorescence. *Nature*. 373:663–64. https://doi.org/10.1038/373663b0

(87) Joseph M. Jez (2022) Connecting primary and specialized metabolism: Amino acid conjugation of phytohormones by GRETCHEN HAGEN 3 (GH3) acyl acid amido synthetases, Current Opinion in Plant Biology, Volume 66, 102194. https://doi.org/10.1016/j.pbi.2022.102194.

(88) Hagen, G.; Kleinschmidt, A.; Guilfoyle, T. (1984) Auxin-regulated gene-expression in intact soybean hypocotyl and excised hypocotyl sections. *Planta*, 162, 147–153. https://doi.org/10.1007/BF00410211

(89) Desjardins P.; Conklin D. (2010) NanoDrop Microvolume Quantitation of Nucleic Acids. *Journal of Visualized Experiments* 45: e2565. https://doi.org/10.3791/2565

(90) Acinas, S.; Sarma-Rupavtarm, R.; Klepac-Ceraj, V.; Polz, M. (2005) PCR-induced sequence artifacts and bias: insights from comparison of two 16S rRNA clone libraries constructed from the same sample. *Applied and Environmental Microbiology*; 71(12):8966-9. https://doi.org/10.1128/AEM.71.12.8966-8969.2005.

(91) Pienaar, E.; Theron, M.; Nelson, M.; Viljoen, H. (2006) A quantitative model of error accumulation during PCR amplification. *Computational Biology and Chemistry.* 30(2):102-11 https://doi.org/10.1016/j.compbiolchem.2005.11.002.

(92) Fulton, T.; Stiller, M. (2011) PCR Amplification, Cloning, and Sequencing of Ancient DNA. Ancient DNA, Volume 840, pages 111–119. https://doi.org/10.1007/978-1-61779-516-9_15

(93) Matsumura, I. (2015) Why Johnny can't clone: Common pitfalls and not so common solutions. *BioTechniques*, *59(3).* https://doi.org/10.2144/000114324

(94) Bhuiyan, A.; Asakawa, S.; (2023) Synthesis and cloning of long repeat sequences using single-stranded circular DNA. *Frontiers in Bioengineering and Biotechnology.* 11:1115159. https://doi.org/10.3389/fbioe.2023.1115159

(95) Takahiro, K. (2003) Bias and artifacts in multitemplate polymerase chain reactions (PCR), *Journal of Bioscience and Bioengineering,* Volume 96, Issue 4, pages 317-323, https://doi.org/10.1016/S1389-1723(03)90130-7.

(96) Pinski, A.; Betekhtin, A. (2023) Efficient *Agrobacterium*-mediated transformation and genome editing of *Fagopyrum tataricum*. *Frontiers in Plant Science*. 14:1270150. https://doi.org/10.3389/fpls.2023.1270150

(97) López-Salmerón, V.; Schürholz, A.; Li, Z.; Schlamp, T.; Wenzl, C.; Lohmann, J.; Wolf, S. (2019) Inducible, Cell Type-Specific Expression in *Arabidopsis thaliana* Through LhGR-Mediated Trans-Activation. *Journal of Visualized Experiments*, (146). https://doi.org/10.3791/59394

(98) Kümpers, B.; Han, J.; Vaughan-Hirsch, J.; Redman, N.; Ware, A.; Atkinson, J.; Leftley, N.; Janes, G.; Castiglione, G.; Tarr, PT.; Pyke, K.; Voß, U.; Wells, D.; Bishopp, A. (2022) Dual expression and anatomy lines allow simultaneous visualization of gene expression and anatomy. *Plant Physiology*. 188(1):56-69. https://doi.org/10.1093/plphys/kiab503

(99) Zhang, X.; Henriques, R.; Lin, S.-S.; Niu, Q.-W.; Chua, N.-H. (2006) *Agrobacterium*-mediated transformation of Arabidopsis thaliana using the floral dip method. *Nature Protocols,* 1(2), *641–646.* doi:10.1038/nprot.2006.97

(100) Harrison, S.; Mott, E.; Parsley, K. (2006) A rapid and robust method of identifying transformed *Arabidopsis thaliana* seedlings following floral dip transformation. *Plant Methods* 2, 19. https://doi.org/10.1186/1746-4811-2-19

(101) De Buck, S.; Podevin, N.; Nolf, J.; Jacobs, A; Depicker, A. (2009) The T-DNA integration pattern in *Arabidopsis* transformants is highly determined by the transformed target cell. *Plant Journal*. 60(1):134-45. https://doi.org/10.1111/j.1365-313X.2009.03942.x

(102) Cogoni, C.; Macino, G. (1999) Homology-dependent gene silencing in plants and fungi: a number of variations on the same theme. *Current Opinion in Microbiology*, Volume 2, Issue 6, pages 657-662. https://doi.org/10.1016/S1369-5274(99)00041-7

(103) Grefen, C.; Donald, N.; Hashimoto, K.; Kudla, J.; Schumacher, K.; Blatt, M. (2010) A ubiquitin-10 promoter-based vector set for fluorescent protein tagging facilitates temporal stability and native protein distribution in transient and stable expression studies. *Plant Journal*. 64(2):355-65. https://doi.org/10.1111/j.1365-313X.2010.04322.x

(104) Pegg, T.; Gladish, D.; Baker, R. (2021). Algae to angiosperms: Autofluorescence for rapid visualization of plant anatomy among diverse taxa. *Applications in Plant Sciences,* 9(6). https://doi.org/10.1002/aps3.11437

(105) Brooks, E.; Elorriaga, E.; Liu, Y.; Duduit, J.; Yuan, G.; Tsai, C.; Tuskan, G.; Ranney, T.; Yang, X.; Liu, W. (2023) Plant Promoters and Terminators for High-Precision Bioengineering. *Biodesign Research.* 7;5:0013. https://doi.org/10.34133/bdr.0013.

(106) Schmid, M.; Davison, T; Henz, S; Pape, U.; Demar, M.; Vingron, M.; Schölkopf, B.; Weigel, D.; Lohmann, J. (2005) A gene expression map of *Arabidopsis thaliana* development. *Nature Genetics*. 37(5):501-6. doi:10.1038/ng1543.

(107) Li, K.; Wang, S.; Wu, H.; Wang, H. (2020) Protein Levels of Several Arabidopsis Auxin Response Factors Are Regulated by Multiple Factors and ABA Promotes *ARF*6 Protein Ubiquitination. *International Journal of Molecular Sciences.* 21(24):9437. https://doi.org/10.3390/ijms21249437

(108) Zhang, L.; Shi, X.; Zhang, Y.; Wang, J.; Yang, J.; Ishida, T.; Jiang, W.; Han, X.; Kang, J.; Wang, X.; Pan, L.; Lv, S.; Cao, B.; Zhang, Y.; Wu, J.; Han, H.; Hu, Z.; Cui, L.; Sawa, S.; He, J.; Wang, G. (2019) CLE9 peptide-induced stomatal closure is mediated by abscisic acid, hydrogen peroxide, and nitric oxide in *Arabidopsis thaliana*. *Plant Cell Environment*. 42(3):1033-1044. https://doi.org/10.1111/pce.13475

Attachments

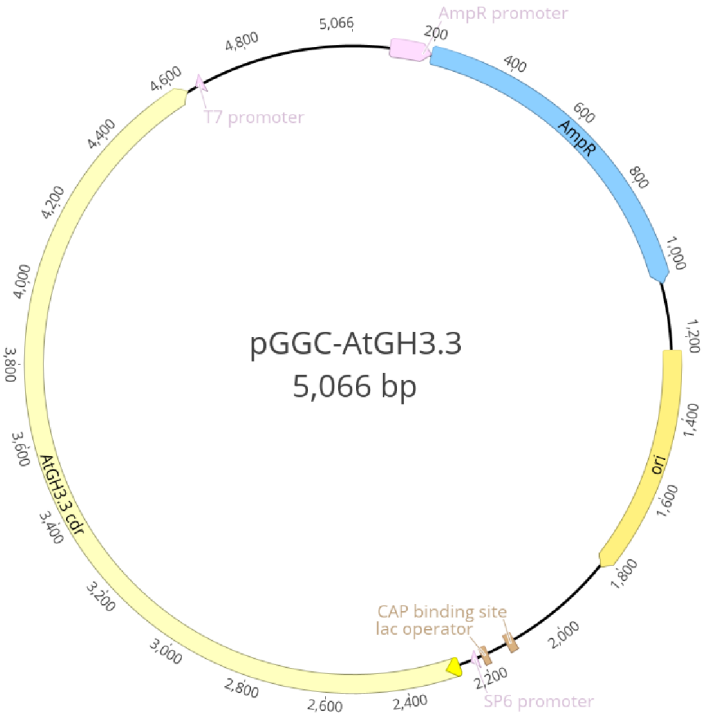

Attachment 1. Representation of pGGC00 plasmid with inserted AtGH3.3 gene, created in Geneious Prime. The plasmid is 5,066 bp and carries the origin of replication ori, lac operator (required for lactose metabolism), CAP binding site (positive regulator of lac operon), SP6 promoter, AtGH3.3 inserted gene sequence, T7 promoter, and ampicillin resistance cassette

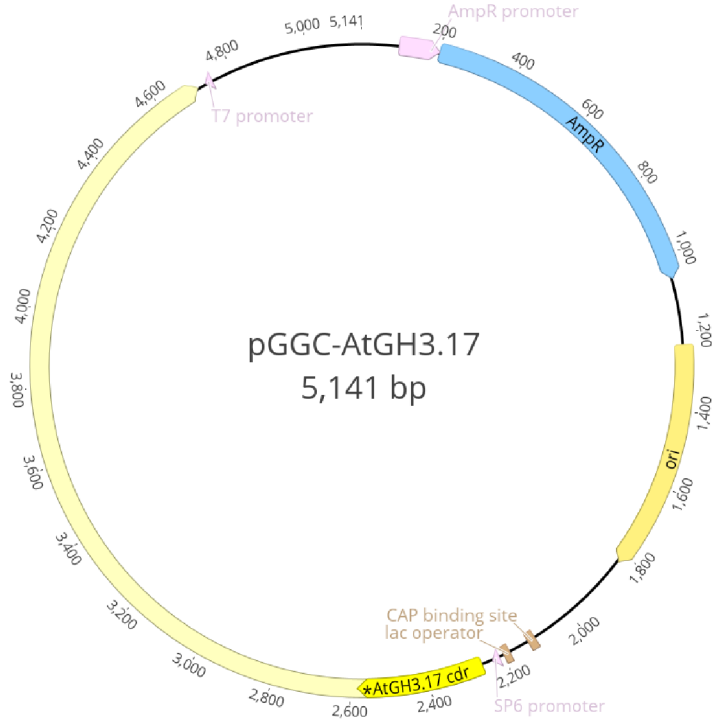

Attachment 2. Representation of pGGC00 plasmid with inserted AtGH3.17 gene, created in Geneious Prime. The plasmid is 5,141 bp and carries the origin of replication ori, lac operator (required for lactose metabolism), CAP binding site (positive regulator of lac operon), SP6 promoter, AtGH3.17 inserted gene sequence, T7 promoter, and ampicillin resistance cassette.

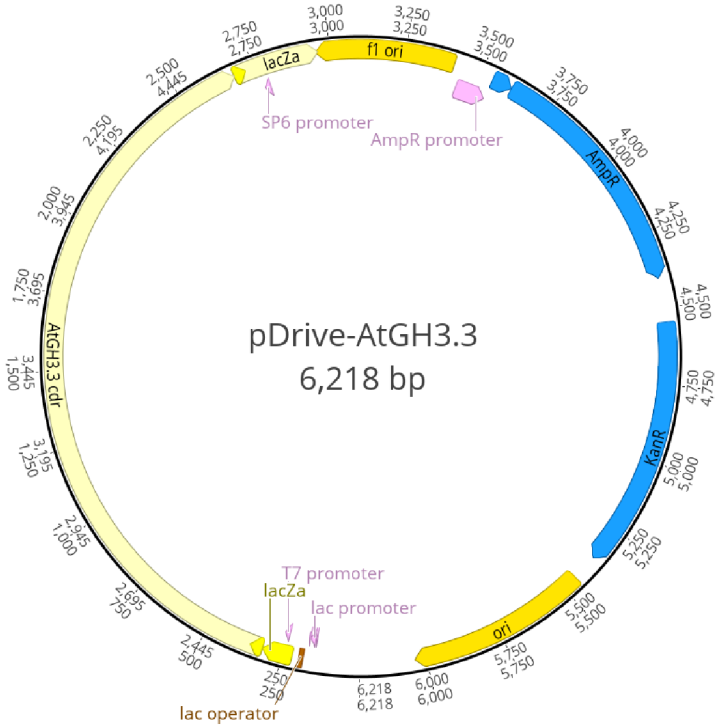

Attachment 3. Representation of pDrive vector with inserted AtGH3.3 gene, created in Geneious Prime. The plasmid is 6,218 bp and carries the origin of replication ori, f1 ori, lac operator with LacZa (required for lactose metabolism), CAP binding site (positive regulator of lac operon), SP6 promoter, AtGH3.3 inserted gene sequence, T7 promoter, ampicillin, and kanamycin resistance cassette.

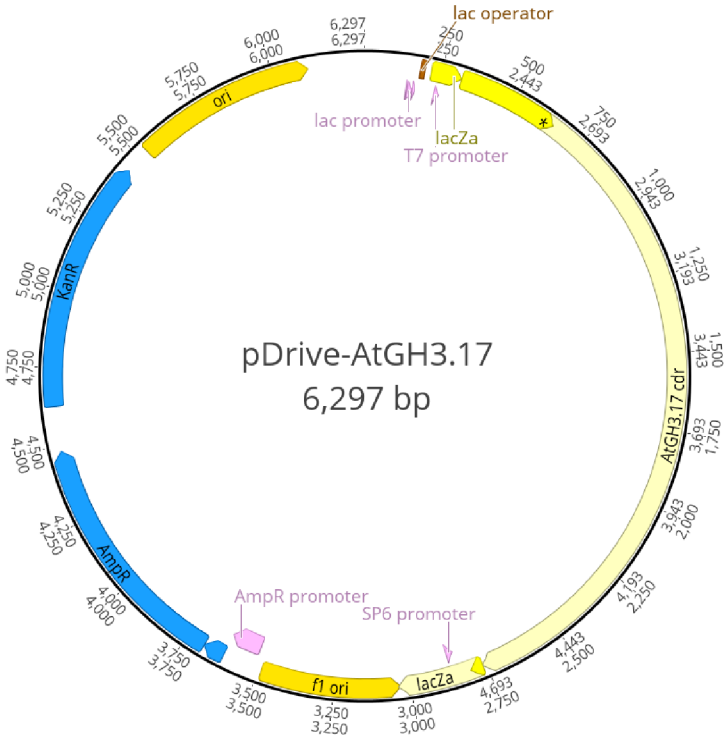

Attachment 4. Representation of pDrive vector with inserted AtGH3.17 gene, created in Geneious Prime. The plasmid is 6,297 bp and carries the origin of replication ori, f1 ori, lac operator with LacZa (is required for lactose metabolism), CAP binding site (positive regulator of lac operon), SP6 promoter, AtGH3.17 inserted gene sequence, T7 promoter, ampicillin, and kanamycin resistance cassette.

```
pDrive-AtGH3.3       ATACGACTCACTATAGGGAAAGCTCGGTACCACGCATGCTGCAGACGCGTTACGTATCGG   300
3_1_1.ab1            ------------------------------------------------------------
3_2_1.ab1 (reversed) ------------------------------------------------------------

pDrive-AtGH3.3       ATCCAGAATTCGTGAT-------------------------CGTTGATTCAGCTCTGCG   334
3_1_1.ab1            ----------------------------------------GTTGATTCAGCTCTGCG    17
3_2_1.ab1 (reversed) ------------------------------------------------------------

pDrive-AtGH3.3       ATCTCCGATGATGCACTCACCGTCCACTAAGGACGTGAAGGCTCTAAGGTTCATTGAGGA   394
3_1_1.ab1            ATCTCCGATGATGCACTCACCGTCCACTAAGGACGTGAAGGCTCTAAGGTTCATTGAGGA    77
3_2_1.ab1 (reversed) ------------------------------------------------------------

pDrive-AtGH3.3       GATGACACGTAACGTCGATTTCGTTCAGAAGAAAGTGATTAGAGAGATACTTAGTCGTAA   454
3_1_1.ab1            GATGACACGTAACGTCGATTTCGTTCAGAAGAAAGTGATTAGAGAGATACTTAGTCGTAA   137
3_2_1.ab1 (reversed) ------------------------------------------------------------

pDrive-AtGH3.3       CTCGGACACTGAGTACCTGAAACGGTTTGGTCTCAAGGGATTCACTGACCGTAAAACATT   514
3_1_1.ab1            CTCGGACACTGAGTACCTGAAACGGTTTGGTCTCAAGGGATTCACTGACCGTAAAACATT   197
3_2_1.ab1 (reversed) ------------------------------------------------------------

pDrive-AtGH3.3       TAAGACCAAAGTTCCGGTGGTTATCTACGATGATCTTAAACCGGAGATTCAACGTATTGC   574
3_1_1.ab1            TAAGACCAAAGTTCCGGTGGTTATCTACGATGATCTTAAACCGGAGATTCAACGTATTGC   257
3_2_1.ab1 (reversed) ------------------------------------------------------------

pDrive-AtGH3.3       CAATGGTGACCGGTCAATGATCTTGTCTTCTTACCCCATCACAGAGTTCCTCACAAGGTA   634
3_1_1.ab1            CAATGGTGACCGGTCAATGATCTTGTCTTCTTACCCCATCACAGAGTTCCTCACAAGGTA   317
3_2_1.ab1 (reversed) ------------------------------------------------------------

pDrive-AtGH3.3       TATACTTAACCCAAAATGTATATTATGTTATCTTAGACTCTTAGACAGAGTTAATCATCT   694
3_1_1.ab1            TATACTTAACCCAAAATGTATATTATGTTATCTTAGACTCTTAGACAGAGTTAATCATCT   377
3_2_1.ab1 (reversed) ------------------------------------------------------------

pDrive-AtGH3.3       ATAATTGTGGATTAATCTTGTTTTGTATCCAGCTCTGGGACATCAGCTGGTGAAAGGAAG   754
3_1_1.ab1            ATAATTGTGGATTAATCTTGTTTTGTATCCAGCTCTGGGACATCAGCTGGTGAAAGGAAG   437
3_2_1.ab1 (reversed) ------------------------------------------------------------

pDrive-AtGH3.3       TTGATGCCAACCATTGATGAAGACATGGACCGACGTCAGCTTTTATACAGTCTTCTCATG   814
3_1_1.ab1            TTGATGCCAACCATTGATGAAGACATGGACCGACGTCAGCTTTTATACAGTCTTCTCATG   497
3_2_1.ab1 (reversed) ------------------------------------------------------------

pDrive-AtGH3.3       CCTGTGATGAATCTGTAAGTTACAGTTATTTAATTTGCAATTAACTTCTATTTTGTAGTA   874
3_1_1.ab1            CCTGTGATGAATCTGTAAGTTACAGTTATTTAATTTGCAATTAACTTCTATTTTGTAGTA   557
3_2_1.ab1 (reversed) ------------------------------------------------------------

pDrive-AtGH3.3       ATATCTACGTGCCAAGATTAATACGTTAAAATTGGAAAAATTATGAATTAATCTAATTTA   934
3_1_1.ab1            ATATCTACGTGCCAAGATTAATACGTTAAAATTGGAAAAATTATGAATTAATCTAATTTA   617
3_2_1.ab1 (reversed) ------------------------------------------------------------

pDrive-AtGH3.3       TATTAAAATTTTAGCAAAAATATTTTAAATCTGAACTTTGGACTCTACATTCTAAATTTA   994
3_1_1.ab1            TATTAAAATTTTAGCAAAAATATTTTAAATCTGAACTTTGGACTCTACATTCTAAATTTA   677
3_2_1.ab1 (reversed) ------------------------------------------------------------

pDrive-AtGH3.3       AAACGTGAAGACTAAATGCTGAGGTTTAAACCATAAATCAGAAACCTTAAACCCTAATTC  1054
3_1_1.ab1            AAACGTGAAGACTAAATGCTGAGGTTTAAACCATAAATCAGAAACCTTAAACCCTAATTC   737
3_2_1.ab1 (reversed) ------------------------------------------------------------

pDrive-AtGH3.3       TTGAAATTTAAAAAATTAACACTAAAATATAAACCAAATCATATATATTTACTTAATTTC  1114
3_1_1.ab1            TTGAAATTTAAAAAATTAACACTAAAATATAAACCAAATCATATATATTTACTTAATTTC   797
3_2_1.ab1 (reversed) ------------------------------------------------------------

pDrive-AtGH3.3       AAAAGATCTAATTAACATGTGTTTTGCTTTAGTTCATATTTTGTCAGATTTTTTTTGTCA  1174
3_1_1.ab1            AAAAGATCTAATTAACATGTGTTTTGCTTTA----------------------------   857
3_2_1.ab1 (reversed) ------------------------------------------------------------

pDrive-AtGH3.3       ATTACGTACATCCTTTAAAATGTTATTTCACTATCGCAATAACGTAACATTTTTTTTTTC  1234
3_1_1.ab1            ------------------------------------------------------------   917
3_2_1.ab1 (reversed) ------------------------------------------------------------
```

Attachment 5. Sequence alignment of pDrive-AtGH3.3cdr with a fragment of the GH3.3 gene resulting from the sequencing and confirming the correctness of the inserted sequence.

```
Consensus       TCGGATCCAGAATTCGTGATGCTGTTGATTCGCTTCTTCAATCTGGGATGGCTTCACCGA   356
pDrive-AtGH3.4 TCGGATCCAGAATTCGTGATGCTGTTGATTCGCTTCTTCAATCTGGGATGGCTTCACCGA   356
AtGH3.4_1       ---------------------------ATTCGCTTCTTCAATCTGGGATGGCTTCACCGA    33
AtGH3.4_2       ------------------------------------------------------------

Consensus       CGACATCTGAGACAGAGGTGAAGGCTCTCAAGTTCATTGAGGAGATTACTCGGAACCCTG   416
pDrive-AtGH3.4 CGACATCTGAGACAGAGGTGAAGGCTCTCAAGTTCATTGAGGAGATTACTCGGAACCCTG   416
AtGH3.4_1       CGACATCTGAGACAGAGGTGAAGGCTCTCAAGTTCATTGAGGAGATTACTCGGAACCCTG    93
AtGH3.4_2       ------------------------------------------------------------

Consensus       ACTCGGTTCAAGAAAAGGTTCTTGGAGAGATACTTAGTCGTAACTCGAACACGGAATATC   476
pDrive-AtGH3.4 ACTCGGTTCAAGAAAAGGTTCTTGGAGAGATACTTAGTCGTAACTCGAACACGGAATATC   476
AtGH3.4_1       ACTCGGTTCAAGAAAAGGTTCTTGGAGAGATACTTAGTCGTAACTCGAACACGGAATATC   153
AtGH3.4_2       ------------------------------------------------------------

Consensus       TGAAACGGTTCGATCTTAATGGTGCCGTTGATAGGAAATCGTTCAAGAGCAAAGTTCCGG   536
pDrive-AtGH3.4 TGAAACGGTTCGATCTTAATGGTGCCGTTGATAGGAAATCGTTCAAGAGCAAAGTTCCGG   536
AtGH3.4_1       TGAAACGGTTCGATCTTAATGGTGCCGTTGATAGGAAATCGTTCAAGAGCAAAGTTCCGG   213
AtGH3.4_2       ------------------------------------------------------------

Consensus       TGGTAATCTACGAAGATTTGAAGACGGATATTCAACGTATATCCAACGGTGATCGTTCTC   596
pDrive-AtGH3.4 TGGTAATCTACGAAGATTTGAAGACGGATATTCAACGTATATCCAACGGTGATCGTTCTC   596
AtGH3.4_1       TGGTAATCTACGAAGATTTGAAGACGGATATTCAACGTATATCCAACGGTGATCGTTCTC   273
AtGH3.4_2       ------------------------------------------------------------

Consensus       CGATCTTGTCTTCTCATCCCATCACCGAGTTTCTCACAAGGTATGTTACTTAAGTCAACC   656
pDrive-AtGH3.4 CGATCTTGTCTTCTCATCCCATCACCGAGTTTCTCACAAGGTATGTTACTTAAGTCAACC   656
AtGH3.4_1       CGATCTTGTCTTCTCATCCCATCACCGAGTTTCTCACAAGGTATGTTACTTAAGTCAACC   333
AtGH3.4_2       ------------------------------------------------------------

Consensus       AACTATATCAATGATTAATATCGTTTCTTTTGTTTTTACAACTTTATCAAGGAGTACCAA   716
pDrive-AtGH3.4 AACTATATCAATGATTAATATCGTTTCTTTTGTTTTTACAACTTTATCAAGGAGTACCAA   716
AtGH3.4_1       AACTATATCAATGATTAATATCGTTTCTTTTGTTTTTACAACTTTATCAAGGAGTACCAA   393
AtGH3.4_2       ------------------------------------------------------------

Consensus       TCCCCTTGTACTAGGTCACCATCCTTTTAGTAATGACTAAAACGTTGTTATAAAAAAATT   776
pDrive-AtGH3.4 TCCCCTTGTACTAGGTCACCATCCTTTTAGTAATGACTAAAACGTTGTTATAAAAAAATT   776
AtGH3.4_1       TCCCCTTGTACTAGGTCACCATCCTTTTAGTAATGACTAAAACGTTGTTATAAAAAAATT   453
AtGH3.4_2       ------------------------------------------------------------

Consensus       CAATGACGGGATTTTGATCACCATAATACAAATTGTTAAAAAATATTTTATAGAATACTA   836
pDrive-AtGH3.4 CAATGACGGGATTTTGATCACCATAATACAAATTGTTAAAAAATATTTTATAGAATACTA   836
AtGH3.4_1       CAATGACGGGATTTTGATCACCATAATACAAATTGTTAAAAAATATTTTATAGAATACTA   513
AtGH3.4_2       ------------------------------------------------------------

Consensus       TACAGTTTTTTTACCGTAATTAATTTGTAATGTTTTGTGTGTATTGCAGCTCTGGAACAT   896
pDrive-AtGH3.4 TACAGTTTTTTTACCGTAATTAATTTGTAATGTTTTGTGTGTATTGCAGCTCTGGAACAT   896
AtGH3.4_1       TACAGTTTTTTTACCGTAATTAATTTGTAATGTTTTGTGTGTATTGCAGCTCTGGAACAT   573
AtGH3.4_2       ------------------------------------------------------------

Consensus       CTGCTGGCGAGAGGAAATTAATGCCGACAATTGAAGAAGACATAAACCGACGTCAGCTTT   956
pDrive-AtGH3.4 CTGCTGGCGAGAGGAAATTAATGCCGACAATTGAAGAAGACATAAACCGACGTCAGCTTT   956
AtGH3.4_1       CTGCTGGCGAGAGGAAATTAATGCCGACAATTGAAGAAGACATAAACCGACGTCAGCTTT   633
AtGH3.4_2       ------------------------------------------------------------

Consensus       TAGGCAATCTTCTCATGCCTGTGATGAATCTGTTAGTATATTACTTTTAACATTATTAAA  1016
pDrive-AtGH3.4 TAGGCAATCTTCTCATGCCTGTGATGAATCTGTTAGTATATTACTTTTAACATTATTAAA  1016
AtGH3.4_1       TAGGCAATCTTCTCATGCCTGTGATGAATCTGTTAGTATATTACTTTTAACATTATTAAA   693
AtGH3.4_2       ------------------------------------------------------------

Consensus       CAAAATTGTAACGATTTATAAAATTAACCAAAAATGTTTAACAACTACAGCTACGTGCCG  1076
pDrive-AtGH3.4 CAAAATTGTAACGATTTATAAAATTAACCAAAAATGTTTAACAACTACAGCTACGTGCCG  1076
AtGH3.4_1       CAAAATTGTAACGATTTATAAAATTAACCAAAAATGTTTAACAACTACAGCTACGTGCCG   753
AtGH3.4_2       ------------------------------------------------------------

Consensus       GGATTAGACAAAGGCAAAGGTTTATACTTCTTATTTGTGAAGTCGGAGTCTACGACATCA  1136
pDrive-AtGH3.4 GGATTAGACAAAGGCAAAGGTTTATACTTCTTATTTGTGAAGTCGGAGTCTACGACATCA  1136
AtGH3.4_1       GGATTAG-------------------------------------------------------   813
AtGH3.4_2       ------------------------------------------------------------
```

Attachment 6. Sequence alignment of pDrive-AtGH3.4cdr with a fragment of the GH3.4 gene resulting from the sequencing and confirming the correctness of the inserted sequence.

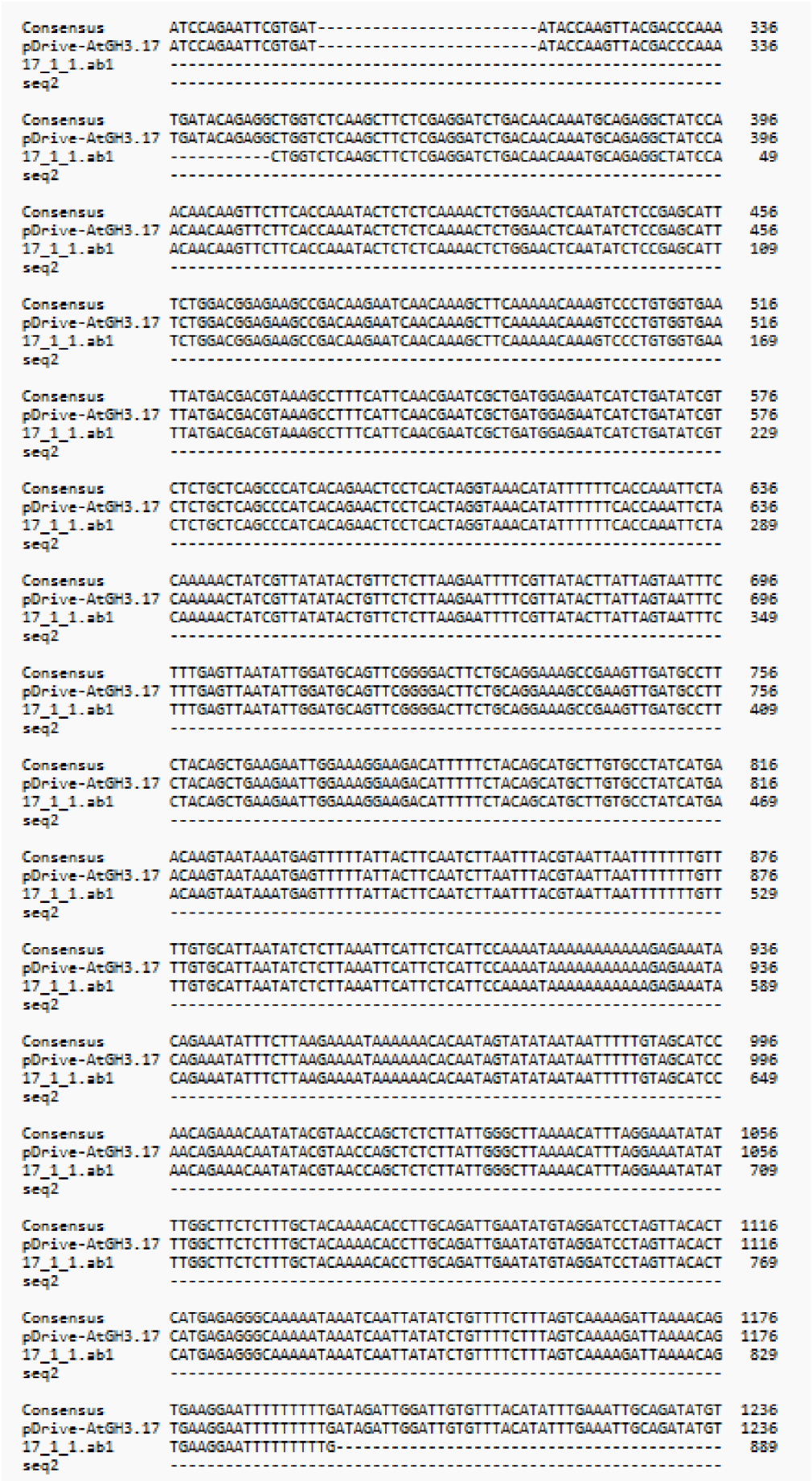

Attachment 7. Sequence alignment of pDrive-AtGH3.17cdr with a fragment of the GH3.17 gene resulting from the sequencing and confirming the correctness of the inserted sequence.

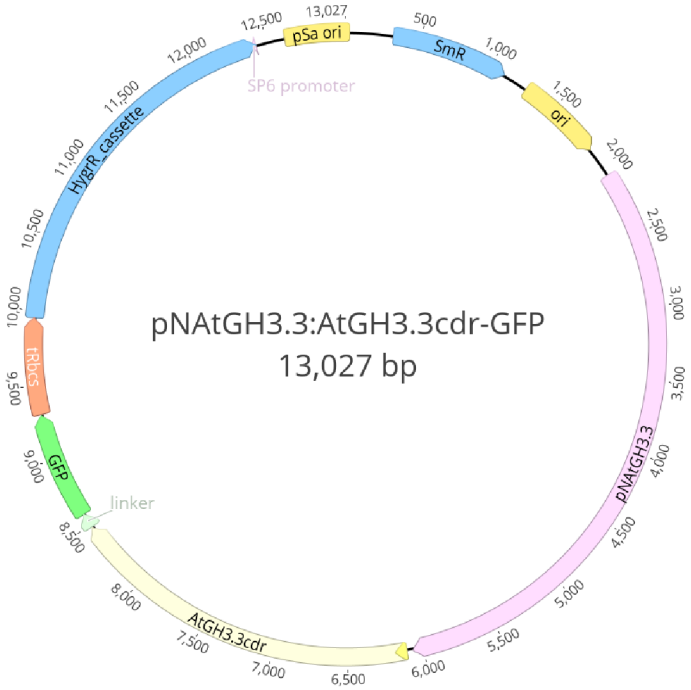

Attachment 8. Representation of pNAtGH3.3:AtGH3.3cdr-GFP vector, created in Geneious Prime. The plasmid is 13,027 bp and carries origin of replication ori, native promoter pNAtGH3.3, AtGH3.3 gene, GFP sequence with a linker, tRbcs (terminator), HygrR (hygromycin resistance cassette), pSa ori (origin of replication for bacteria), SmR (spectinomycin resistance cassette)

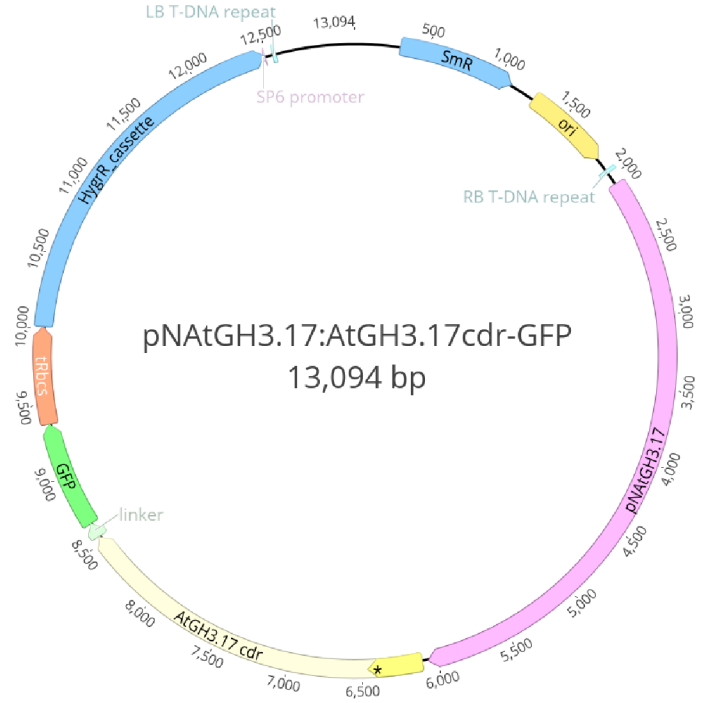

Attachment 9. Representation of pNAtGH3.17:AtGH3.17cdr-GFP vector, created in Geneious Prime. The plasmid is 13,094 bp and carries origin of replication ori, native promoter pNAtGH3.17, AtGH3.17 gene, GFP sequence with a linker, tRbcs (terminator), HygrR (hygromycin resistance cassette), pSa ori (origin of replication for bacteria), SmR (spectinomycin resistance cassette)

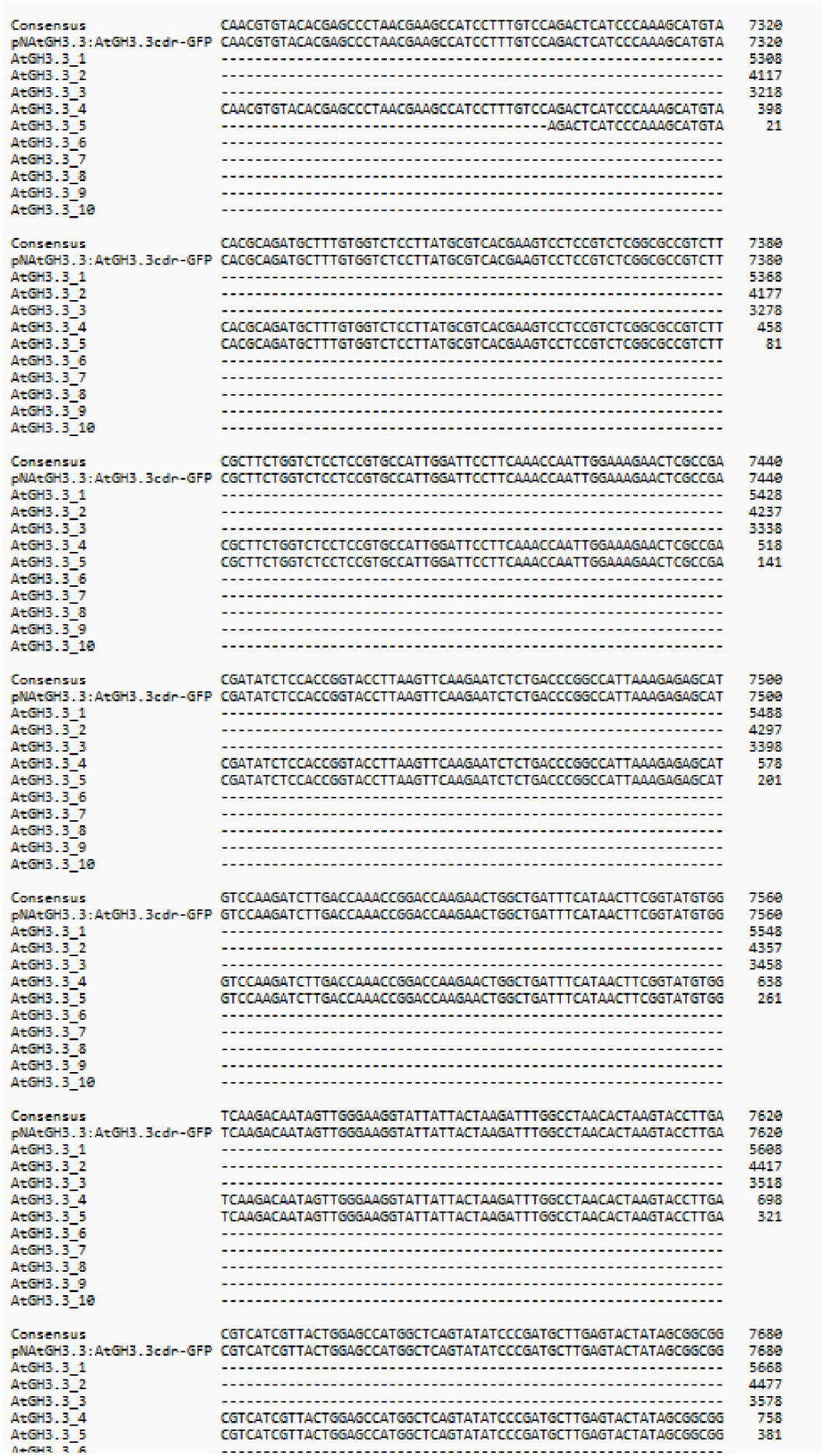

Attachment 10. Sequence alignment of pNAtGH3.3:AtGH3.3cdr-GFP with a fragment of AtGH3.3 coding region resulting from the sequencing and confirming the correctness of assembly (part 1).

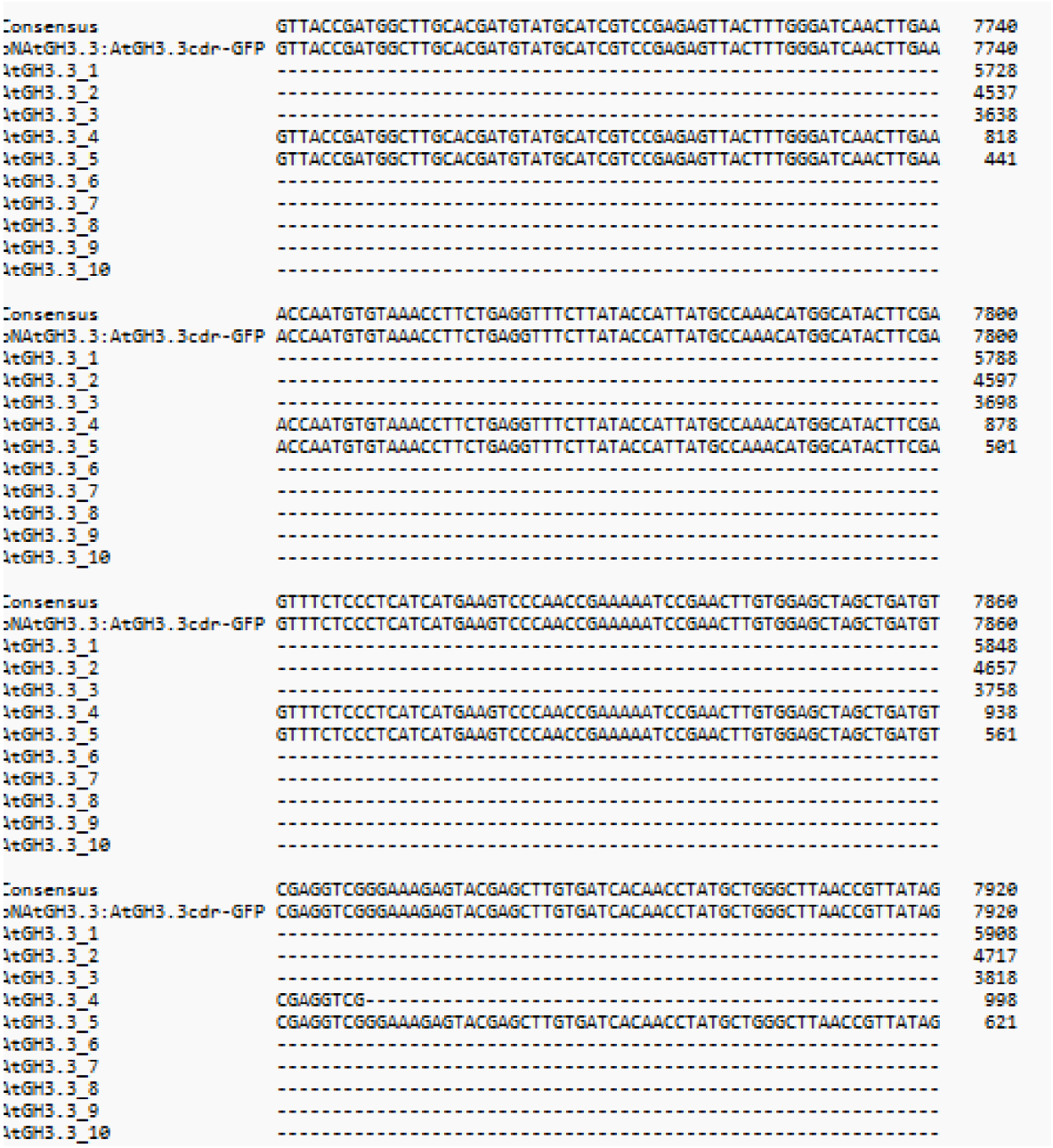

Attachment 11. Sequence alignment of pNAtGH3.3:AtGH3.3cdr-GFP with a fragment of AtGH3.3 coding region resulting from the sequencing and confirming the correctness of assembly (part 2).

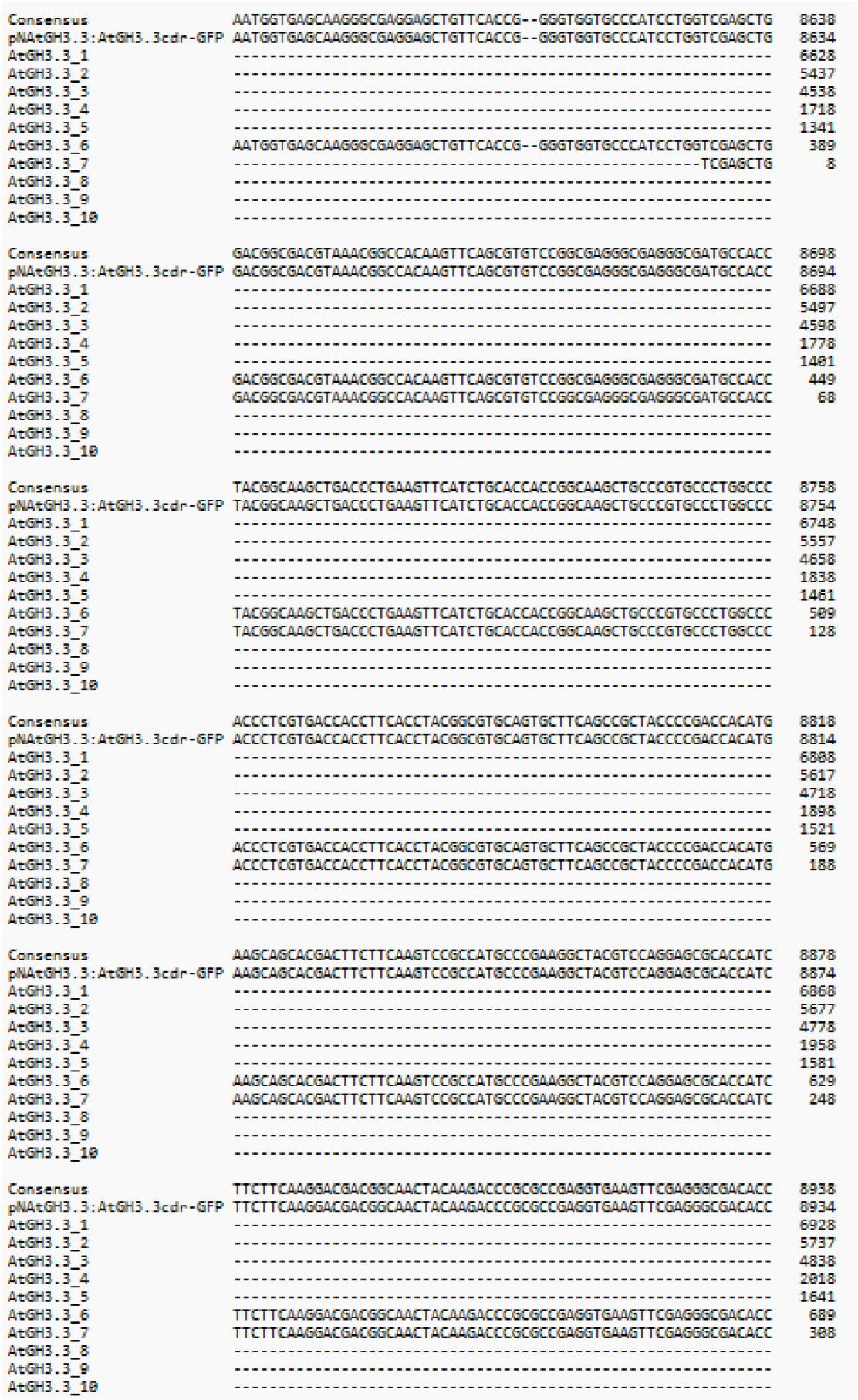

Attachment 12. Sequence alignment of pNAtGH3.3:AtGH3.3cdr-GFP with a fragment of GFP coding region resulting from the sequencing and confirming the correctness of assembly (part 1).

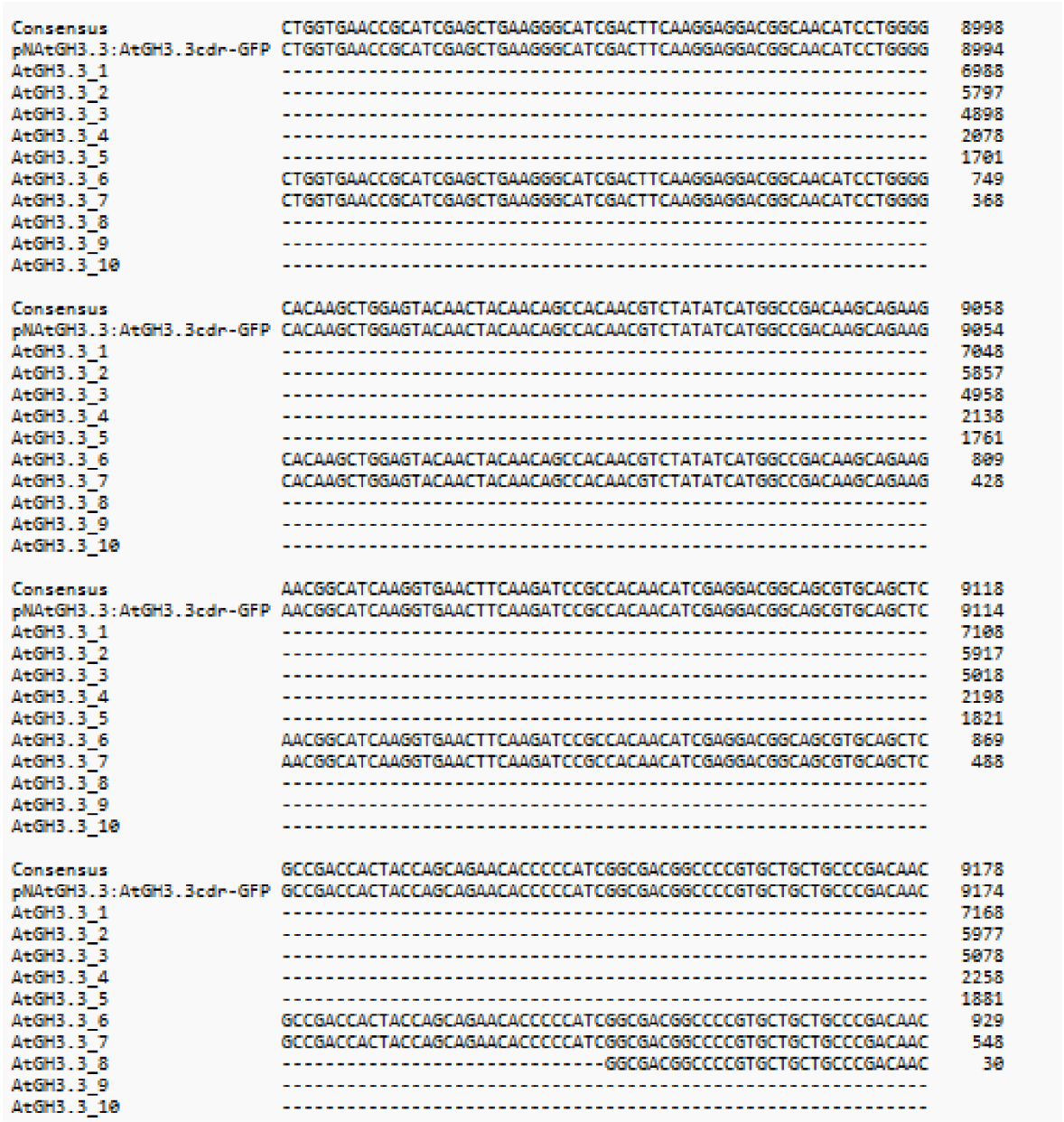

Attachment 13. Sequence alignment of pNAtGH3.3:AtGH3.3cdr-GFP with a fragment of GFP coding region resulting from the sequencing and confirming the correctness of assembly (part 2).

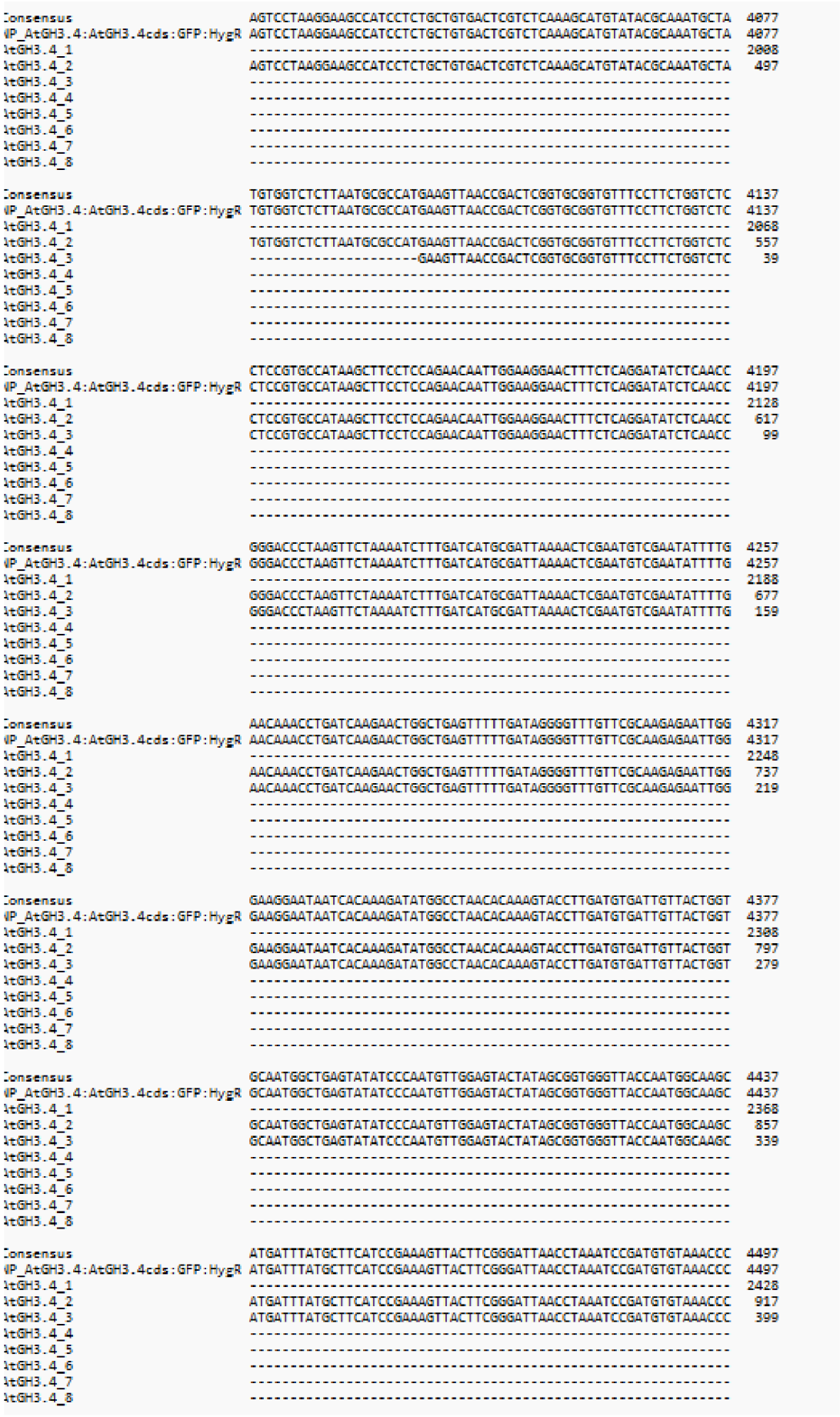

Attachment 14. Sequence alignment of pNAtGH3.4:AtGH3.4cdr-GFP with a fragment of AtGH3.4 coding region resulting from the sequencing and confirming the correctness of assembly (part 1).

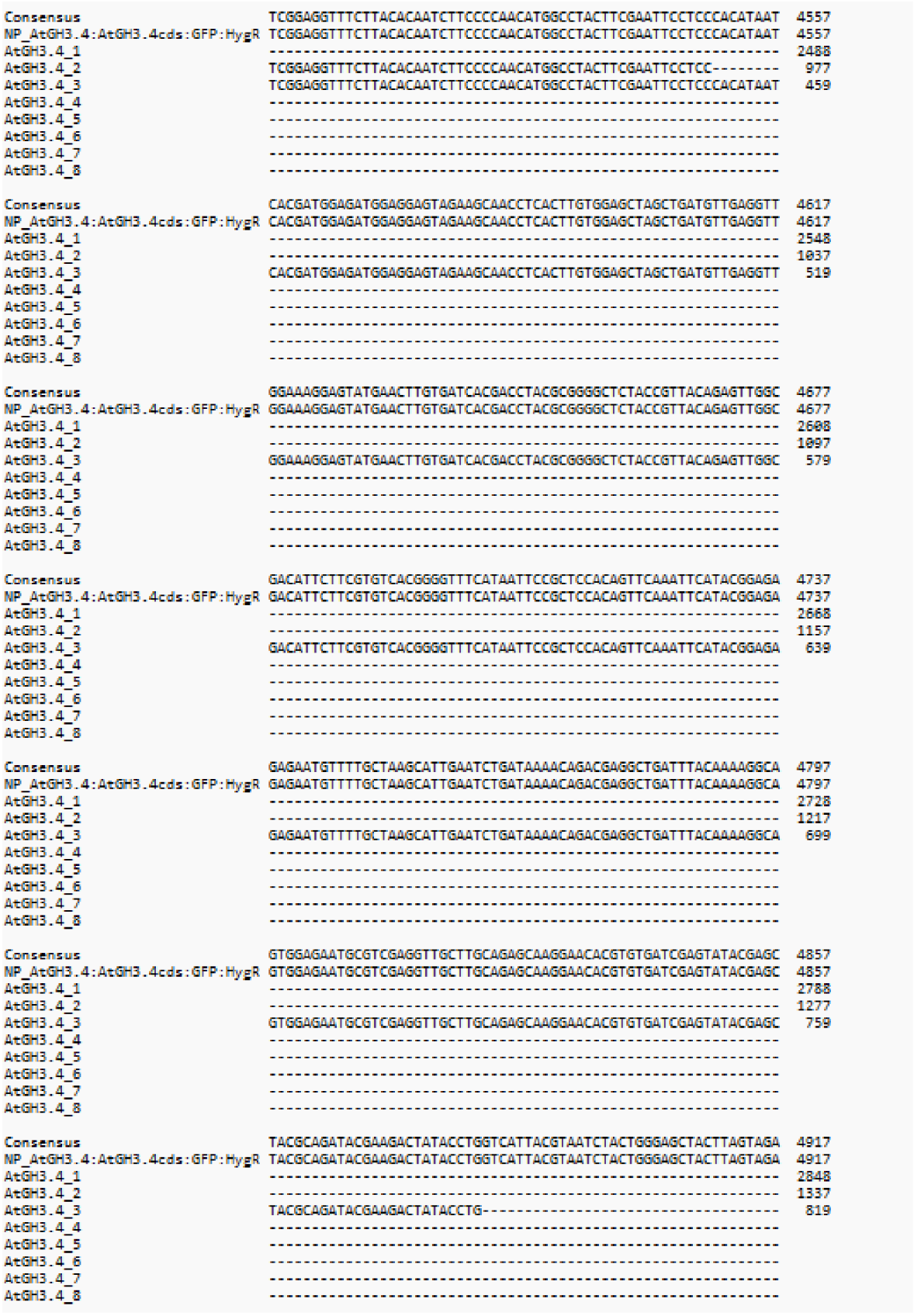

Attachment 15. Sequence alignment of pNAtGH3.4:AtGH3.4cdr-GFP with a fragment of AtGH3.4 coding region resulting from the sequencing and confirming the correctness of assembly (part 2).

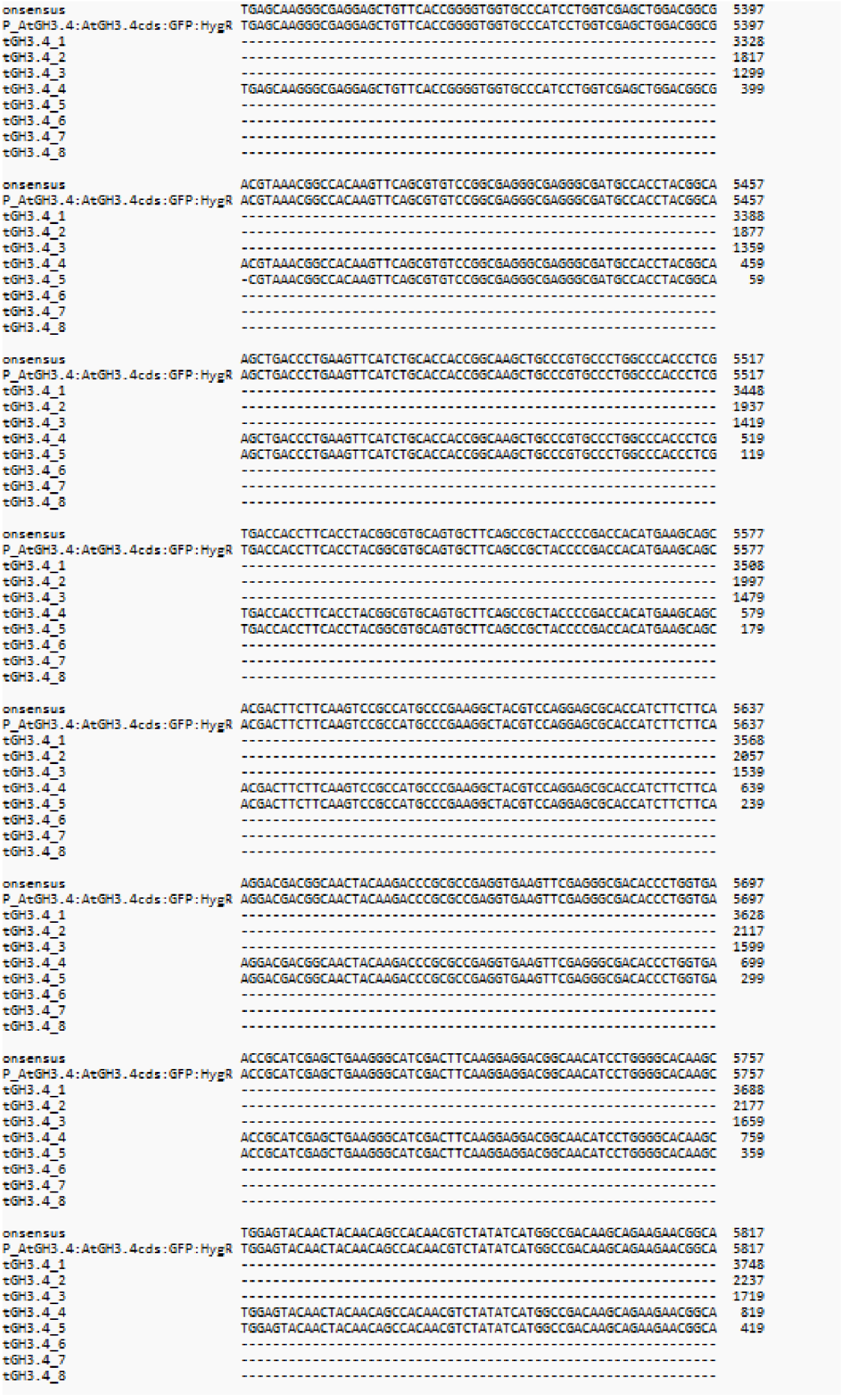

Attachment 16. Sequence alignment of pNAtGH3.4:AtGH3.4cdr-GFP with a fragment of GFP coding region resulting from the sequencing and confirming the correctness of assembly (part 1).

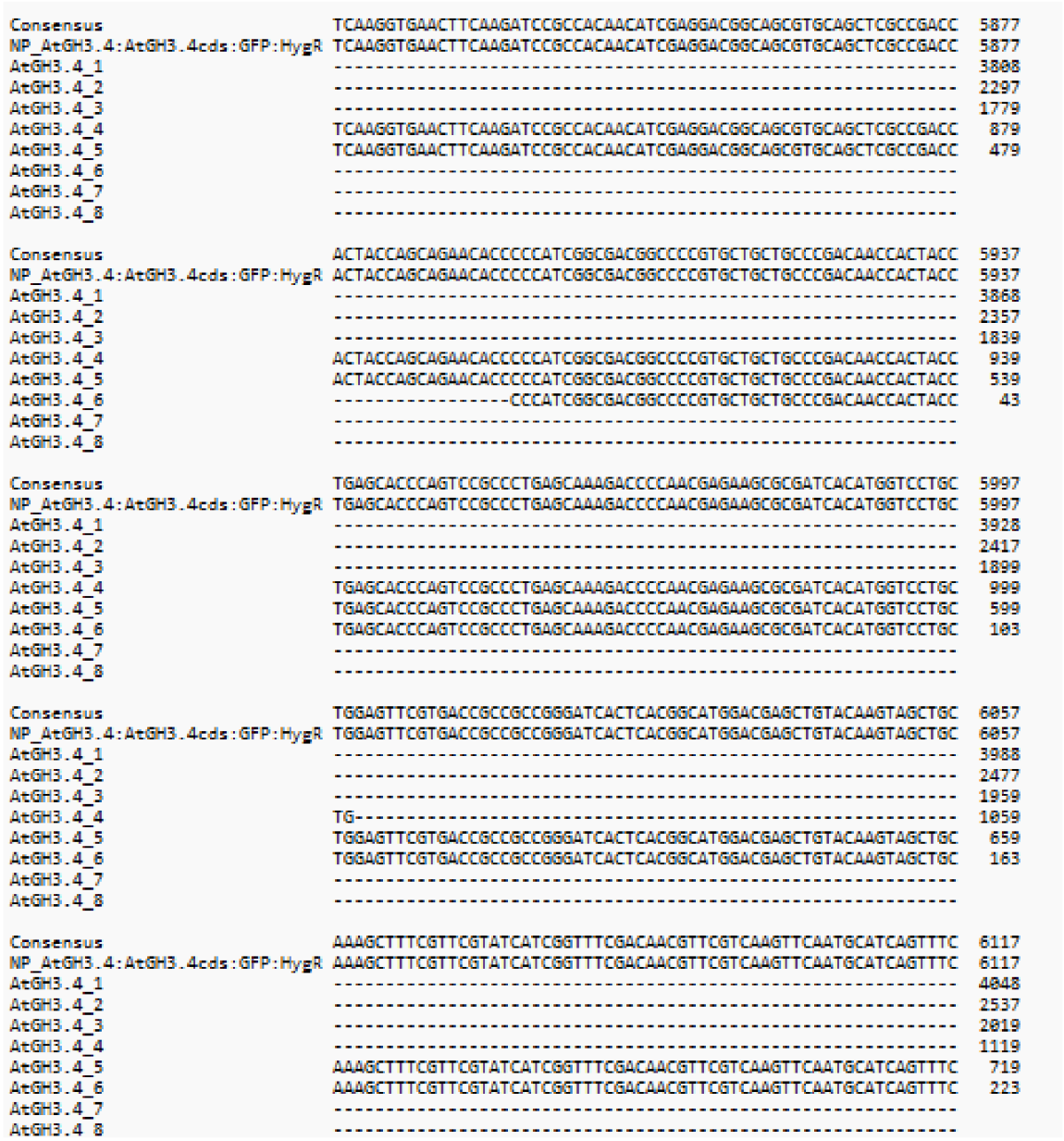

Attachment 17. Sequence alignment of pNAtGH3.4:AtGH3.4cdr-GFP with a fragment of GFP coding region resulting from the sequencing and confirming the correctness of assembly (part 2).

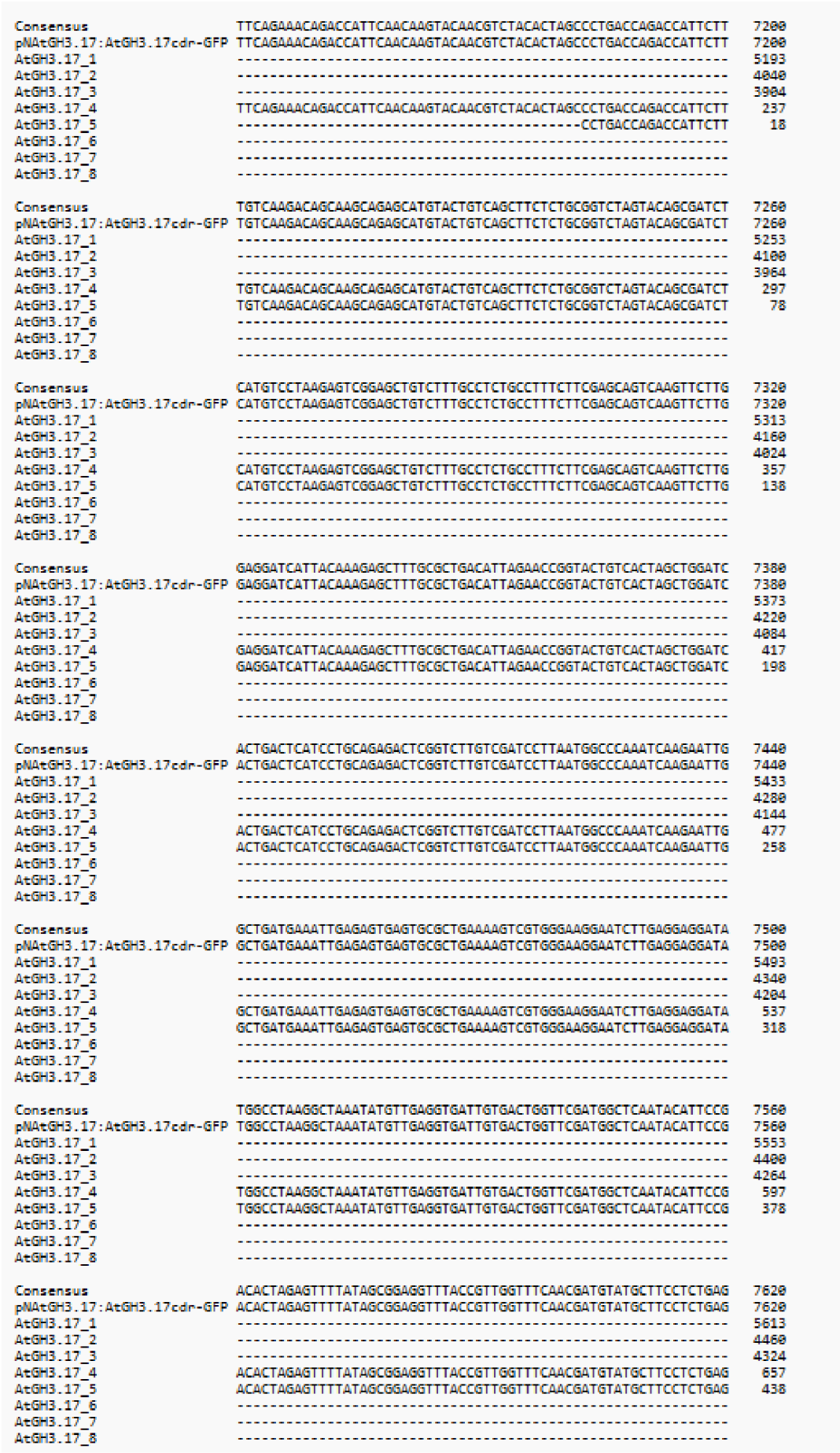

Attachment 18. Sequence alignment of pNAtGH3.17:AtGH3.17cdr-GFP with a fragment of AtGH3.17 coding region resulting from the sequencing and confirming the correctness of assembly (part 1).

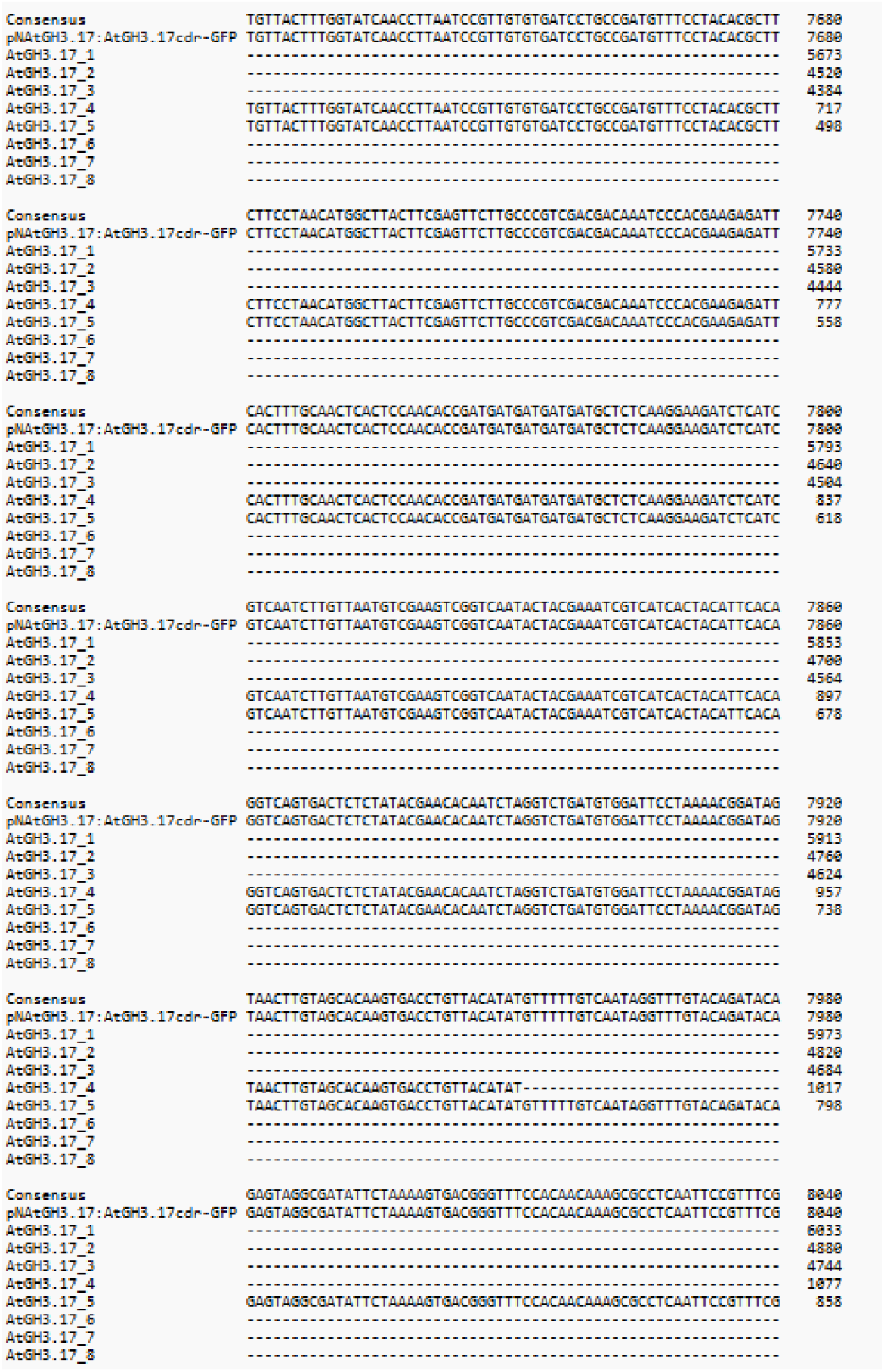

Attachment 19. Sequence alignment of pNAtGH3.17:AtGH3.17cdr-GFP with a fragment of AtGH3.17 coding region resulting from the sequencing and confirming the correctness of assembly (part 2).

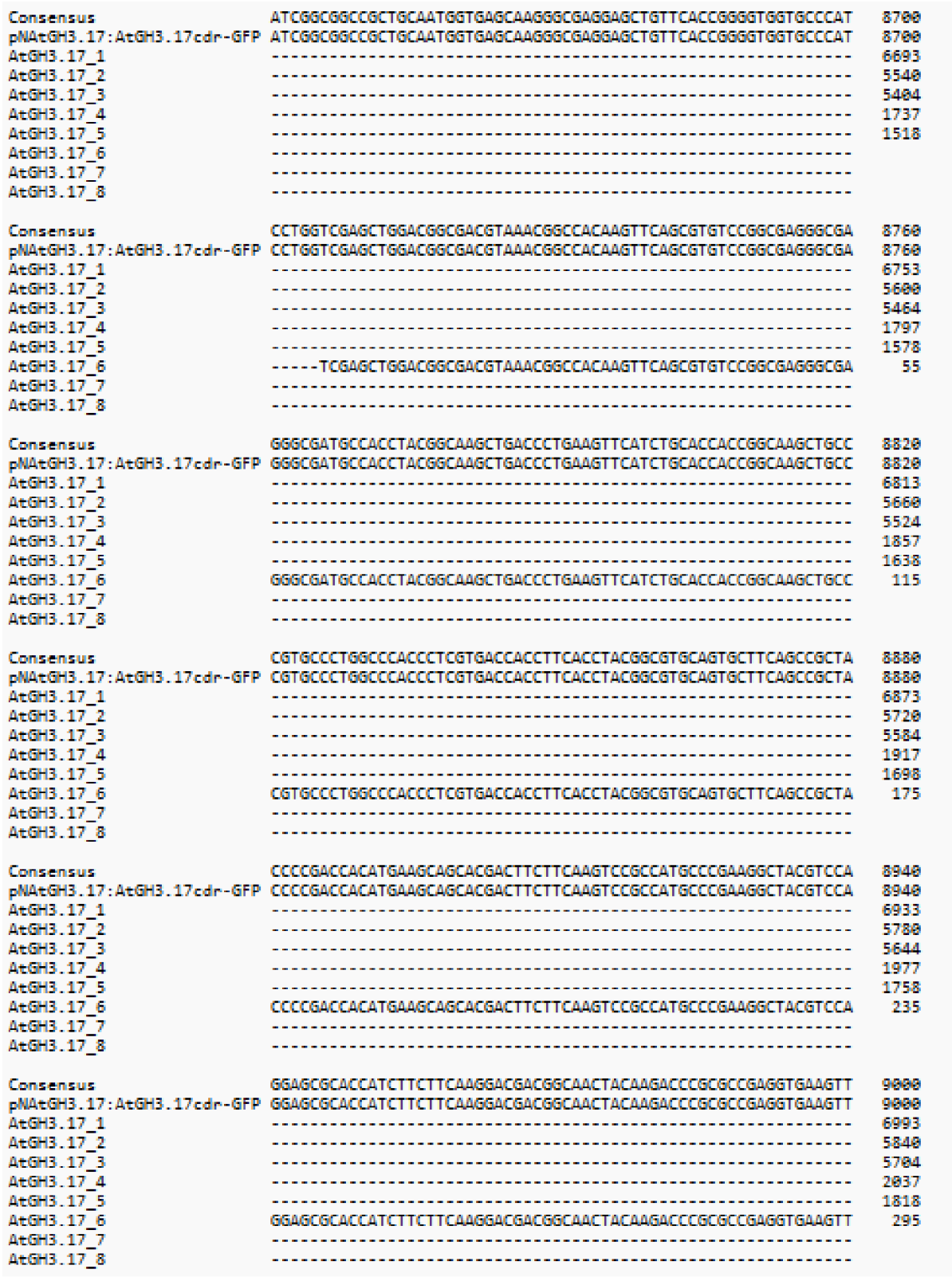

Attachment 20. Sequence alignment of pNAtGH3.17:AtGH3.17cdr-GFP with a fragment of GFP coding region resulting from the sequencing and confirming the correctness of assembly (part 1).

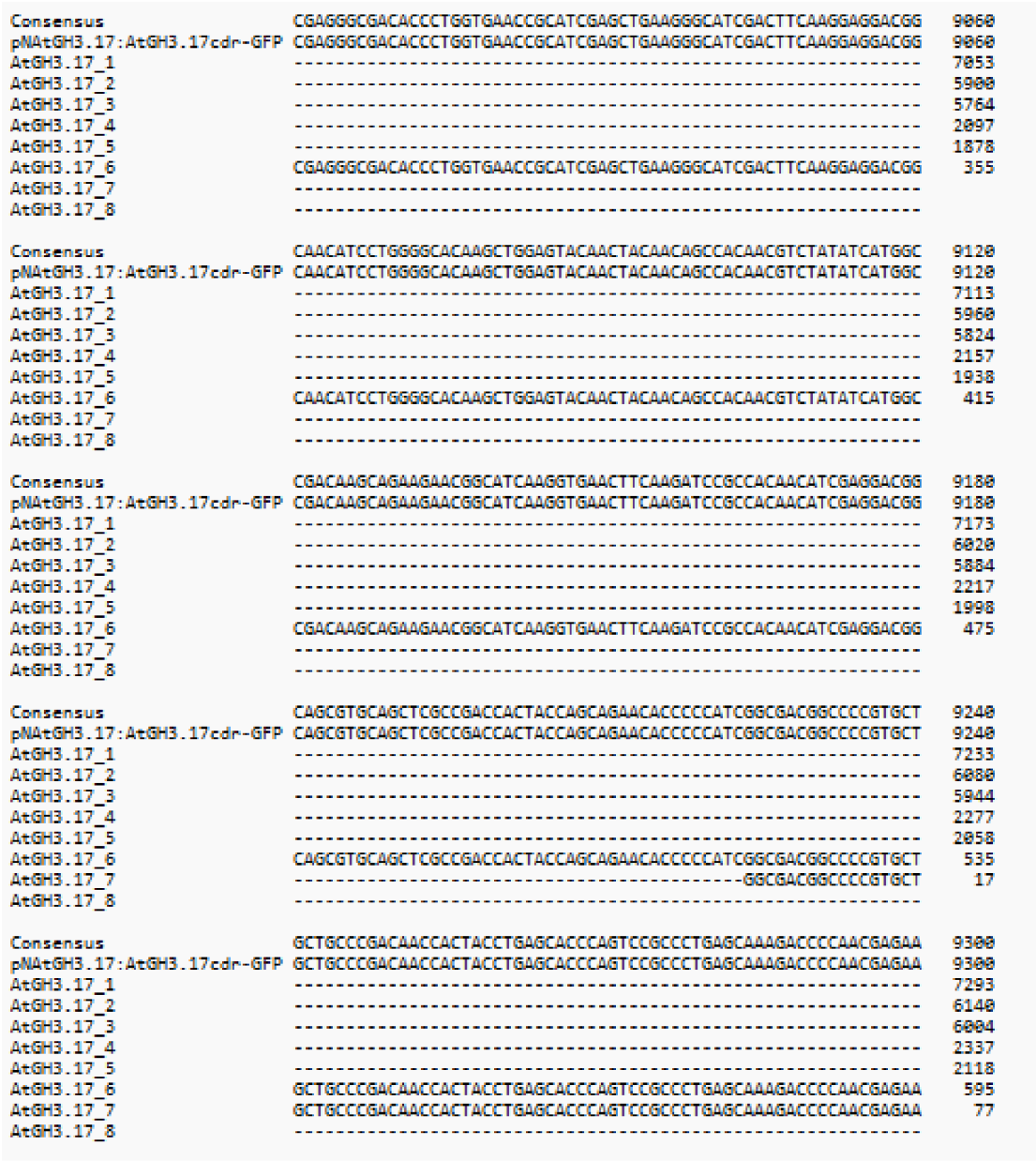

Attachment 21. . Sequence alignment of pNAtGH3.17:AtGH3.17cdr-GFP with a fragment of GFP coding region resulting from the sequencing and confirming the correctness of assembly (part 2).